Gelling properties of milk gels using rennet as a coagulant

DEPARTMENT OF FOOD TECHNOLOGY, ENGINEERING AND NUTRITION | LTH | LUND UNIVERSITY
ELIN BENGTSSON AND DRAGOŞ VOICU | MASTER THESIS 2022

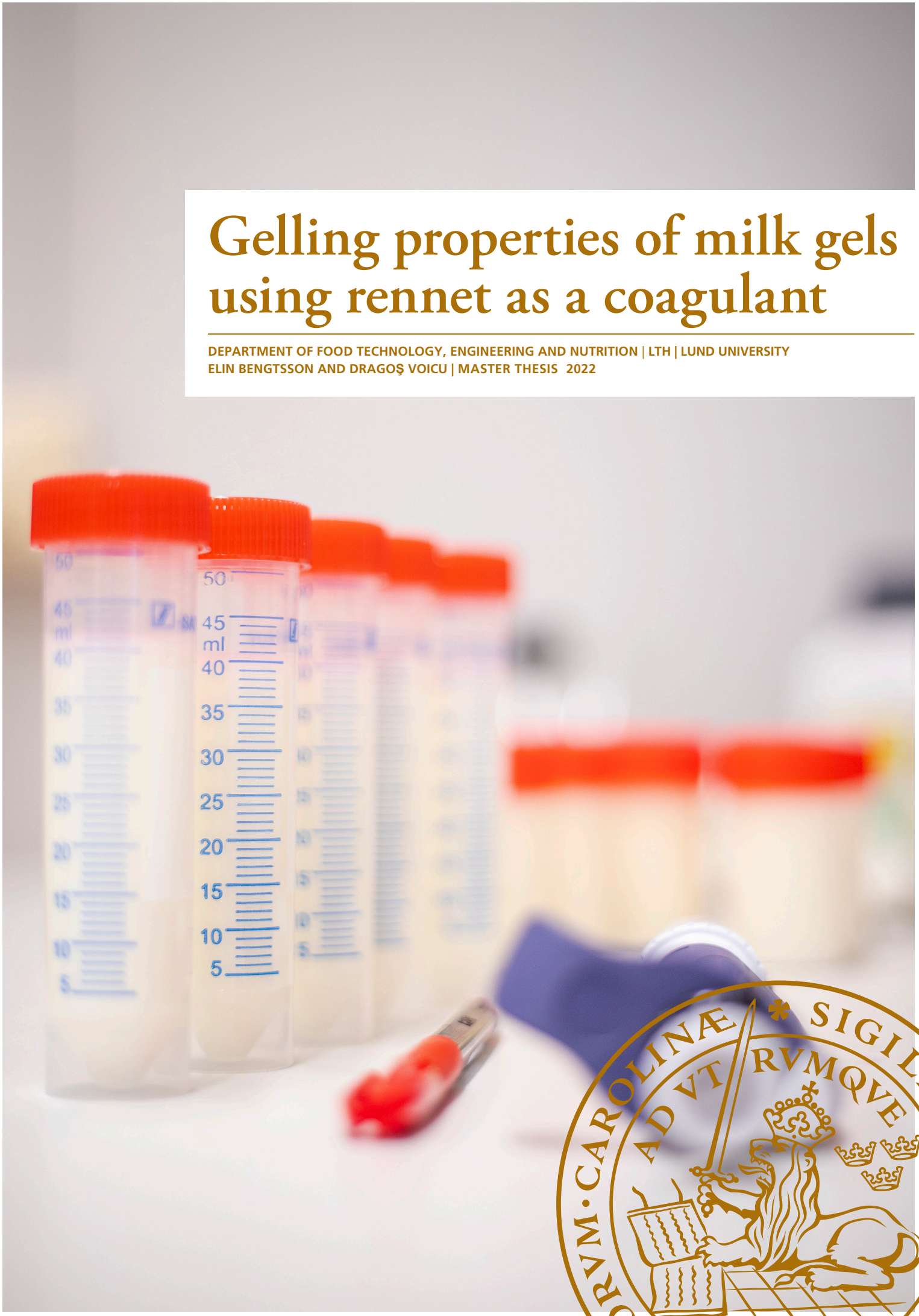

Gelling properties of milk gels using rennet as a coagulant

Elin Bengtsson and Dragoș Voicu

Department of Food Technology Engineering and Nutrition, Lund University, Sweden

KLGM10 – Examensarbete i Livsmedelsteknologi – Civilingenjörsutbildning i Bioteknik

KLTM01 – Degree Project in Food Technology – Master's in Food Technology and Nutrition

Supervisors: Frida Lewerentz and Maria Glantz

Examiner: Marie Paulsson

Lund 2022

Preface

This thesis represents the final assignment of the Civilingenjörsutbildning i Bioteknik programme and Master's Programme in Food Technology and Nutrition from the Faculty of Engineering at Lund University. The report was made in collaboration between Elin Bengtsson and Dragoș (Eva) Voicu at the Department of Food Technology, Engineering and Nutrition. This master thesis was performed in Lund from the end of January to the beginning of June 2022

We want to acknowledge the fructuous collaboration with Frida Lewerentz, Maria Glantz, Marie Paulsson, Shruti Lalwani, Hans Bolinsson, Olexandr Fedkiv and we would also want to thank them for their support.

As a Swedish and international student, the previous two years have been tumultuous, due to the current situation in the world. We would like to thank Lund University for its openness to everyone, regardless of identity, nationality and for creating a save space for all students during this time.

Elin Bengtsson

Dragoș (Eva) Voicu

Lund, Sweden, June 2022

Abstract

As the consumption of dairy is a common staple in the Nordic and European diet and culture, better understanding of the dairy industry as a whole, and especially the cheese industry is needed to aim for a more sustainable production. This project aims to offer an extended approach on the rennet coagulation of milk, analysing the gelling properties of skim milk samples at different pH values (5.5-6.7) with various additions of $CaCl_2$ (1.0-10 mmol/L), as well as the impact of the presence of fat and the fat content (2%-3%) of the milk samples.

Two trials were performed during this project, the Response Surface method trial, and the Effect of fat on gelation-trial. The Response Surface method trial contained skim milk samples with a varying degree of added $CaCl_2$ at different pH, to investigate how pH and $CaCl_2$, and the interaction of these factors affect the gelling properties of the skim milk. The Effect of fat on gelation-trial contains both skim milk and full fat milk samples, with varying fat content (2%-3%), to establish if the fat content, or the presence of fat had a significant impact on gelling properties of the milk. Methods used in order to measure the gelling properties of the milk samples during these trials include Rheometer to establish G' at 30 min, Turbiscan to establish the Δ Back Scatter (ΔBS) and Malvern Master sizer to establish particle size. Statistical methods such as Minitab21 and its response surface method was used to not only plan the Response surface method trial, but also to generate contour plots, pairwise parson correlations and 2-Sample T-test. Matlab was also used to generate plots of gelation curves.

The results concluded that pH is an important factor regarding gelling properties of rennet milk gels, as it had a significant effect on both gelation time and G' 30 min. $CaCl_2$ does not have a statistically significant effect on the variables of gelation time, G' 30 min and ΔBS 30 min. The fat content and the presence of fat had no significant effect on the gelation time, G' at 2x gelation time and G' 30 min, while the fat content had a significant effect on the ΔBS 30 min. It was expected that the pH would be significant for gelling properties, but unexpected that $CaCl_2$, fat content and presence of fat did not have a bigger impact on the results obtained. In order to verify the results presented in this report, more research and trials, especially on the impact of fat content, presence of fat and $CaCl_2$ needs to be made.

Popular science summary

How does the pH, fat content and addition of calcium chloride effect gelling properties of milk gels?

pH, calcium chloride and fat content are all factors with an integral role in the cheese making process, or is it so? By understanding these factors and their significance for the milk gel formation, steps are taken towards a more sustainable and knowledgeable production that the dairy industry is in desperate need of.

Cheese, and dairy products in general have been around for a very long time, albeit in more simple forms than the products available in the grocery store today. But now over 8000 years later, fermented milk products are still a staple in the Nordic and European diets. As the call for more sustainable food production becomes louder, and introduction to plant-based version of beloved dairy products are growing by the dozen, the dairy industry needs to act and not only take responsibility of their environmental impact, but also to implement change. But how would this be possible? “With great power comes great responsibility”, a quote most commonly known from Marvels the Spider-Man comics, but something that should be taken to heart by everyone, as it is the responsibility, and burden of the people today, to ensure a better future for tomorrow.

In order to instill change in any production process, a deep knowledge of said process and its components is crucial. During the production of cheese, the incoming milk goes through a pre-treatment, where the milk is pasteurized, and spores are removed. It is then centrifuged and standardized to achieve the right fat content. It is here that lactic acid bacteria, or lactic acid is added in combination with calcium chloride and rennet to achieve coagulation of the milk. It is through the coagulation of the milk that a gel network consisting of casein micelles and fat globules can be created, that lays the foundation for remaining steps of the cheese making process. The gel is then cut, pressed, salted and ripened to finally be available for consumers to purchase.

Having a deeper understanding for how the fat content of the milk used during coagulation and gel formation affect the final gel properties, but also the impact of pH and addition of calcium chloride, makes it possible to assess the effect and necessity of these factors. Perhaps the addition of calcium chloride can be minimized or even removed, as its contribution of gel properties are minute? This would in turn render the process more streamlined and even more specialized to certain types of cheese.

In this thesis project, the composition of cow’s milk used ahead of alterations is looked closer at using the Milkoscan. The particle size of casein micelles and fat globules were established using the Mastersizer 2000. The Kinexus Rheometer and Turbiscan Lab were used to look closer at gelling properties such as gelation time, G’ at 2x gelation time, G’ at 30 min and ΔBack Scatter at 30 min. This was used in combination with software such as MATLAB and Minitab to establish the significance of the result achieved and how the factors of fat, pH and calcium chloride influence the gelling properties of milk gels.

Abbreviations

ΔBS – ΔBack Scatter
CCP – Colloidal Calcium Phosphate
CLSM – Confocal Laser Scanning Microscopy
CMP – Caseinomacropeptide
DOE – Design of Experiment
DSS – Defined-strain cultures
DVS – Direct vat set
FTIR – Fourier Transform Infrared Spectroscopy
HTST – Regular High Temperature, Short Time
ISA – Ionic Strength Adjuster
LAB – Lactic acid bacteria
MFGM – milk fat globule membrane
MSS – Mixed-strain cultures
NSC – Natural starter cultures
NSLAB – Nonstarter LAB
SNF – Solid non-fat
SEM – Scanning Electron Microscopy
SOP – Standard Operating Procedure
TS – Total solids

Table of Contents

1. Introduction

Milk and dairy products are very much a part of the European and Nordic way of living. It has been this way since around 6500 BC [1], and it is to this day still shaping consumer habits and influencing the food market. It is interesting how a primitive discovery made in ancient times [2] [3], have developed into a dominating industry that keeps evolving to create new food products. Nowadays in the dairy industry, there are observed 2 types of gels being classified in: caseins aggregates and combination between whey proteins and caseins aggregates [4]. With a better understanding of this field, the production flows in the cheese making process can be optimised. For the cheese and yoghurt industry, the gelling properties of the milk are very important. It is of interest to explore how the addition of acid to the milk changes the properties of the coagulating milk. This could be seen by studying the firmness of the gel in question. Another important aspect in cheese making is the addition of $CaCl_2$, as it is used to improve gelling. Can there be an amount added that worsen the properties of the gel, or is it possible to remove the addition of $CaCl_2$ entirely and still achieve the same quality product? As the knowledge of gelling properties of cow's milk is deepened, changes to current products can be made, as well as proposing new products for the market. In addition, a better production flow can be translated into a higher yield and improved economic sustainability. Better utilization of raw material and residual products would enable the creation of other revenue streams as for food and pharmaceutical industry.

1.1. Scope

For this project, the comparison of gelation properties in whole milk and skim milk, depending on how two important factors correlate; the addition of $CaCl_2$ and the pH of the milk at start of gelation, will be investigated. The milk used for this research project comes from cows located in Skåne, Sweden.

1.2. Aim

The overall aim for this project is to increase the knowledge of how gelling properties of cow's milk are affected by properties of the milk and additions made at the start of gelation.

1.2.1. Research question

Based on the aim for this thesis project, 3 research questions will be explored, as listed below.

- What is the difference in gel properties in skim milk and whole milk?
- What is the effect of $CaCl_2$ addition in different levels on gel properties?
- What is the effect of pH adjustment on gel properties?
- What is the combined effect of pH and $CaCl_2$ on gel properties?

1.3. Delimitations

Some choices were made in order to limit the topics of this report, focusing on the effect on pH and calcium chloride and fat content, excluding other factors, which were not investigated, such as temperature, lactose content in the milk, the size of casein micelles and fat droplets, CO_2 and $NaNO_3$ addition. The focus of this project is the gelling properties of cow's milk. On the other hand, the time limit of about 4 months limited a deeper look in the topic.

2. Theoretical background

Understanding the importance of dairy products in history is the key to understanding the interest in them today. Cheese has been considered a very appreciated product due to its taste but also shelf-life properties. As technology is improving, so is knowledge, offering a new perspective on the world of cheese making

2.1. History of cheesemaking

Since the early times, the humankind has appreciated fermented products due to their special properties such as extended shelf life, taste, and even nutritional value. Fermented milk products were first mentioned originating from Mesopotamia, Egypt and India around 9000 BC. All the civilisations created their own variants of fermented dairy products such as Dahi, Chhash, Khad, Leben or Zabady. According to legend, the first cheese was developed accidentally by a merchant from the Arabic Peninsula. He kept his drinking milk in a pouch made from the stomach of a sheep while crossing the desert. The historians consider that the evolution of civilization determines the evolution of cheese, with cheese making being considered a way of art in the zone of Mediterranean Sea but also around the globe. There are also references about cheese in the Bible and in ancient Greek and Roman reports. [1] [2] [5] [6]

2.2. Composition of milk

Milk is characterised as a fluid which is secreted by female mammals [7]. Its composition differs between mammal species. Cheese can be made from any milk provided by any mammal, but mostly used are: cow, sheep, buffalo, and goat. For this project, cow's milk will be used. This type of milk is characterised by an average of 3.5% protein, 3.7% fat, 4.8% carbohydrate and 0.7% solids. These values can be changed by different external conditions as the animal feed, the existing climate or breeding. [8] [9]

2.2.1. Proteins

It is considered that the milk proteins are the most studied out of the food proteins. They contain essential amino acids which are important for the balanced development of the body, including maintaining the tissues with protein containment and the binding metal ions or vitamins [9]. There are 2 types of milk proteins: caseins and whey proteins. The challenge faced by the scientific community is to fully understand the caseins, their tertial structure and why they are not crystallizing. Usually, the milk provided by bovines contains around 30 g of proteins/L. From this quantity around 80% is represented by caseins and 20% by the whey proteins.

Caseins are described as spherical large micelles composed by 92% proteins and 8% inorganic salts with low molecular mass [10]. There are 4 types of recognised caseins: α_s-caseins (α_{s1} (Figure 1) and α_{s2} (Figure 2)), β-casein (Figure 3) s and κ-caseins (Figure 4), all with different genetic variants. [8] All of them contain an important amount of non-polar amino acids such as proline. Due to the presence of proline, there are low amounts of α-helix and β-sheet structures in the secondary structure of the casein. Because of this the proteolysis can occur without a pre-treatment as acid addition or heat treatment. [9]

Figure 1: Structure of α_{s1}-caseins [11].

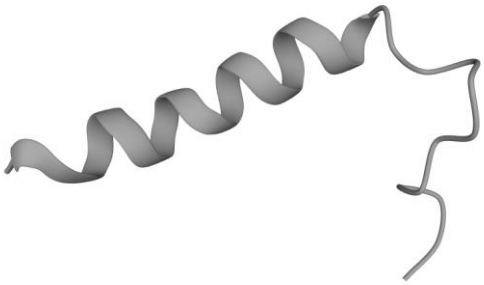

Figure 2: Structure of α_{s2}-caseins [12]

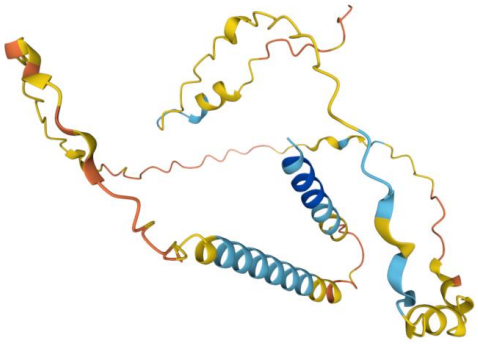

Figure 3: Structure of β-caseins [13].

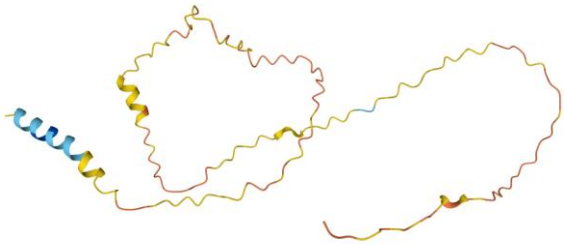

Figure 4: Structure of κ-caseins [14].

Several models try to predict the structure of the casein micelle, and while there is no definitive answer as to which model is the "correct" one, there are similarities and differences between these models. 3 models are of particular interest, the extended sub-micelle casein model proposed by Walstra [15] and two internal structure models proposed by Holt [16] and Horne [17]. The Walstra model came out as the one who has the most common acceptance, being suggested in 1984. The main idea of it is that the casein micelles are formed by subunits, called sub-micelles which are considered spherical. They are merged together due to the in between protein hydrophobic linkage and also the calcium phosphate ones. It was considered that the sub-micelle diameter is around 15 nm, containing about 25 casein molecules. Walstra considers the existence of 2 different kinds of submicelles. The first one is formed by α_s- and β-caseins. The other one is formed by α_s- and κ-caseins. The κ- caseins are located at the external part of the micelle forming the "hairy" structure. [15] In his model Holt mainly focused on the location of the protruding κ-caseins and on the role of the colloidal calcium phosphate (CCP). The casein micelle was limited to a gel-like structure created by the flexible casein network. The CCP form micro-granules that are present in the centre of the casein phosphate. The stability of the casein is attributed to two main factors, the protruding C-terminal of the κ-casein as it creates steric stabilization, as well as the surface potential of the casein micelle. Horne proposed in his dual binding model that the casein micelle is held together by electrostatic repulsion that limit the growth of polymers, and hydrophobic interactions that are the forces behind the casein micelle formation. The hydrophobic regions are also where the caseins first bond together. The CCP is considered the link between casein micelles as it binds to phosphoserine residues. κ-caseins will act as a termination propagator due to their lack of phosphoserine to bind to

calcium and will therefore only interact hydrophobically. [18] While all of these models have differences and similarities, it is very possible that a combination of all three is closer to the "true" structure of the casein micelle.

Some micrograph images [19] show casein micelles with larger diameters as 300-350 nm but usually the average dimension of the micelle is around 200 nm. It was proven that the micrograph images are bringing more details than the usual SEM image. This provides an update to what was already known, that the submicelles have a "raspberry" appearance [19].

The reduction of pH needed for casein precipitation can be obtained using either lactic acid bacteria (LAB) or lactic acid, methods which result in reaching the specific milk caseins isoelectric point of pH 4.6. The other way of precipitating the caseins is through the use of enzymes breaking the linkage between the amino acid 105 and 106 from the k casein molecule (example: chymosin affect Phe_{105} and Met_{106}). The whey proteins are divided in α-lactalbumin and β-lactoglobulin. [8] Casein micelles of smaller sizes generally contribute to a faster coagulation, as the smaller casein micelles have a higher level of κ-caseins compared to larger casein micelles [20].

In the following Figure 5, a casein micelle is presented.

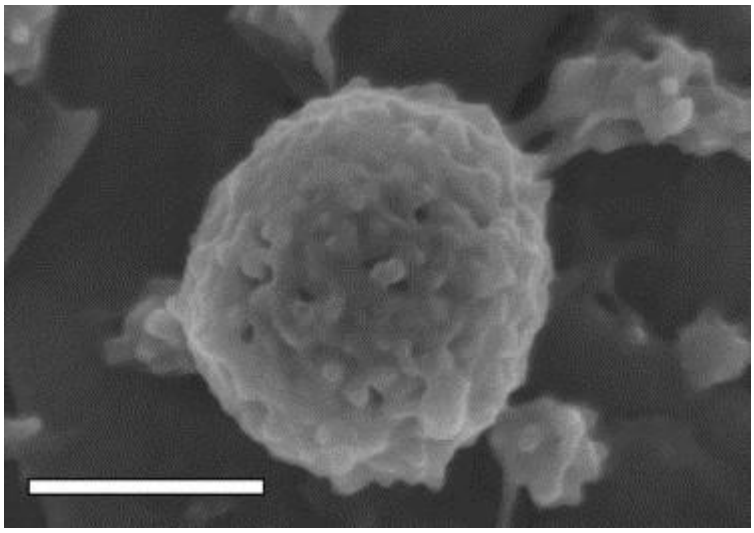

Figure 5 Micrograph of casein micelle scale bar 200 nm- cross section [19].

2.2.2. Fat

One of the most important uses of lipids is as source of energy. The different fat content from different sources of milk explains the difference in the needs of each species. Lipids are an important origin of essential fatty acids and function as solvent for A, D, E, K vitamins. [9] They are also responsible for the milk rheology. For example, the state of the fat, if it is solid or liquid, influences the milk's flow behaviour. Also, the milk with a higher fat concentration would present higher viscosity levels. [21] It is known that from the total lipids, around 98% are triglycerides. There are 400 different fatty acids in the milk of bovines. [9] A significant part of them is found in very low concentrations, but which are enough to be traced. There are different fatty acids featured in milk, depending on the animal origin of it. For example, the butanoic acid (C4:0) concentration might reach around 7% in the milk of some mammals, but in the cow's milk it reaches just about 3.3%. In the cow's milk there are also other short chain saturated fatty acids such as 1.6% caproic acid (C6:0), 1.3% caprylic acid (C8:0) and 3.0% capric acid (C10:0). Regarding long chain saturated fatty acids, in cow's milk, there are 26.3% palmitic acid (C16:0) and 14.6% stearic acid (C18:0). The highest concentration, however, is represented by the monounsaturated oleic acid (C18:1) 29.8%. There are no high concentrations of poly unsaturated fatty acids in cow's milk, just 2.4% is represented by linoleic acid (C18:2) and 0.8% by alpha linoleic acid (C18:3). The quantity of fatty acids might

differ depending on the season. Most fatty acids peak in the summer, with only palmitic acid peaking in the winter. [9] [22].

The globules of milk fat represent droplets rich in triglycerides with their origin in the membrane of the endoplasmic reticulum, being released in cytosol. After this, they are secreted from the cell in a special exocytosis mechanism with cytoplasmic vacuoles. The milk fat globule membrane (MFGM) is formed from 3 structures (some regions from the apical plasma membrane, endoplasmic reticulum, and some other intracellular parts). The part originating from the apical plasma membrane, presents bilayer aspect which is dense in electrons in the inner part of it. The membrane from the other 2 parts appear to present a protein monolayer. Also, there are lipids covered by triacylglycerols remaining from before secretion [23]. Usually, the diameter of the milk fat globule is on average about 4 μm. It has been observed that the cheese produced from milk with smaller fat globules maintains more moisture than the cheese obtained from milk with bigger fat globules [20].

2.2.3. Carbohydrates

Lactose, also known as β-D-galactosyl-D-glucose, is a disaccharide found exclusively in milk. As in the case of fats, each mammal species has a different amount of carbohydrates in their milk. Lactose has significant nutritional and pharmaceutically importance. In the cheese production, a part of lactose is converted by the starter cultures into lactic acid, but the biggest quantity of lactose is separated with the whey. It is estimated that there is around 5g of lactose in 100mL whey. [24]

2.2.4. Solids

The milk solids are presented as different salts (carbonates or bicarbonates of Ca, which is important in cheesemaking process, Mg, K, Na or chlorides, sulphates). There are also around 20 elements found in traceable quantities such as Cu, Fe, Zn or I. They have an important impact on the nutritional aspect and influence the processing and storage of the milk. [9] Ca can be found either bound to casein micelles or in complexes with citrate and phosphate. The calcium in the milk can also be found in its ionized form (Ca^{2+}). [25]

2.3. Steps of cheesemaking

In Sweden, 83.5 thousand tons of cheese were produced in 2020 [26]. With many different types of cheese available on the market today, consumers have many options to choose from. Some cheeses are more alike, while some have more unique characteristics setting them apart. This is also reflected in the cheese making process. While many cheeses share common steps within the production process, diversification during production enables the unique characteristics of each kind of cheese to be created.

2.3.1. Pre-treatment of milk

To ensure high quality of the produced cheese, measures are put into place to only use high quality milk to produce the cheese. One of these measures is that milk from sick cows or milk from cows undergoing treatment with antibiotics should not be used to make cheese [8]. It is also of importance that the milk is held at the temperature of 4 °C during collection and transportation of the milk to the cheese plant. After arrival at the cheese plant, the milk will go through pasteurization at 72-73 °C for 15-20 seconds for Regular High Temperature, Short Time (HTST) pasteurization. However, this can vary, as for some types of cheeses, the milk used should not be heated above 40 °C, such as parmesan, as it will affect the aroma, flavour, and whey expulsion. Pasteurization is often performed in a plate heat exchanger. The plate heat exchanger consists of several heat transfer plates with gaskets, providing a two-channel flow system. This enables a counter-current flow to be used

where the primary and secondary media do not mix, as the media flow through single channels. As the two different media is separated, the heat transfer from the secondary medium goes through the metal to the primary medium. In the counter-current flow, the milk meets the heating medium when they are both at their coldest state. As the milk moves through the channel, it encounters heating medium at increasing temperature. After the milk has been heated, it needs to be cooled in order to be used for further processing. Therefore, the outgoing heated milk is sometimes used to heat the incoming cold milk. This saves energy in comparison to chilling and heating the respective outgoing and ingoing milk separately. [27] The purpose of performing pasteurization is to kill potential pathogenic bacteria, as well as coliforms that could affect the quality of the cheese. [8]

After pasteurization of the milk, it is often put through a mechanical removal of spore-forming microorganisms in their spore state. Spores will survive regular HTST pasteurization and trying to remove these spores using a more intense heat would be detrimental to the cheese making process. Therefore, microfiltration and beatification is often used to remove spores that could pose a problem during ripening. [8]

2.3.2. Centrifugation and standardization

Separation of cream and skim milk can be done through the usage of a centrifugal separator. [8] The vessel is filled with a liquid and is spun around a center point. This creates a centrifugal force that will change depending on the distance from the center of rotation, and the speed of rotation. [8]. The rate of separation also depends on the difference in density between the continuous phase (skim milk) and dispersed phase (fat globules), the viscosity of the milk, as well as the radius of the fat globules [9]. When the milk is introduced into the separator, it will flow towards distribution holes. The solid particles have a lager density compared to the medium, which is skim milk. These solid particles will move radially outwards in the separation channels and will settle in the sediment space. Due to their lower density compared to the medium, the fat globules will move radially inwards in the separation channels and leave the centrifugal separator separate from the medium and other solid particles. [8]

After separation of skim milk and cream, some of the cream is mixed back into the skim again to achieve the right fat content of the pasteurized milk that is used during the production of cheese. Seasonal variations of the fat and protein content are common in cow's milk. Therefore, it is important to adjust the fat content to achieve the proper fat content, as cheeses are often classified by fat in dry solid basis. [8]

2.3.3. Additions

2.3.3.1. Rennet

Rennet was discovered by accident thousands of years ago and can be found in the fourth compartment, the abomasum, in the stomachs of ruminants. Animal rennet is very commonly used, but other forms of rennet exist, one being the microbially-derived rennet substitutes secreted by different fungi species. These mainly purified proteases act upon the milk in a similar fashion compared to animal rennet. Recombinant clotting enzymes produced by transgenic microorganisms can produce different types of chymosin originating from different animals. [8]

Animal rennet consists of two main proteolytic enzymes; pepsin and chymosin [28]. Chymosin cleaves the peptide bond at $Phe_{105} - Met_{106}$ of κ -casein, cleaving the caseinomacropeptide (CMP) from the main body of the κ-casein. However, pepsin is less specific in its cleaving of residues such as Val, Tyr, Leu and Phe. [29] Calf chymosin has a high milk clotting activity, but a low proteolytic activity. However, as the calf continues to age and is fed more solid food, the amount of chymosin secreted is lowered and the amount of pepsin is increased [28]. There are three types of calf chymosin. Chymosin A has a molecular size of 35.71 kDa and is more proteolytically active

compared to the other genetic variants of chymosin but undergoes autocatalytic degradation. Chymosin B has a molecular size of 35.65 kDa and only differs from chymosin A concerning one amino acid at position 254. Chymosin C is a degradation product of chymosin A due to its autolytic cleaving at Tyr_{285} – Asp_{286} and Phe_{288} – Asp_{289}, resulting in the tripeptide Asp_{286} – Glu_{287} – Phe_{288}. [28] Chymosin has been proven to have a high milk clotting activity, but as the coding gene responsible for its production is rare there are often low levels of chymosin C in commercial rennet. [29] The optimum pH for rennet is found at around pH 6.0 [30] and at 40 °C [8].

There are mentioned factors as stability, the direct dependence of gelling to variables as pH, temperature or ionic strength, or even proteolytic activity during ripening. The following figure 6 shows the effect of the concentration of chymosin, temperature, pH and free calcium ions on chymosin inactivation, splitting of κ -casein, aggregation and clotting time [31].

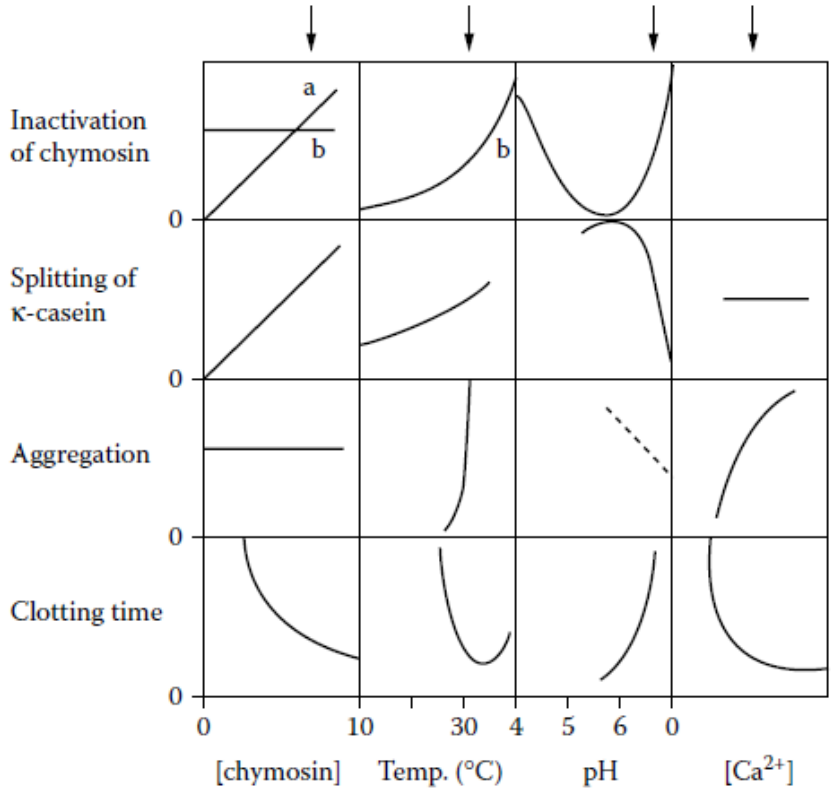

Figure 6 The effect of different variables on chymosin inactivation, splitting of κ -casein, aggregation and clotting time. "a" represents pH 3.5 and "b" represents pH 7 also the blank represents no effect and the dot line an estimated effect. [31]

2.3.3.2. Calcium chloride ($CaCl_2$)

$CaCl_2$ is a common addition within the making of hard cheese using rennet coagulation. During production of cheese, 5-20 g of $CaCl_2$ per 100 kg of milk ($5 \cdot 10^{-5}$ – $2 \cdot 10^{-4}$ %) is usually sufficient for coagulum firmness and constant coagulation. This addition serves more than one purpose. During the first stage of coagulation, as mentioned below, the $CaCl_2$ lowers the pH of the milk and accelerates the rate of coagulation through the increase in enzymatic activity [32]. It is in the second stage of coagulation where $CaCl_2$ is very important, and the coagulation of the milk is dependent on the $CaCl_2$ concentration. The addition of $CaCl_2$ may make the gel firmer, making the gel less brittle and less susceptible to shatter. However, the addition of $CaCl_2$ may also cause a curd with a lower moisture content due to syneresis. [32] The addition of $CaCl_2$ will also change the salt equilibrium between the serum and micellar phases [33]. Generally, a stronger connection between pH compared to that of $CaCl_2$ is seen in regard to improved coagulation properties [20].

The effects of the addition of different amounts of $CaCl_2$ (0, 2, 4, 9, 36, 54, 72 mmol/L) on acid-rennet milk gels were investigated by Tarapata et al. [34]. The milk used for this study had a 2 % fat content and was inoculated using DVS starter culture. Coagulation ended after the samples had reached the desired pH of 4.6-4.7. At the two highest concentrations of $CaCl_2$, the gel had a more homogenous protein network and smaller pore sizes. This translates into high water holding capacity and slightly higher protein hydration, but also a lower cohesiveness of the gel. Meanwhile, the consistency and the firmness levels remained roughly constant regardless the amount of $CaCl_2$ addition. In the end it was concluded that 4 mmol/L of $CaCl_2$ is the best for acid-rennet coagulation. Cottage cheese and cream cheese are examples of products that is made using acid-rennet coagulation [35].

2.3.3.3. Lowering of pH through addition of lactic acid or lactic acid bacteria

The pH ahead of and during fermentation is of major importance to the quality of the produced cheese. As mentioned before, the optimum pH for rennet is around pH 6.0 [30], and it is very common to add lactic acid bacteria at the start of fermentation in order to reduce the pH of the milk, and therefore obtain a faster coagulation [30].

The pH of the milk at start of coagulation have been proven in several studies to be of big importance for several properties such as casein micelle size and gelling properties. Sinaga et al. [36] bring up several questions and concluded that the size of casein micelles decreased by adding acid down to pH 5.5. Around pH 5.5-5.0 however, the size increased again. The opposite effect could be seen when increasing the pH, as casein micelle size increased between pH 6.6-8.5, but decreased from pH 8.5-10.5. Changes to the size of casein micelles where reversible when restoring the milk pH to its normal level within the pH range of 6-7. It was also noted that coagulating the acidified milk created firmer gels and shortened the gelation time. The change in native casein micelle size due to pH was also noted by Glantz et al [37].

Esteves et al. [38] found in their research that the pH of the milk greatly influences the properties of rennet induced gels. When lowering the pH from 6.7 to 6.3 and 6.0, the gelation time was shortened, and the rate of which the gel firms was increased. It was noted that the G' -value decreased as the gel was ageing. This was especially prevalent in the gels using the plant coagulants but could also be seen in the chymosin gels.

As pH is decreased from optimum 6.0 to 5.7 the amount of calcium phosphate attached to the micelles has been halved. When lowering the pH even more, to 5.4, the gel firmness is decreased due to a lower amount of colloidal calcium phosphate [39].

2.3.3.3.1. Lactic acid bacteria/ lactic acid

Lactic acid bacteria (LAB) are very commonly used for production of cheese. The main function of LAB is to produce lactic acid from lactose found in the milk during the ripening of the cheese. Several different species are typically used, these include: *Lactococcus lactis*, *Streptococcus thermophilus* and other *Leuconostoc* species [40].

The primary starter culture is mainly added in order to convert lactose to lactic acid. This will in turn lower the pH of the curd. The primary starter culture is usually either thermophilic or mesophilic. The secondary microbiota is more diverse compared to the primary starter culture, as it includes nonstarter LAB (NSLAB), yeast, molds, as well as staphylococci, propioniacteria and coryneforms. This microbiota is inactive during the production of acid at the start of gelling, but active during the ripening of the cheese. The starter cultures are split into three main divisions: natural starter cultures (NSC), mixed-strain cultures (MSS) and defined-strain cultures (DSS). These are defined by the complexity of the culture and how the strain is reproduced. [40]

Natural starter cultures are produced each day at the cheese plant by backslopping. This entails the usage of an old, fermented batch to inoculate a new batch. Some cheese varieties are protected and registered as being traditional and are specifically connected to certain NSC. It is believed that a specific relationship exists between these two that enables the desired quality of the cheese. [40]

Mixed strain cultures like the natural starter cultures contain an undefined mix of different strains of bacteria, usually mesophilic or thermophilic. However, the MSS are produced under more controlled conditions and is obtained through the natural starter cultures. Nevertheless, he DSS, as the name implies, have a known strain or species composition. It was first implemented as a response to the problems arising concerning texture and variable starter activity that was found in MSS produced cheddar cheese. These types of culture strains are being implemented more and more, due to their known composition making the strains highly reproducible, something that is highly desired in the large-scale production industry. [40]

As the group of lactic acid bacteria contains bacteria of different kinds, the metabolisms of the major carbohydrate in milk, lactose, will differ depending on species and strain in the culture. Fermentation can be achieved through two pathways, the glycolytic pathway using obligatory homo-fermentative LAB such as *L.bulgaricus* and *L.helveticus* [41], where the lactose will be converted into glucose, then pyruvate and lastly converted into lactic acid. The lactic acid is the only product of this fermentation. [41] Or it can be done through the phosphoketolase pathway using hetero-fermentative LAB such as *Leuconostoc* spp [40]. During the hetero fermentation with the phosphoketolase pathway, lactose is converted into glucose, then acetealdehyde, and lastly lactic acid, ethanol, and CO_2 [40] [41].

2.3.4. Formation of the gel

After the standardization, $CaCl_2$, rennet, and lactic acid bacteria are added in order to start the coagulation [8]. The gelation is performed at 30-35 °C for 40 minutes [42] [8] [31]. The optimum temperature for rennet, around 40 °C, is not used, as the lower temperature allows for the coagulum's hardness to be controlled. [8] The lactic acid bacteria added lowers the pH of the milk as the lactose in the milk is converted into lactic acid [40]. Depending on the type of cheese produced, the pH during gelation decreases from the native pH of the milk (6.7) to around 6.5 [43]. The addition of $CaCl_2$ and the lowering of pH through the addition of lactic acid, increases the rate of hydrolysis of the κ-casein [30]. The coagulation will occur faster as the rennet reaches its optimum pH [39]. The coagulation process of the cow's milk using rennet can be divided into different stages. During hydrolysis of the κ -casein, chymosin cleaves at amino acids $Phe_{105} - Met_{106}$ [28]. The para- κ -casein is located at the surface of the casein micelle, with the hydrophobic end, amino acids 1-105. The rest of the protein, the CMP amino acids 106-169, is hydrophilic, negatively charged and protrudes into the solution. Within the first stage of coagulation, one of the enzymes of rennet, chymosin, hydrolyses the protein κ -casein. The protruding κ-casein creates a physical barrier between casein micelles, and together with electrostatic repulsion, effectively prevents the micelles from aggregating [32]. The CMP will be cleaved from the casein micelle and the para- κ -casein that is still attached to the casein micelle. This will reduce the electrostatic repulsion and in extension, the steric repulsion between micelles. The surface tension of the para-casein micelles is reduced as the Ca^{2+} ions, through electrostatic cross linkages, bind to the casein micelles. The charge of the para-casein micelles is neutralized as the Ca^{2+} ions bind to carboxylic acid groups of α – and β- caseins [32]. This is part of the primary enzymatic reaction as the micelles are getting more and more destabilized. It is during the secondary aggregation process when the destabilized micelles start to aggregate. The micelles start to form strands, and, as more strands are formed, a network is created. Large pores are formed around the thicker strands of micelles. [33] The free Ca^{2+} still left are either found in the serum or in complexes with other proteins and anions [32].

2.3.4.1. Structure of the cheese gel

The literature considers the microstructure of the curd to be a complex one. It is described as a distribution in space of its components as protein aggregates, fat and vast spaces filled by whey, being associated with a matrix. When analyzing with Scanning Electron Microscopy (SEM) (Figure 7), it can be observed that the protein structure forms a "porous" network made of the calcium phosphate para-casein. The spherical fat globules are also observed as spread through this network. The literature also mentions that it was observed that the porosity of the network increases with the increasing of rennet concentration. [44] [45] [46] Soodam et al. observed in their studies that this fact is not seen in analysis of the image ($P>0.05$) due to the high variation of data. [47] Another paper [32] found the influence of the $CaCl_2$ on the curd microstructure and the properties of the obtained gelation. Ong et al. suggest that the porosity decreases significantly ($p<0.05$) with the addition of $CaCl_2$. The samples were analyzed with confocal laser scanning microscopy (CLSM). The fat droplets are represented by the red color and the proteins are represented by green as seen in (Figure 7) [32]

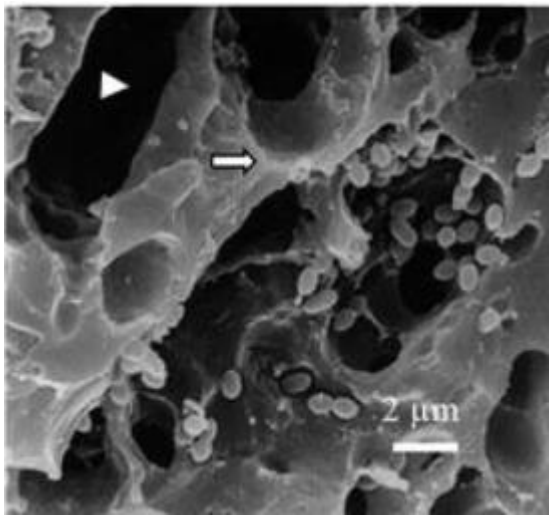

Figure 7 Scanning Electron Microscopy (SEM) [44]. The arrow shows the matrix of para-casein while, the arrowhead marks the area occupied by fat.

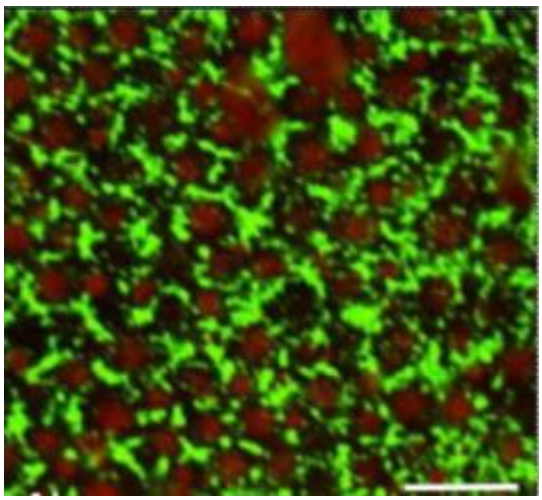

Figure 8 Confocal Laser Scanning Microscopy (CLSM). The fat droplets are represented by the red color and the proteins are represented by green [32]

2.3.5. Cutting of gel and removal of whey

After the coagulation has taken place, the gel is cut into small pieces [8]. Here the pH is around 6.5 [43]. The size of the grains is connected to the type of cheese that is produced, where the finer cut result in a lower moisture content in the cheese [8]. A healing time of 5-10 minutes is implemented after the cutting of the cheese gel, as it gives the cheese curd the time to form a thin skin on the cut edges, which gives the grains better mechanical stability [39]. Depending on the type of cheese that is being produced, the amount of whey that is removed after the cutting of the coagulum is different, but it is normal to remove 30% of the total batch volume [8]. Syneresis is the act of when whey is removed after cutting of the cheese gel. The firmness of the coagulum at the time of cutting influences the quality of the product. If the gel is too soft at the time of cutting, there is an increased loss of curd fines and fat, causing a decline in yield. If the coagulum is too hard at the time of cutting, the resulting cheese is left with a high moisture content, as syneresis is hampered. Depending on the type of cheese that is being produced, the amount of whey that is removed after the cutting of the coagulum is different, but it is normal to remove 30% of the total batch volume [8]. It is common and recommended to have a second drainage of whey after heat treatment and final stirring. [8] During this process the pH of the cheese curds continues to decrease to about 6.3 [43].

2.3.6. Processing of curd

When the whey has been removed, the cut cheese curds are pressed into molds to achieve the desired shape. This also allows for a film to form on top. This process can be done in open or closed execution depending on the level of hygiene and capacity of the lines. For the salting of the cheese, it can be performed using two different methods, either dry salting or brine salting. For dry salting, a controlled amount of salt is added to the curd before pressing. Brine salting utilizes a pool containing a brine solution. The already pressed cheeses are submerged in the brine solution for a set time. The brine solution must be kept under controlled conditions to ensure the quality of the solution. Using brine solution with <16% salt raises the risk for microbiological disturbances. [8].

After the salting, the cheese moves to ripening, where the cheese goes through several physical, microbiological, and biochemical changes. During ripening, both lactose and protein degradation will occur, as well as fat lipolysis. Temperature during ripening and time is very much dependent on the cheese type. Some cheeses are wrapped in film or bag during ripening. After months to years, of maturing and a pH of around 5.3 and above [43], the cheese is ready for packaging and distribution. [8]

2.5. Processes flow diagram

For a better understanding of the cheese making process, a simplified flow diagram was designed as presented in Figure 9.

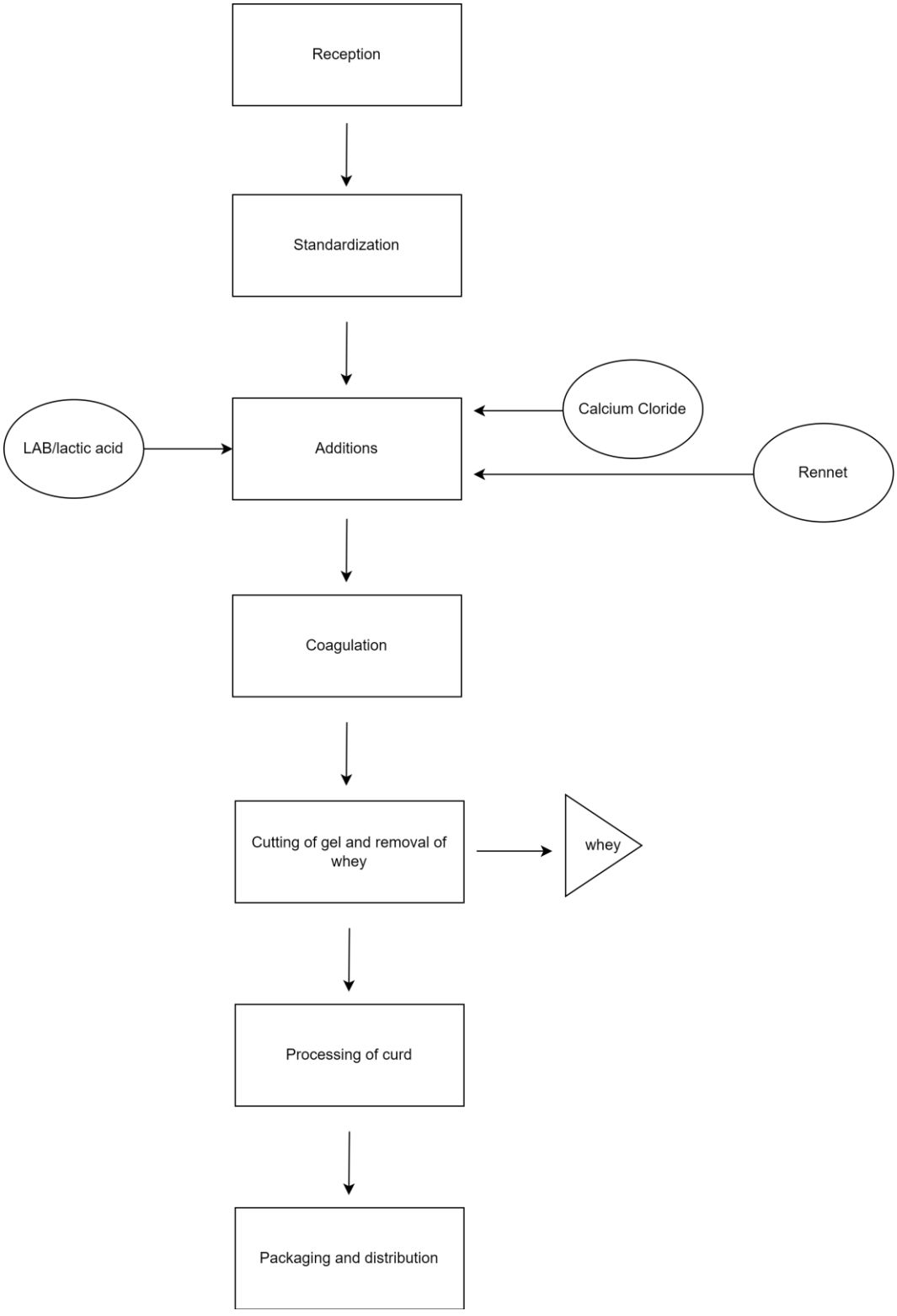

Figure 9 Simplified figure of the flow diagram for the cheese making process.

2.6. Rheology

Understanding the fluids' flow and the matter's deformation represents the science of rheology [48] [49], the word stemming from the Greek word of "rhei" [50] which means "to flow". The first definition of rheology as "The study of the deformation and flow of matter" [48] was accepted in the USA in 1929. This field is important in order to understand the products' flowing behaviour and to be able to define the unit operations and equipment needed. As a result, knowing the structural and textural details of a product, a positive impact could be achieved regarding the quality control of food. [49] The strain and the stress are the important variables for the understanding of deformation of a material after force was applied to it. The strain refers to the change in the length, while the stress refers to the force's magnitude on the application surface.

Since the 17th century, scientists have tried to describe these phenomena. The law of Hooke provides the link in the relationship between strain and stress. According to Hooke's law, a material is defined as linear elastic, but it does not flow. Later, Isaac Newton gave more attention to fluids. There are different types of flowing fluids classified by behaviour as: Newtonian, non-Newtonian, shear thickening, pseudoplastic and Bingham plastic. There were also other models proposed, showing other behaviours, such as rheopectic or thixotropic. All liquids are considered a dispersion of molecules with different sizes. In the moment where the applied force creates motion, those molecules are sliding, developing resistance when flowing and interacting with each other. A larger resistance between molecules creates higher viscosity values. For rheometric analyses, there are rotational viscometers or oscillatory rheometers can be used. While a rheometer can run different tests such as uniaxial tensile and oscillatory, a viscometer can run viscosity tests such as rotation. [48] [49] [50]

The shear stress, τ, is defined by the shear force (F) into a specified area (A) being measured by a rheometer and 1 stress unit being equivalent with 1 Pa. Meanwhile, the shear strain or deformation, γ, is defined as the ratio between the deflection path (s) and shear gap (h). The shear strain is dimensionless and usually has the value written as a percentage. The shear modulus, G, is defined as the ratio between τ and γ. In order to test the shear, the easiest way is to use the 2-plates model, which can also also used for measuring the viscoelastic behaviour by using oscillatory tests. As an illustration of the method there are 2 parallel plates (as in Figure 10), with the upper one presenting a wheel for driving and a rod for pushing. The upper plate deflections can be found at different angles, δ, from 0° to 360°. Originating from this, the complex shear modulus, G*, is the ratio between shear-stress amplitude (τ_A) and strain amplitude (γ_A). The shear modulus elastic component or the storage modulus, written as G', measured in Pa [38] [48] [49] [50] (the stress divided by the strain in sinusoidal conditions), is described as the elastic portion of the viscoelastic behaviour. The shear modulus viscous component or the loss modulus written as G'', measured in Pa, is described as the viscous portion of the viscoelastic behaviour. [50]

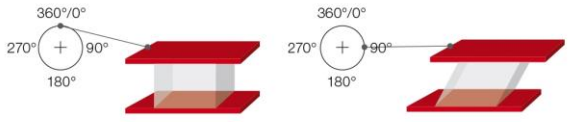

Figure 10: 2 parallel plates method [50].

Usually, the milk's behaviour before coagulation from the rheology point of view can be influenced by different factors impacting directly the outcoming product. G' is one of the is one of the parameters who indicate the coagulation properties as the time needed for coagulation, the rate of aggregation and the firmness of the curd [51].

2.6.1. The Rheometer

In order to observe the rheological properties of the milk with different additions of $CaCl_2$ and different starting pH, a rheometer was used (Kinexus PRO). A rheometer station consists of different elements, the rheometer as the measuring device, a computer for controlling the device and checking the results, and an environmental controller cartage which houses the slot for the lower geometry as it is explained in figure 11. The last component is the heat exchanger which ensures the right temperature of the samples. The rheometer is composed of the head which is held by the crossbar and contains a motor (air bearing). From the head, a chuck is found as a slot for the upper geometry and functions to secure the upper geometry. Near the head there is a keypad for a smoother control. On the lower part there is the cartridge securing the lower geometry, and underneath, its lock as it is shown in Figure 12. [52]

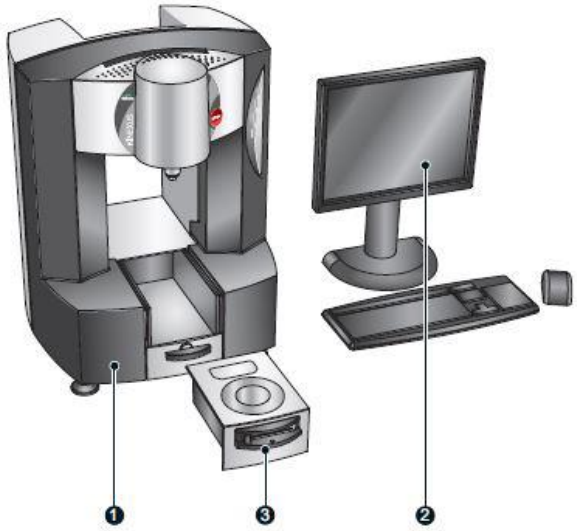

Figure 11: Rheometer Unit: 1. The Rheometer Device, 2. The Controlling Computer 3: Environmental Controller Cartridge [52].

Figure 12: Rheometer device: 1. Head, 2. Chuck, 3. Upper geometry, 4. Lower geometry, 5. Cartridge [52].

2.7. Turbiscan

It was observed that a luminous beam creates a highlight spot which is composed of 2 photon elements (long path and short path) which are backscattered when a sample (considered thick dispersion) is introduced in a glass recipient for measuring. [53] The Turbiscan as a device measures the transmission of light through a cuvette filled with sample. The milk is a very turbid fluid, so it is impossible for photons to travel through the sample. The analysing unit is a compact one, formed by the device connected to the computer. The device manual presents what the sample in the cuvette should look like before the start of analysis (Figure 13).

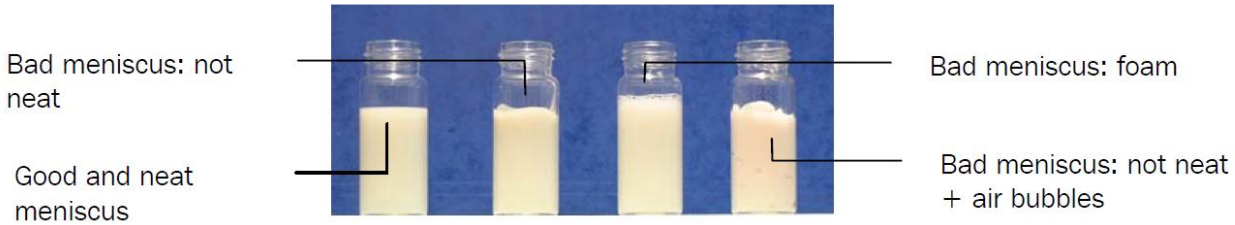

Figure 13: Examples of samples in cuvette exemplifying different types of meniscuses [53].

The measurement is done with light provided by a diode which is electro luminescent, with a wavelength of $\lambda = 880$ nm. The light is sent through the sample and is received by 2 optical sensors that are synchronized. The optical sensor for measuring backscattering is positioned at 45°, while the sensor measuring the incident light for transmission is positioned at 180° as it is presented in Figure 14. [53]

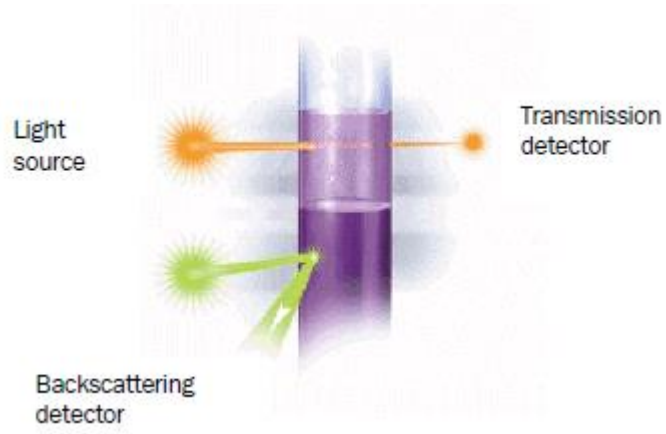

Figure 14: Turbiscan Lab Principle [53].

2.8. Particle size analysis

One of the most important elements in maintaining the quality of a product is connected to the particle size and their distribution [54]. It is proven that smaller casein micelles form a stronger gel [37]. As it was mentioned before, the average dimension of the milk fat globules is about 4 μm. Also, as it was discussed before, the cheese formed with smaller fat globules has more water retention than the cheese formed with bigger fat globules [20]. There are different ISO references created for determining the sizes. There are also different ranges to measure these sizes (from nm to mm). The goal and the challenge of the analysis is to determine a single value for the size of a 3D object. Some of the most popular methods include: laser diffraction, dynamic light scattering, sedimentation, electrozone sensing as well as Image analysis and sieving [54].

In order to determine the size of the particles found in milk samples for this thesis, a device called Mastersizer 2000 was used. This device uses the light scattering method. To understand the light's behaviour, the device uses the "Mie theory". This theory works to predict behavior of the light and the laser when it meets spherical particles. For this method it is important to have information on the sample such as adsorption and refraction index. The analyser contains 3 different key units: the optical bench described in figure 14, the unit for the sample dispersion, and computer unit. The raw data from the milk sample is collected through the optical bench, and the sample is loaded through the dispersion unit. Attached to the dispersion unit is an RPM controller used to set the speed of the mixer. The computer system is represented by a computer running the device manufacture's software. The bench has different components including the protection cover for the cell area. The protection cover prevents any obscuration from dirt or dust to occur. The protection window is located next to the protection cover and cell area and is there to protect internal components. The cell is used to connect the dispersion unit, where the sample is loaded, to the bench. The cell contains two windows that allow the laser beam to go through the cell and analyse the sample. Other components of the bench include the cell holder, window tool, backscatter material, power indicator, and an end panel. [55]

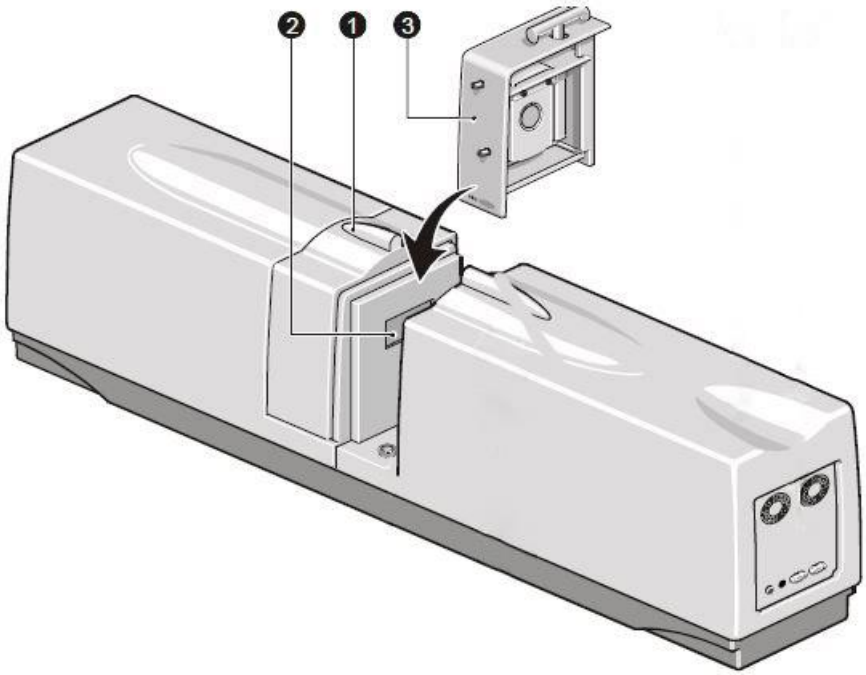

Figure 15: The bench 1. Cell area protection cover, 2. Protection window, 3. Cell [55].

2.9 Composition using IR

It is of importance to ensure that the milk used during production of cheese contains the minimum of required components, such as protein and fat quantity [56]. Any deficit might be translated into a product that fails to prove its authenticity. To meet this requirement, different methods were developed, but most of them are lengthy, hard to apply, and mainly impossible to be used in a routine [56]. One of the most convenient methods is the Fourier transform infrared spectroscopy (FTIR) method. It is viewed as a "daily routine" in the milk industry, due to its simplicity and economic sustainability, as only a small quantity of sample is used to perform the analysis [57].

To analyse the composition of milk samples during this thesis project, the device MilkoScan^{TM} was used. It is described as presenting "ready-to-use calibrations" for controlling different types of dairy samples such as milk, cream, or whey. It can analyse fat, protein, lactose, total solids (TS), non-fat solids, and just for the milk samples, the freezing point. The device works in a large range of ambient temperatures and presents a wide measuring range (0-48% for fat, 0-6% for protein, 0-6% for lactose, 0-50% for total solids and 0-12% for non-fat solids). [58]

3. Materials and methods

3.1. Materials

Åsens lantmjölk Orginal (1.7-1.9 % fat) (Skånemejerier AB, Malmö, Sweden), Åsens lantmjölk Gammaldags (2.9-3.1 % fat) (Skånemejerier AB, Malmö, Sweden), Lactic acid 90% (VWR, Radnor, Pa, United States), $CaCl_2$ powder (Sigma-Aldrich, St. Louis, MO, United States), Rennet 0.45 mL/L (Chy-Max Plus, 202 international milk clotting units (IMCU)/L, Christian Hansen A/S, Hørsholm, Denmark), Allegra X-15R Centrifuge (Beckman Coulter, Brea, CA, USA), Kinexus PRO (Malvern Instruments Ltd, Worcestershire, UK), Turbiscan Lab (Formulaction SA, L'Union, France), Mastersizer 2000 (Malvern Instruments Ltd, Worcestershire, UK), Milkoskan (FOSS analytical A/S, Hillerød, Denmark), Minitab21 (Minitab, Pennsylvania USA), MATLAB (MathWorks, Massachusetts USA), Calcium electrode 9720-BNWP (Thermo Fisher Scientific Inc), pH electrode (Metrohm AG, Switzerland), Water bath, 50mL test tubes, 200 µL micropipette, 20 mL glass pipette, Peleus ball.

3.2 Preparation

3.2.1. Preparation for the Response Surface Method trial

The following steps were performed to prepare the samples for the Response Surface Method trial. First, the milk is introduced into a test tube and then centrifuged (section 3.3.4). The Ca^{2+} concentration was then measured in mV using a $CaCl_2$ electrode (section 3.3.6). $CaCl_2$ was then added according to the schedule presented in Table 2 and remeasured. Following this step, the pH is adjusted using lactic acid (section 3.3.7) according to the schedule presented in Table 2. The test tube was then kept for a minimum of 30 minutes in a 32°C water bath.

3.2.2. Preparation for the Effect of fat on gelation-trial

The following steps were performed to prepare the samples for the Effect of fat on gelation-trial. First, part of the milk was centrifuged (section 3.3.4). The sample milk was introduced in a test tube and lactic acid was added (section 3.3.7) under constant agitation in order to adjust the pH, so that all samples had a constant pH 6.7. The test tube was then kept for a minimum of 30 minutes in a 32°C water bath.

3.3. Methods

During this project, two trials were performed, the Response Surface method trial and the Effect of fat on gelation-trial. During the Response Surface method trial, two factors were varied, the pH and addition of $CaCl_2$. This was done to investigate the impact of changing these factors and how they might interact. For the Effect of fat on gelation-trial, the effect of fat content and the presence of fat was investigated. Two types of fat content if the milk was used, in combination with skim milk and full fat versions of these fat contents. These trials are explained in more detail in the following sections.

3.3.1. Response Surface method trial

As explained briefly earlier, in the Response Surface method trial, the pH and addition of $CaCl_2$ to the milk samples was varied to establish the effect of these factors and if they are statistically significant. The Response surface method was created using Minitab21, which enables the

simultaneous screening of several factors, while minimizing the number of runs that needs to be performed. Generated 3D plots give insight as to how the different factors correlate. [59]

In Table 1 below, the high and low values of the two factors, pH and $CaCl_2$ are presented. It is between these values that the factors are varied. The amounts of $CaCl_2$ added (1.0-10.0 mmol/L) is translated to 10.8 g – 108 g of $CaCl_2$ per 100 kg of milk ($1.08 \cdot 10^{-4}$ – $1.08 \cdot 10^{-3}$ %)

Table 1 The low and high values for the two factors (pH and CaCl2) in the Response Surface Method trial are presented.

Factor	**Low**	**High**
pH	5.5	6.7
$CaCl_2$ [mmol/L]	1.0	10.0

In total 28 runs were created over two blocks, with 14 runs in each block. Block 2 contains the replicates of the samples run in block 1. These 28 runs were divided over 4 days. The duplicates of day 1 is represented by those on day 3 and duplicates of day 2 were run on day 4. Duplicate were run on different days to the original sample to account for any differences between days when the samples were investigated. During day 1 and day 2, the Åsens lantmjölk Gammaldags (2.9-3.1 % fat) was used, where the fat has been removed through centrifugation. As for day 3 and day 4, another carton of the same Åsens lantmjölk Gammaldags (2.9-3.1 % fat) milk was used. The runs and the values for pH and $CaCl_2$ used for each day, as provided through the Response Surface Method, can be found in Table 2. This method enables a smaller samples size to be used as it does not test every combination possible for these two factors. All samples are numbered after their running order and at which day the sample was run, so, the first sample of day 1 is sample S1,1. This was done in order to look at specific day and their running order to determine why, if any inconsistencies between samples of the same duplicate could be seen. There are two identical versions of each sample, one run in the Turbiscan, and one run in the Mastersizer and Rheometer. The methods of the Turbiscan, Mastersizer and Rheometer are described further below along with the trial set up for the Response Surface method trial.

Table 2: The table presents the pH value and amount of added $CaCl_2$ for each duplicate and each sample during the 4-day Response Surface Method trial.

Duplicate	**Sample**	**pH**	**$CaCl_2$ [mmol/L]**
1	S1,1	6.1	5.5
	S3,3		
2	S2,1	6.5	8.7
	S5,3		
3	S3,1	6.5	2.3
	S4,3		
4	S4,1	5.7	8.7
	S2,3		
5	S5,1	6.1	5.5
	S6,3		
6	S6,1	5.7	2.3
	S1,3		
7	S7,1	6.1	5.5
	S7,3		
8	S1,2	6.7	5.5
	S4,4		
9	S2,2	6.1	5.5
	S1,4		
10	S3,2	5.5	5.5
	S6,4		
11	S4,2	6.1	1.0
	S7,4		
12	S5,2	6.1	5.5
	S2,4		
13	S6,2	6.1	5.5
	S3,4		
14	S7,2	6.1	10.0
	S5,4		

3.3.2. Effect of fat on gelation-trial

In order to look closer at differences in milk with different fat content the Effect of fat on gelation-trial was created. Two types of milk were used for this comparison, Åsens lantmjölk Orginal (1.7-1.9 % fat) and Åsens lantmjölk Gammaldags (2.9-3.1 % fat). For each type of milk, one skim milk

version was created through centrifugation, using the same method by Gustavsson et al. [60] as mentioned in section 3.2.8. In Table 3 below, the two types of milk, with their skim milk version is presented. Each sample is given a specific name to help differentiate between samples and their characteristics. As in the Response Surface Method trial, there are two identical versions of the same sample, where one is run in the Turbiscan and the second one in the Rheometer and Mastersizer. A M or SM is added to the name of the sample, representing milk and skim milk respectively. The milk sample contain fat and the skim milk sample do not contain any fat. The first number in the sample name represents the fat content of the milk sample, so the Åsens lantmjölk Orginal (1.7-1.9% fat) is represented by the number 2 and Åsens lantmjölk Gammaldags (2.9-3.1 % fat) is represented by the number 3. The very last number of the sample name represents if it was the first or the replicate run for this specific sample.

Table 3 The table describes the name for each sample during the Effect of fat on gelation-trial dependent on 4 factors, the fat content of the milk, if the sample contain any fat or not, if the sample is run in the Turbiscan or Rheometer and the samples order.

	Turbiscan	**Rheometer**
Milk 2%	SM 2,1	SM 2,1
	SM 2,2	SM 2,2
Skim milk 2%	SSM 2,1	SSM 2,1
	SSM 2,2	SSM 2,2
Milk 3%	SM 3,1	SM 3,1
	SM 3,2	SM 3,2
Skim milk 3%	SSM 3,1	SSM 3,1
	SSM 3,2	SSM 3,2

The samples of this comparison had no addition of calcium chloride, in contrast to the Response Surface method described in section 3.2.4. The pH for all samples were adjusted to 6.7 if the sample in question had a pH that differed from this number initially. This was done in order to remove differences in the pH of the milk samples, as they differed between 6.7-6.9 in pH. Only two samples did not receive an addition of 5% lactic acid, this being both versions of sample SSM 3,1. This is due to the pH of these samples being 6,74 initially. The samples were run on the Turbiscan as well as the Rheometer and Mastersizer according to methods presented in sections 3.2.1, 3.2.2 and 3.2.3 respectively.

3.3.3. Response surface method (Minitab)

A response surface method was created using Minitab 21 for the Response Surface method trial. This was done by creating a new project in the file tab. In the Stat tab, DOE is selected, then Response Surface and Create Response Surface Design. When creating the Response Surface Design, the central composite type of design was used with 2 continuous factors. This can be seen in Figure 16.

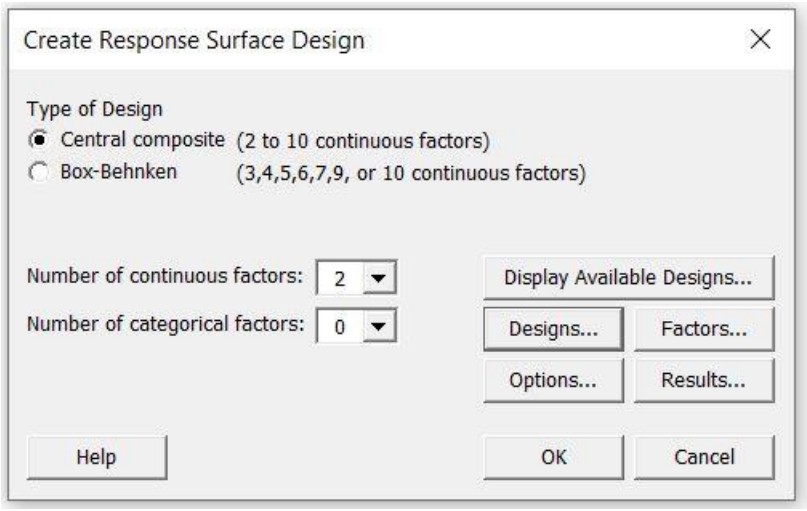

Figure 16: Minitab screen creation of Response Surface Design

Next go to design. A full run with 14 runs divided into two blocks is chosen together with number of replicates being 2. The rest of the settings can be set at default. This can be seen in Figure 17.

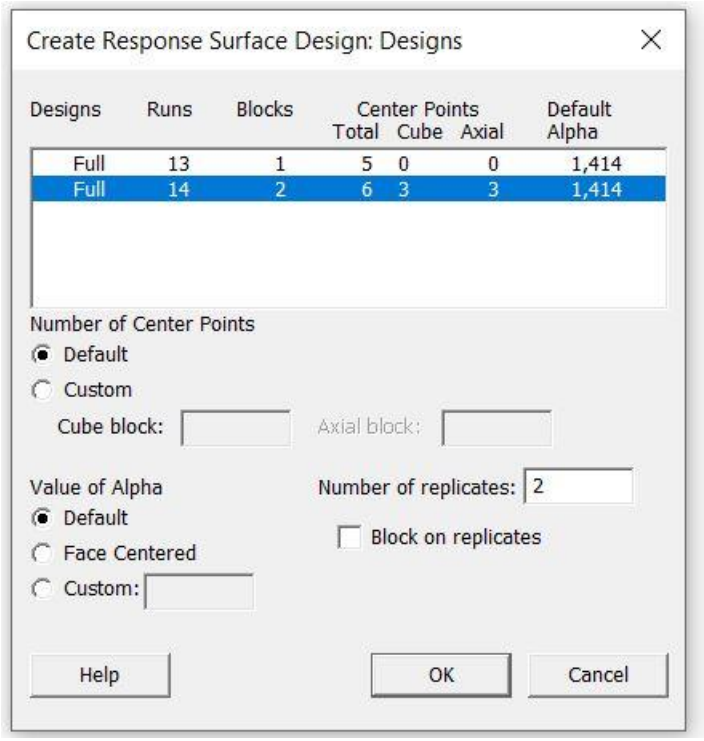

Figure 17: Minitab screen creation of Response Surface Design choosing details

Then the factors are address. For Levels Define, axial points were chosen to ensure that values between the highs and lows of factor A and B were tested, which makes it possible to study potential curvature in the effect of pH and $CaCl_2$. Regarding the factors, two factors were altered during these trials, the pH of the milk ahead of addition of rennet, as well as the addition of $CaCl_2$. The names are added to each factor (pH and $CaCl_2$) and the high and low values, seen in Table 1 are added. These settings can be seen in Figure 18.

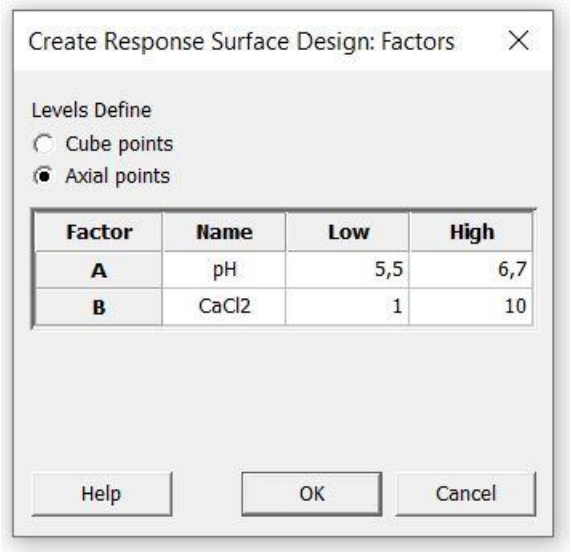

Figure 18: Minitab screen creation of Response Surface Design setting up the factors

3.3.4. Centrifugation (Centrifuge)

According to method by Gustavsson et al. [60] the raw milk was centrifuged at 2000 × g and 4 °C for 30 min. The fat was then separated from the milk from the solid fat by pouring the skim milk from the centrifugated tube. The composition was checked immediately afterwards using the Milkoscan, as described in section 3.3.5.

3.3.5. Milk composition using IR (Milkoscan)

To perform the analysis of skim milk samples, the device was first cleaned using its own cleaning program. From there the "Milk" program is selected and by pressing start, the device's pipette takes 10 mL of sample to perform the analysis. If the samples contain a higher fat content, the sample need to be heated to perform the analysis. This measure was taken in order to make sure that all the fat is in liquid state lowering the risk of clogging the device.

3.3.6. Calcium ion concentration (Calcium electrode)

In order to determine the quantity of free Ca^{2+} ions that are present in the milk samples before and after addition of $CaCl_2$, a calcium electrode is used. The milk was taken out of the fridge and measured after adjusting to room temperature. An addition of $CaCl_2$ was then made and the sample was again measured after mixing the $CaCl_2$ and milk. It was noted during measurements that the temperature of the milk at the time of measurement greatly affected the results. Therefore 5 new samples were created, using the skim milk created from Åsens lantmjölk Gammaldags (2.9-3.1 % fat). The concentrations used are all used during the Response surface trial (section3.2.4). This includes the concentrations of 1.0 mmol/L, 2.3 mmol/L, 5.5 mmol/L, 8.7 mmol/L and 10.0 mmol/L. The milk used here originates from the same package as the milk used for the comparison of fat and non-fat milk (section 3.2.9). 30 mL of skim milk was poured into tubes and left in a water bath at 32 °C for 30 minutes. The samples are then removed from the water bath and the Ca^{2+} concentration was measured. An addition of $CaCl_2$ was made and after agitating the tube, the Ca^{2+} concentration was measured again. This trial removes the uncertainty stemming from the impact of milk temperature at time of measurement.

A calibration curve was also created in order to determine the concentration of Ca^{2+} before and after the addition of $CaCl_2$. According to the Calcium electrode Standard Operating Procedure (SOP), the following steps were performed:

1. 22.5 mL of Milli-Q Water was mixed with 2.5 mL of 0.1 M standard (10^{-2} M)

2. 2.5 mL of the previous solution was added with 22.5 mL of Milli-Q water in a new container (10^{-3} M).

3. Step two was recreated two more times in order to create standard solutions with the concentrations of 10^{-4} M and 10^{-5} M. 2.5 mL was removed from the standard solution with 10^{-5} M concentration in order to have the same volume in all solutions.

4. 0.45 mL of ISA solution was added to all solutions.

4. The standard solutions were put in a water bath at 32 °C for 15 minutes for the solutions to reach the appropriate temperature.

5. All solutions were measured in mV using the calcium electrode, starting with the lowest concentration among the solution (10^{-5} M) and finishing with the solution with the highest concentration (10^{-2} M)

An equation was created using linear regression: $y = 3.1358546 \cdot 10^{-4} \cdot X - 0.015253664$, where X is the measured value in mV. From here it is possible to calculate the concentration of Ca^{2+} ions in the milk before and after addition of $CaCl_2$.

3.3.7. pH determination (pH electrode)

In order to adjust the pH of the milk before coagulation occurs, the pH before adjustment was determined, as well as the pH after adjustment. The standard buffer solutions used to calibrate the electrode had the pH of 4, 7 and 9. The pH was adjusted after the addition of $CaCl_2$ according to the schedule presented in Table 2 using lactic acid at 5%. The lactic acid was diluted from 90% to 5% by adding water. After the pH of the sample had been adjusted, the sample was put into a water bath for a minimum of 30 minutes to allow the samples to adjust and reach the desired temperature of 32 °C.

3.3.8. Particle size analysis (Mastersizer)

In order to start the analysis, it is necessary to rinse the cell through the dispersion unit with Milli-Q water. After cleaning Milli-Q water is again added to the disruption unit and the mixer is set to 1500 RPM. It is desirable to have the laser intensity around 75% and 2 detectors under a certain level (detector no 1 under 150 and detector no 20 under 20), which is checked on the software. The background containing only Milli-Q water is then measured. This is done by doing a manual measurement. Here the name of the sample is edited, and the refraction index is changed to either fit the casein micelles at 1.57 (for all milk samples without fat) or the milk fat at 1.463 (for all samples containing fat). The software will then request the addition of a sample and confirmation to start the measurement. For measurements made with samples that do not contain any fat, a laser obscuration of 5% was used. For samples containing fat, a slightly higher laser obscuration level was used, around 6-7 %. The results of the measurements were presented as histograms of different particle diameter and a frequency curve, both displaying the concentration of the particles at different sizes. Also, the report shows the weighted residual which should be under 1% in order to have the confirmation of a good measurement. For milk samples containing no fat, the obtained distribution graphic was cut having the maximum value of 0.56 μm. This action was performed in order to obtain the dimensions just for the casein micelles, excluding the values from any fat or undissolved $CaCl_2$. For samples containing fat, a cut was made to the graphic distribution. The zone of interest was between 0.9 μm and 15 μm. This is due to the interest in these samples of other components present in the milk samples, and not only the casein micelles. For both types of samples, the interest was on value of "Volume Weighted Mean" also named the "Diameter of Mass Moment

Mean" (D[4,3]). This value, also called "De Brouckere mean diameter" which can be described as the middle point in the histogram. [61] [62]

3.3.9. Formation of gel (Rheometer, Turbiscan,)

The software used in operating the rheometer is called rSpace and is used to control the device and to record the obtained data. A standard procedure is used each time when turning on the device. The air supply to the device is turned on as well as the device itself. After starting the device, the upper and lower geometries are installed. The software then starts the initialization, measuring the zero gap. After this, it is required to set the temperature to 32°C. To initialize the loading of the sample, the "ADD SAMPLE" from the software's menu is used. 13 µL of rennet is added to 30 mL of milk, according to method by Gustavsson et al [60]. 17.6 mL of this samples is then added to the lower geometry. After confirming that the sample is loaded, the thermal cover is placed over the lower geometry and the analyse program can start. The program measures every 10 seconds for 42 minutes and provides several outputs, among them being G', G'' and tan δ . However, for this analysis, the focus will be on G'. A model of outcome result is presented by the graph from Figure 19. After the program is done, the sample is unloaded, and the geometry cleaned. For this project, the G' at 2 times gelation time is also important. To determine it, the gelation time is necessary to be determined, then that value doubled. Then using the double gelation time value, the G' value can be found in the results table generated by rSpace.

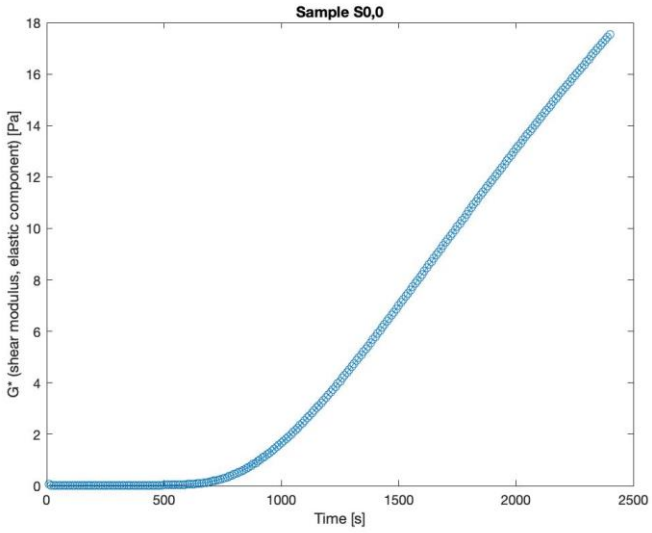

Figure 19: Example of Rheometer result for the reference sample, no adjustment, no CaCl

For the gel formation analysis, the "Turbiscan Lab" was also used. The devices and its accompanying computer are both turned on and the Turbiscan software is started. The temperature of the device was set to 32 °C. According to the same method by Gustavsson et al. [60] 13 µL of rennet was added to 30 mL of milk. The sample was agitated and then added to a glass cuvette. The cuvette was then added to the device and a smart program was started. This program measures the sample every 25 seconds for 40-45 minutes. The results are then exported into the design software on the computer, where the backscattering is of most interest for this analysis. As result example there are Figures 20 and 21.

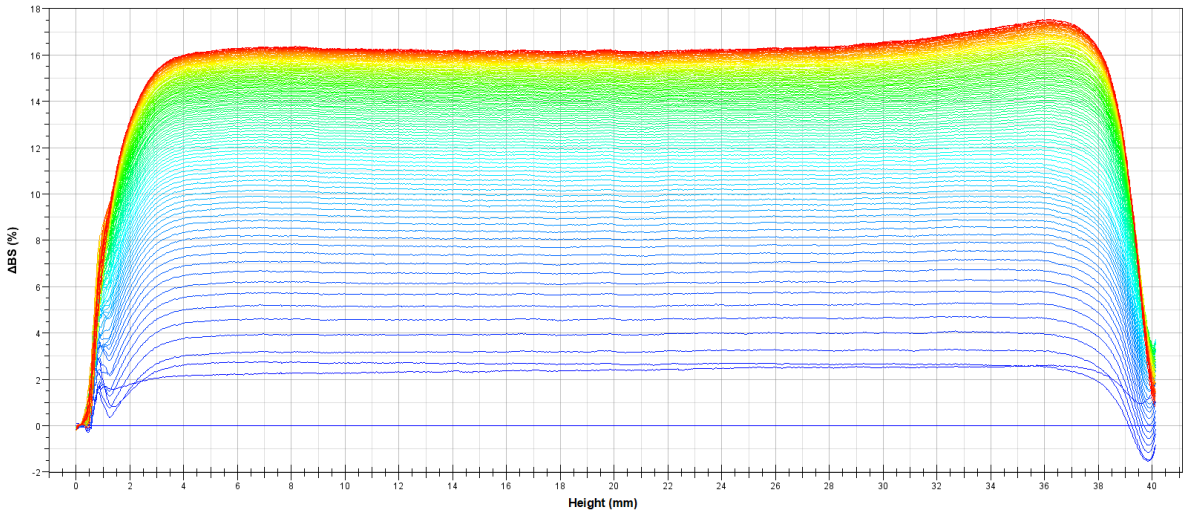

Figure 20 Obtained result ΔBS (%) vs Heigh (mm)

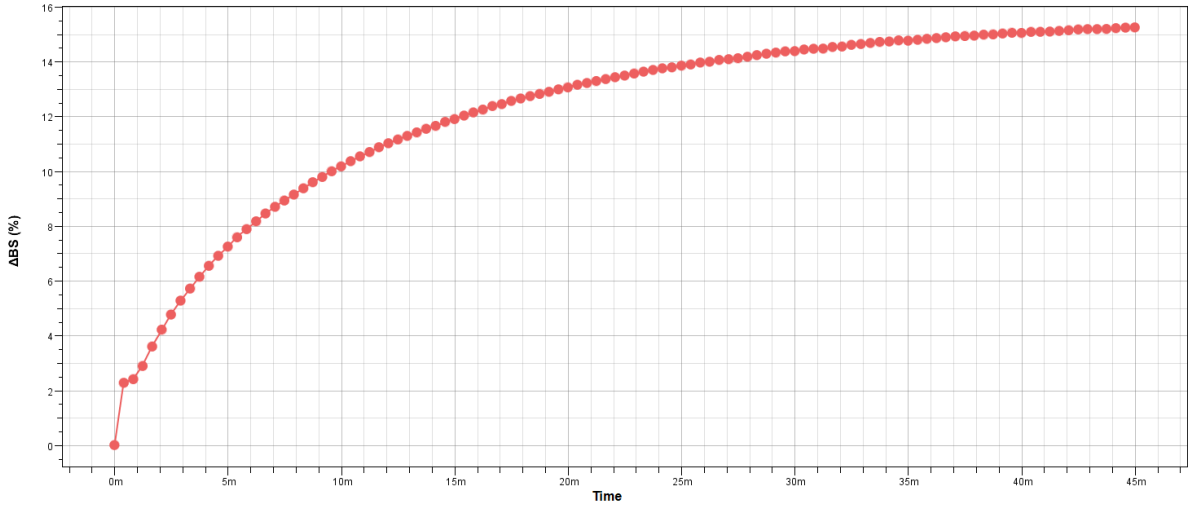

Figure 21 Obtained result of average ΔBS (%) vs Time (min)

3.3.10. Statistical methods

3.3.10.1. Pairwise Pearson Correlation (Minitab)

After response surface was established as it was shown above, the Pairwise Pearson Correlation was obtained as well with Minitab21. In order to obtain that the steps are: "Stat" > "Basic Statistics" > "Correlations…". In the new appeared window, the variables are selected and then at the Results… menu, "Pairwise Pearson Correlation" has to be ticked and then confirmed by "Ok". A final "Ok" is required in order to obtain the correlation in the software's output section.

3.3.10.2. 2-sample t test (Minitab)

For the 2-sample t test, Minitab21 was used. In order to obtain that the steps are: "Stat" > "Basic Statistics" > "2-Sample t…". In the new opened window, it is needed to choose the column for "Samples" and the column for "Sample IDs". It is necessary to have "Both samples are in one column". From the "Options" submenu, the confidence level and the alternative hypothesis has to be selected and from the "Graphs…" submenu, "Boxplot" has to be ticked. A final "Ok" is required in order to obtain the correlation in the software's output section.

3.3.10.3. Average and standard deviation

In order to determine the average and standard deviations for duplicates A-D in the Effect of fat on gelation-trial equation 1 and 2 were used respectively. $\bar{x}$ is the average of each duplicate, x the sample of a specific duplicate and n is the number of samples in each duplicate.

$$\bar{x} = \frac{\sum x}{n} \quad (1)$$

σ in equation 2 is the standard deviation within a duplicate.

$$\sigma = \sqrt{\frac{1}{n}\sum (x - \bar{x})^2} \quad (2)$$

4. Result and Discussion

4.1 Milk ahead of trial start

In this section, the content of fat, protein, lactose, solids non-fat (SNF) and total solids (TS) of all milk used in the Response Surface Method trial and the Effect of fat on gelation-trial, along with the Ca^{2+} concentration of the milk before and after addition of $CaCl_2$ used in the Response Surface Method trial. The particle size of the of casein micelles and fat globules in the skim milk and full fat milk used during both trials is also presented. This is done to determine if there are any initial differences with the milk that could have an impact on the achieved results. The initial pH of the milk samples were not recorded and the adjusted pH match the values presented in Table 2.

4.1.1. Response Surface method trial

4.1.1.1. Milk content

For the Response Surface method trial, two cartons of the same milk, Åsens lantmjölk Gammaldags (2.9-3.1 % fat) were used. Below in Table 4, the content of fat, protein, lactose, solids non-fat (SNF) and total solids (TS) of the skim milk used in this trial for both milk carton 1 and milk carton 2 are presented. As seen in the table the differences in the interest parameter categories are minimal, indicating that at the start of this trial, both cartons of milk are equal and any differences in the following result should not be due to the initial milk used. It was almost impossible to remove all of the fat from the centrifugation tubes as small parts of the solid fat on top would break apart and follow the skim milk out of the tube. It was deemed that this fat content was acceptable, due to the inability to remove all of the fat using the method mentioned in the Materials and Methods, as well as the low-fat content in comparison to the full fat milk.

Table 4 The content of fat, protein, lactose, solids non-fat (SNF) and total solids (TS) for the two milk cartons used during the Response Surface method trial.

Type	Fat [%]	Protein [%]	Lactose [%]	SNF [%]	TS [%]
Skim milk 3% Carton 1	0.175	3.44	4.66	8.97	9.25
Skim milk 3% Carton 2	0.179	3.42	4.69	8.98	9.27

4.1.1.2. Calcium chloride addition

As the milk during the Response Surface method trial had been centrifugated and the contents of the milk had been established and determined sufficient, an addition of $CaCl_2$ was performed. In Figure 21, the concentration [mM] of free calcium ions (Ca^{2+}) before the addition of $CaCl_2$ (0 mmol/L added $CaCl_2$) and after addition of $CaCl_2$ (1.0, 2.3, 5.5, 8.7, 10.0 mmol/L added $CaCl_2$) can be seen. 5 sample tubes containing 30 ml of milk were used, where one addition was added to one tube. Therefore, the Ca^{2+} concentration before addition was measured to establish a baseline for each samples tube. The black * seen in Figure 22 is the average of the Ca^{2+} concentration for all five samples before addition. An error bar was added to this point to demonstrate the standard deviation. It was unexpected that not all samples had the same Ca^{2+} concentration before additions started, as the same milk was used for all sample tubes. It was noted during the Response Surface Method trial that the temperature of the sample during analysis had a big effect on the result. Therefore, each sample was heated to 32 °C to mitigate this effect, but some differences are still noticed. Regardless of starting concentration for the samples, it is evident that the highest addition of $CaCl_2$ (10 mmol/L)

results in the highest Ca^{2+} concentration and the lowest addition of $CaCl_2$ (1 mmol/L) resulted in the lowest Ca^{2+} concentration. It is also noticeable that the response is not linear, as the absolute Ca^{2+} concentration does not increase between 8.7 mmol/L and 10.0 mmol/L. This could be due to that not all of the added $CaCl_2$ can be found as Ca^{2+} but could bind to the casein micelles in the milk or to other complexes with mainly citrate.

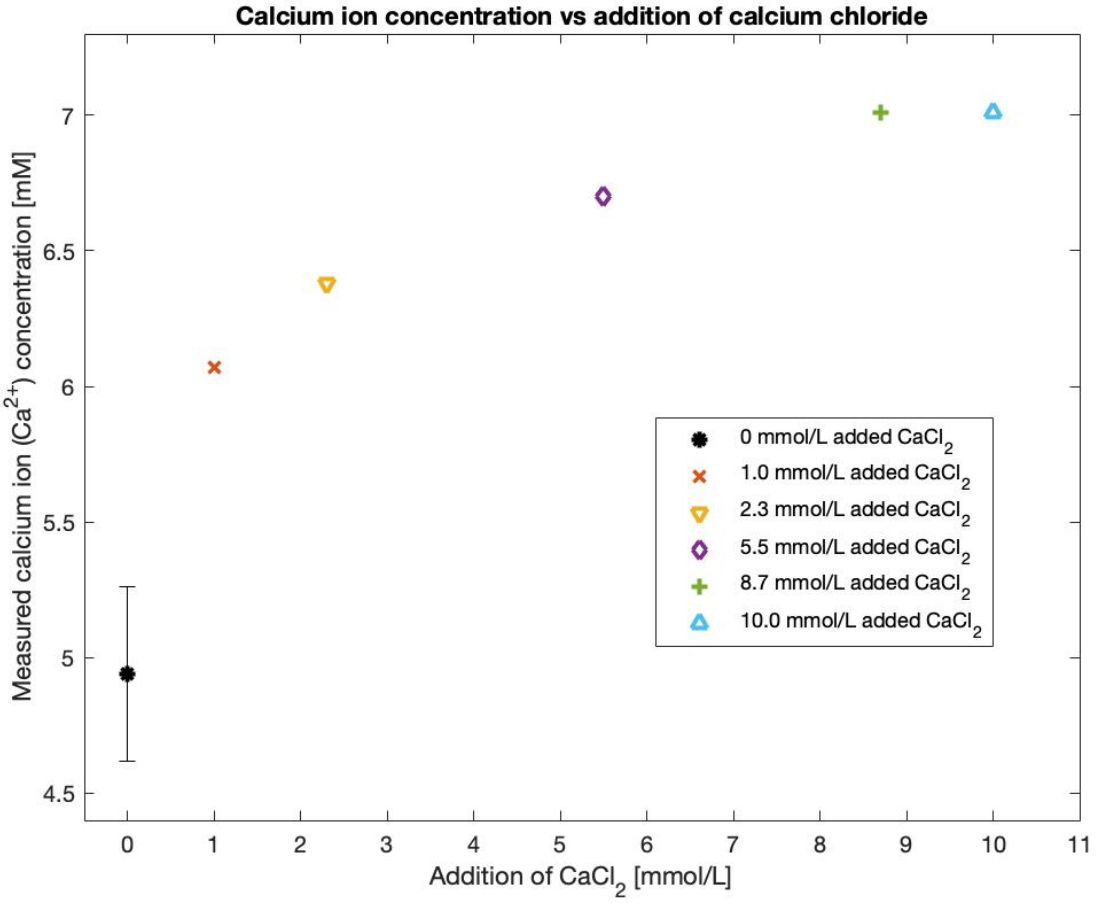

Figure 22 Calcium ion concentration vs addition of CaCl2. Black ∗ represents the average Ca^{2+} concentration of the milk at 0 mmol/L (before addition), with error bar indicating the standard deviation. × represents addition of 1.0 mmol/L, ∇ represents addition of 2.3 mmol/L, ⋄ represents addition of 5.0 mmol/L, + represents addition of 8.7 mmol/L and Δ represents addition of 10.0 mmol/L.

4.1.1.3. Particle size

Figures 23 and 24 describe a result obtained from the Mastersizer2000 device on skim milk. In Figure 23, there are 3 noticeable peaks, the first one representing the casein micelles, the second one representing some remaining fat globules and the third one undissolved $CaCl_2$. As it was described before, in order to obtain the size distribution for just the casein micelles the graph was cut, creating a graph with a smaller particles size range. From this cut, it was possible for the software to obtain the d[4,3] value just for the casein micelles seen in Figure 23. The obtained values of d[4,3] are in the table 1A in Appendix A

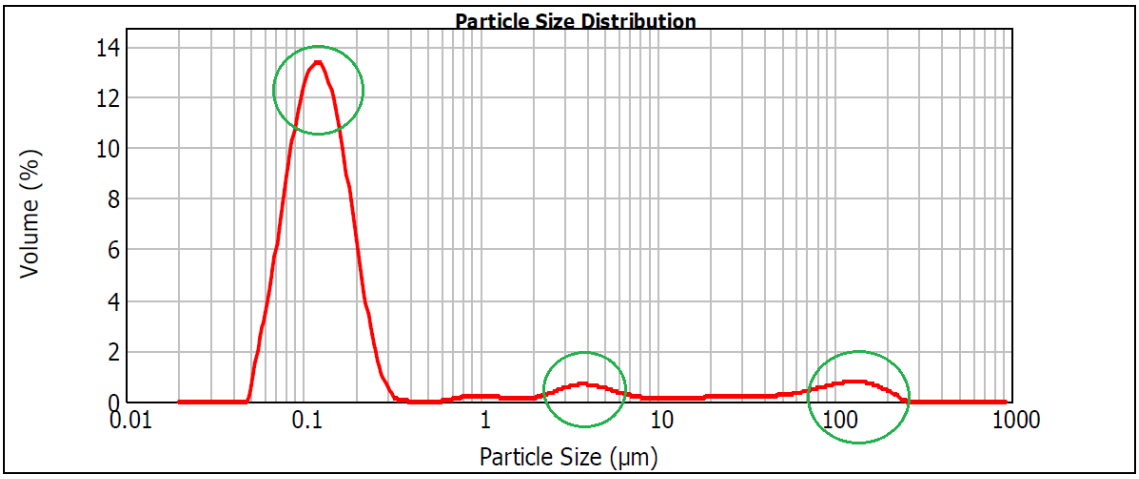

Figure 23 Particle size distribution graph of a skim milk sample after pH adjustment and $CaCl_2$ addition. The first peak is represented by the casein micelles, the second one by the remained fat globules and the third one by the undissolved $CaCl_2$.

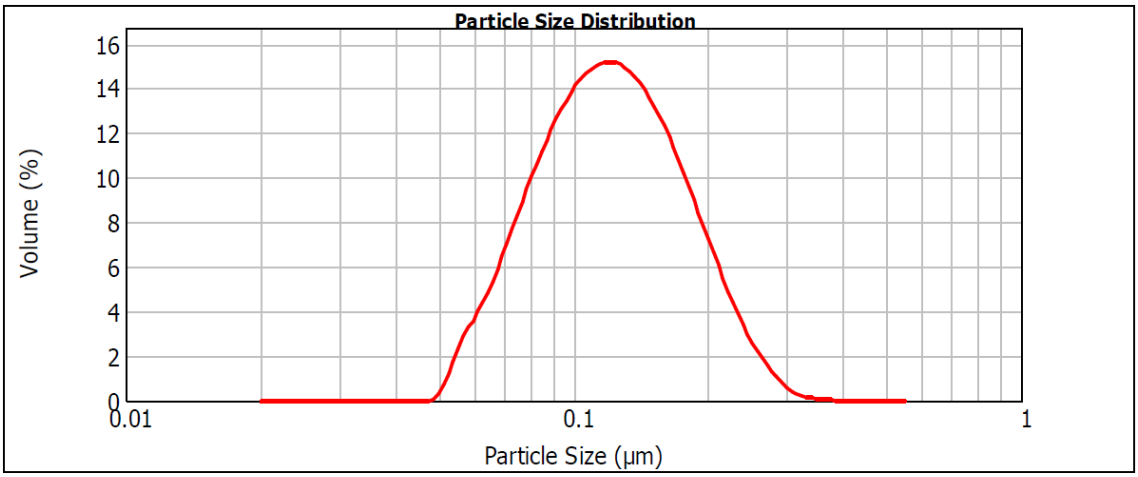

Figure 24 Particle size distribution graph highlighting casein micelles at around 0.1 µm.

In Figure 25 a contour plot is presented, created in Minitab21. In this figure, the impact of pH and $CaCl_2$ on particle size is investigated. A darker blue color represents a smaller particle size, while a darker green color represents a bigger particle size. This suggests that a bigger particle size can be found at lower pH and higher additions of $CaCl_2$. The smallest particles can be found at higher pH and higher additions of $CaCl_2$. The significance of pH in regard to the particle size of casein micelles was investigated by Sinaga et al [36] which stated that a decrease in pH would result in a decrease in the size of casein micelles. It is therefore perplexing that the particle size for the most part present very small differences despite large changes in pH. It is even more perplexing that a decrease in pH would result in an increase of particle size. It is noticeable that the pH has a statistically significant effect on the particle size, according to Table 5. In this table, it is also noticeable that the addition of $CaCl_2$ is not significant. The pH*pH is significant, indicating that there is a curvature in the model. This implies that the response of added pH to particle size is not linear. Like with the factor of $CaCl_2$, the $CaCl_2$* $CaCl_2$ factor is not significant. The combination between pH and $CaCl_2$ is however almost significant (α (0.05)), hinting of a relationship between pH and $CaCl_2$ and their effect on particle size.

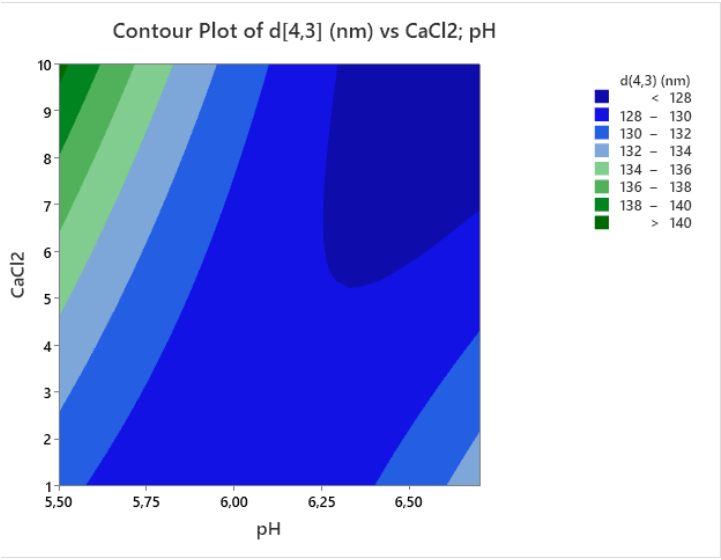

Figure 25 Contour plot of particle size [nm] vs $CaCl_2$ and pH.

Table 5 Response Surface result of d(4,3) [nm] vs pH; $CaCl_2$.

Term	**P-Value**
pH	0.014
$CaCl_2$	0.511
pH*pH	0.049
$CaCl_2$* $CaCl_2$	0.688
pH* $CaCl_2$	0.070

The interaction between the terms and the response from the model can be expressed algebraic by the regression equation. That has the general form of:

$$y = b_0 + b_1X_1 + b_2X_2 + \cdots + b_kX_k \quad (3)$$

where: "y" represents the variable of response, "b_0" the constant, "b_1", "b_2", "b_k" the coefficients, and "X_1", "X_2", "X_k" the term's value [63]. For the response surface, the uncoded units were chosen in order to have freedom in creating and using the worksheet in Minitab21 [64].

The contour plot from the figure 24 was designed by the following regression equation in uncoded units in Minitab21.

$$d(4,3)(nm) = 459 - 112.1\,pH + 9.41\,CaCl_2 + 9.49\,pH * pH + 0.0329\,CaCl_2 * CaCl_2 - 1.574\,pH * CaCl_2 \quad (4)$$

Due to the multicollinearity, the predictors which are highly correlated, are described as "problematic" [65]. In the end the software offers a model summary with values for S, R-sq, R-sq (adj) and R-sq (pred). "S" shows if the response is correctly described by the model. It is measured in units, and the lower S value is, the assumption is considered to be met by the model. "R-sq" shows how well the data is fitted by the model. It is characterized by percent (from 0 to 100). "R-sq (adj)" represents a way to compare the different set of predictor models in order to find the correct model. "R-sq (pred)" measures the level of prediction in the case of new observations. The value of R-sq (pred) smaller than R-sq suggests that the model overfits. [66] In this case the overfit can be explained as the situation when the added terms are not relevant for the model. The model correctly

describes the results but does not fit the data very well and the overfit occurs as well as it is seen in Table 6.

Table 6 Model summary of d(4,3) [nm] vs pH; $CaCl_2$.

S	R-sq	R-sq (adj)	R-sq (pred)
3.14931	46.49%	31.20%	0.00%

4.1.2. Effect of fat on gelation-trial

4.1.2.1. Milk content

For the Effect of fat on gelation-trial, two cartons of different milk were used. A third carton of Åsens lantmjölk Gammaldags (2.9-3.1 % fat) was used in combination with the only carton of Åsens lantmjölk Orginal (1.7-1.9 % fat). Below in Table 7, the content of fat, protein, lactose, solids non-fat (SNF) and total solids (TS) of the skim milk and the full fat milk used in this trial for both milk carton 3 (2.9-3.1 % fat) and milk carton 1 (1.7-1.9 % fat) As seen in the table 7, there are some differences between the five categories. The major one being the fat content of the different types of milk. It is noticeable that the fat content of the third carton of skim milk is slightly higher compared to the first and seconds carton of (2.9-3.1 % fat) milk. As mentioned previously, it was difficult at times to remove the skim milk from the centrifugation tubes without including some of the more solid fat. In this case the challenge was higher and therefore the fat content is slightly higher. The 3% skim milk of carton 3 also has lower protein content, slightly lower lactose and SNF content and lower TS content. These are no major differences and while these differences are considered, the results obtained using the skim milk from carton 3 is never compared to the results when using carton 1 and carton 2. Therefore, it is not of utmost importance to have similar values in all of these categories. The skim milk of 2% shows a higher fat content compared to all of the 3% skim milks. It was harder to remove the fat after centrifugation for this fat content, as there was a less solid layer of fat due to the lower fat content. It was deemed slightly higher, but it was believed that it would still be sufficient for the analysis going forward. Otherwise, the skim milk 2% is quite similar to the skim milk 3% of carton 3, where only the protein content is slightly higher, something that is reflected in the TS.

The fat content of full fat milk 2% is slightly lower compared to what the carton states, at 1.7-1.9 % according to the carton, while the measured fat content was slightly lower at 1.6 %. This could be due to inconsistencies when performing the measurements. The fat content of the 3% full fat milk is at the range which the carton states. The protein, lactose, SNF and TS content is quite similar between the skim milk 3% and the full fat milk 3%, except regarding the TS, which is excepted due to the much higher fat content of the full fat milk 3%. The same thing can be seen for the 2% skim milk and full fat milk, where some small inconsistencies are present, but the biggest difference is seen in the TS content, which is due to the higher fat content of the full fat milk.

Table 7: Milk cartons and the obtained skim milk comparison for the Effect of fat on gelation-trial.

Type	Fat [%]	Protein [%]	Lactose [%]	SNF [%]	TS [%]
Skim milk 3% Carton 3	0.21	3.14	4.60	8.61	8.88
Full fat milk 3% Carton 3	2.88	3.14	4.52	8.49	11.2
Skim milk 2% Carton 1	0.30	3.24	4.63	8.70	9.05
Full fat milk 2% Carton 1	1.56	3.23	4.56	8.64	10.1

4.1.2.2. Particle size

For the milk samples with 3% fat, without any addition of $CaCl_2$, the size distribution graph (Figure 26) looks different compared to Figure 23 above. It is expected that the peak representing the casein micelles is absent in Figure 26. This is due to the volume fraction of the fat globules is significantly larger compared to the volume fraction of the casein micelles as the size of casein micelles significantly smaller compared to the size of the fat globules. A special case is observed at the milk samples with 2% fat. After the refraction index was changed from 1.570, specific for casein micelles to 1.463, specific to milk fat, a peak appeared between 0.03 and 1.00 µm (Figure 27). It is expected that the peak is representing the casein micelles due to the lower fat concentration and the change of refraction index.

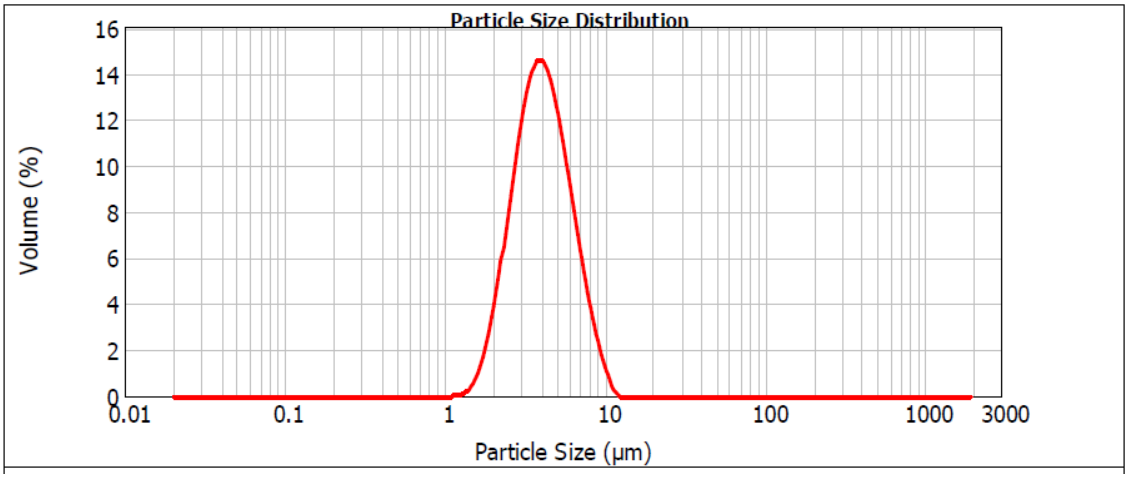

Figure 26 Particle size distribution graph for the milk with 3% fat after changing the refraction index.

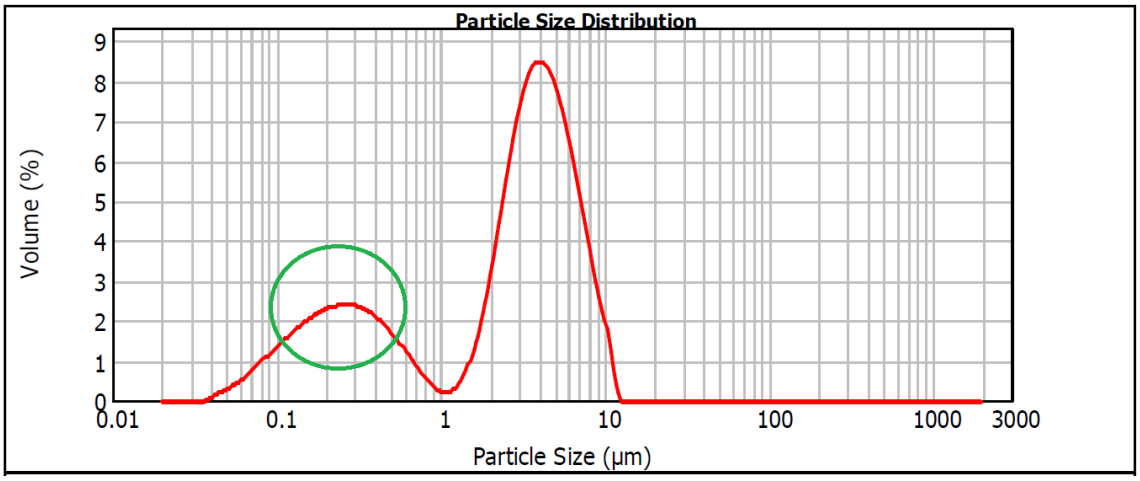

Figure 27: Particle size distribution graph for the milk with 2% fat after changing the refraction index.

In order to obtain a specific, clear result on the size of the fat globules, a graph cut between 0.9 µm and 15 µm (figure 28) was performed, keeping just the specific peak for the fat globules. From the obtained size distribution graphs for samples with a fat percentage of 2% or 3%, the value of d[4:3] for each sample was achieved. The obtained results can be seen in Table 2A, Appendix A.

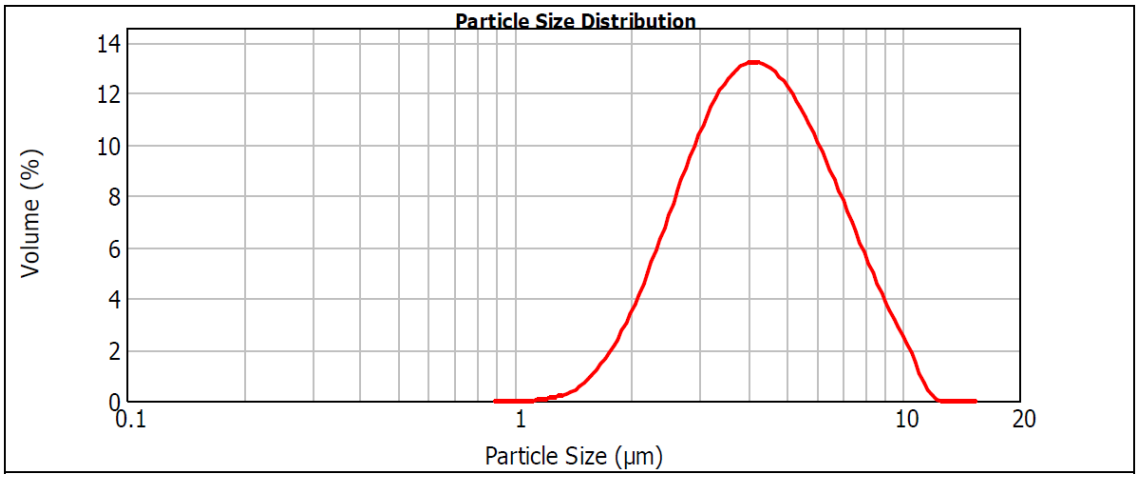

Figure 28 Particle size distribution graph for the milk with 2% and 3% fat after the cut was performed between 0.9 µm and 15 µm.

Looking at the size of the fat globules it is visible that for both cartons, they have similar size. Meanwhile averaging the values, the size of the particles for the 3%, $4.147 \cdot 10^3 \pm 0.147 \cdot 10^3$ µm, milk is slightly higher than the 2% one, $4.070 \cdot 10^3 \pm 0.004 \cdot 10^3$ µm, as it will be seen in Table 19.

4.2 Response surface method trial

4.1.1. Compilation table

Table 8 presents the average and standard deviation for gelation time, G' 30 min, particle size (d[4,3]) and ΔBS 30 min for duplicates 1-14 of the Response Surface method trial. The result for each sample in all 14 duplicates in the Response Surface method trial are presented in Table A1 in Appendix A. In Appendix B and C, the samples of each duplicate are plotted against each other, regarding the result derived from the Rheometer and Turbiscan respectively.

Table 8 Compilation table, containing average and standard deviation for gelation time, G' 30 min, particle size (d[4,3]) and ΔBS 30 min for duplicates 1-14 of the Response Surface method trial.

Sample	**Duplicate**	**pH**	**$CaCl_2$ [mmol/L]**	**Gelation time [s]**	**G' 30 min [Pa]**	**Particle size (d[4,3]) [nm]**	**ΔBS 30 min [%]**
S1,1	1	6.1	5.5	50 ± 0	53.6 ± 1.44	127 ± 1.00	13.1 ± 1.28
S3,3							
S2,1	2	6.5	8.7	135 ± 25	43.5 ± 0.245	137 ± 4.50	12.9 ± 1.14
S5,3							
S3,1	3	6.5	2.3	195 ± 75	43.1 ± 3.38	130 ± 0.500	13.8 ± 0.485
S4,3							
S4,1	4	5.7	8.7	55 ± 5.0	54.4 ± 0.98	129 ± 0.500	12.0 ± 1.62
S2,3							
S5,1	5	6.1	5.5	55 ± 15	53.6 ± 0.980	136 ± 8.00	15.0 ± 0.0938
S6,3							
S6,1	6	5.7	2.3	40 ± 10.0	51.8 ± 0.330	128 ± 1.00	10.5 ± 2.24
S1,3							
S7,1	7	6.1	5.5	65 ± 15	53.5 ± 1.42	130 ± 0.500	13.9 ± 1.73
S7,3							
S1,2	8	6.7	5.5	205 ± 25	46.1 ± 4.28	129 ± 0.500	13.7 ± 0.264
S4,4							
S2,2	9	6.1	5.5	65 ± 5.0	54.4 ± 0.0350	129 ± 0	14.2 ± 0.811
S1,4							
S3,2	10	5.5	5.5	70 ± 10.0	50.4 ± 1.34	128 ± 0	10.7 ± 0.363
S6,4							
S4,2	11	6.1	1.0	70 ± 40	50.6 ± 2.14	129 ± 0	14.6 ± 0.402
S7,4							
S5,2	12	6.1	5.5	55 ± 45	58.7 ± 6.07	129 ± 0	13.8 ± 0.951
S2,4							
S6,2	13	6.1	5.5	75 ±5.0	53.5 ± 0.230	129 ± 0.500	14.8 ± 0.232
S3,4							
S7,2	14	6.1	10.0	80 ± 30	56.8 ± 1.85	130 ± 1.50	13.9 ± 0.284
S5,4							

4.2.2. Effect of pH on gelation time, G' 30 min ΔBS 30 min

Below, the impact of factor pH for gelation time, G' 30 min and ΔBS 30 min is investigated.

4.2.2.1. Gelation time

When comparing the gelation time of duplicates 8 (pH 6.7, $CaCl_2$ 5.5 mmol/L), 10 (pH 5.5, $CaCl_2$ 5.5 mmol/L) and 13 (pH 6.1, $CaCl_2$ 5.5 mmol/L), as seen in Table 8, duplicate 8 with the higher pH has a much longer gelation time compared to that of duplicate 10 and duplicate 13. Duplicates 10 and 13 have very similar gelation times at 70 s and 75 s respectively with the standard deviation of duplicate 10 being slightly higher than that of duplicate 13. This indicates that the lower pH result in a shorter gelation time, while the higher pH results in longer gelation time. The same observation can be made when comparing duplicates 2 (pH 6.5, $CaCl_2$ 8.7) and 4 (pH 5.7, $CaCl_2$ 8.7), it is noticeable that duplicate 2, with the higher pH also has a longer gelation time compared to duplicate 4 with the lower pH at the same $CaCl_2$ addition. Similar differences can be seen with duplicates 3 (pH 6.5, $CaCl_2$ 2.3) and 6 (pH 5.7, $CaCl_2$ 2.3), where duplicate 6 with the lower pH also has a shorter gelation time compared to duplicate 3 with a higher pH and a longer gelation time. This indicates that a lower pH will result in a shorter gelation time, while a higher pH will result in a longer gelation time. This observation is supported by the Pairwise Pearson Correlations test performed (Table 9). The Factor here is pH and the variable investigated is the gelation time. The "N" column represents the number of samples used in the analysis, while the "Correlation" column shows if the variables present a negative or positive correlation. The correlation values are between (-1), representing strong negative correlation, and (+1), representing strong positive correlation. A negative correlation represents that an increase of a variable, means that the decrease of the other one. Meanwhile a positive correlation represents that an increase in a variable result in an increase in the other variable. The next column represents the confidence interval for ρ, which in this case was selected to be 95%, and an α of 0.05. Usually, a confidence interval is used in order to obtain the range where the coefficients or correlation are likely to be. [67] [68] The last column is the p-value, where if the p-value < α (0.05), the pH factor is significant for the variable. This is expected as a lower pH would result in a faster gelation time according to Figure 6 by Walstra [31]. According to Figure 6, the clotting time drastically decrease with a decrease in pH, as the effect of aggregation and splitting of the κ-casien is higher at lower pH.

Table 9 Pairwise Pearson Correlation of gelation time [s] vs pH.

Variable	Factor	N	Correlation	95% CI for ρ	P-Value
Gelation time (s)	pH	28	0.684	(0.418; 0.842)	0.000

Here the correlation supports the previous observation, that with an increase in gelation time, there is also an increase in the pH. As the p-value < α (0.05), the pH is highly statistically significant.

4.2.2.2. G' 30 min

In Figure 29, the G'-values [Pa] of duplicate 8 (pH 6.7, $CaCl_2$ 5.5 mmol/L), duplicate 10 (pH 5.5, $CaCl_2$ 5.5 mmol/L) and duplicate 13 (pH 6.1, $CaCl_2$ 5.5 mmol/L) are plotted against time [s]. In this figure, the G' is labelled G*, and should not be confused with the complex shear modulus mentioned in section 2.6. Here it is evident that at the beginning of the gelation curve, as mentioned in the previous section, the gelation time for duplicate 10 and duplicate 13 are quite similar, while duplicate 8 differs quite a lot. Duplicates 10 and 13 continue to follow a very similar pattern up until 1000 s, where they start to differentiate. The G' 30 min-value for these duplicates are 46.1 Pa, 50.6 Pa and 53.5 Pa respectively for duplicate 8,10 and 13. At this point, the duplicates are quite different, with the highest G' 30 min-value for duplicate 13 with the middle pH value, while both duplicates with lower and higher pH-values have lower G' 30 min-values. As the gelation continues from this point duplicate 10 are nearing duplicate 8 and are both quite separated from duplicate 13. When studying the vertical bars representing the standard deviation at certain points in the gelation curve, it is evident that the biggest standard deviations in general are found before 500 s and are for the

most part decreasing from there. This is however not true for duplicate 8, where the standard deviation is roughly the same throughout the gelation curve. It is also evident that the upper limit if the standard deviation of duplicate 8 almost reaches the gelation curve of duplicate 13. Duplicate 10 has a smaller standard deviation than duplicate 8 and stays for the most part right in between the other duplicates. This means that the duplicate with the lowest pH does not have the highest G' 30 min value, but the duplicate with the highest pH has the lowest G' 30 min value.

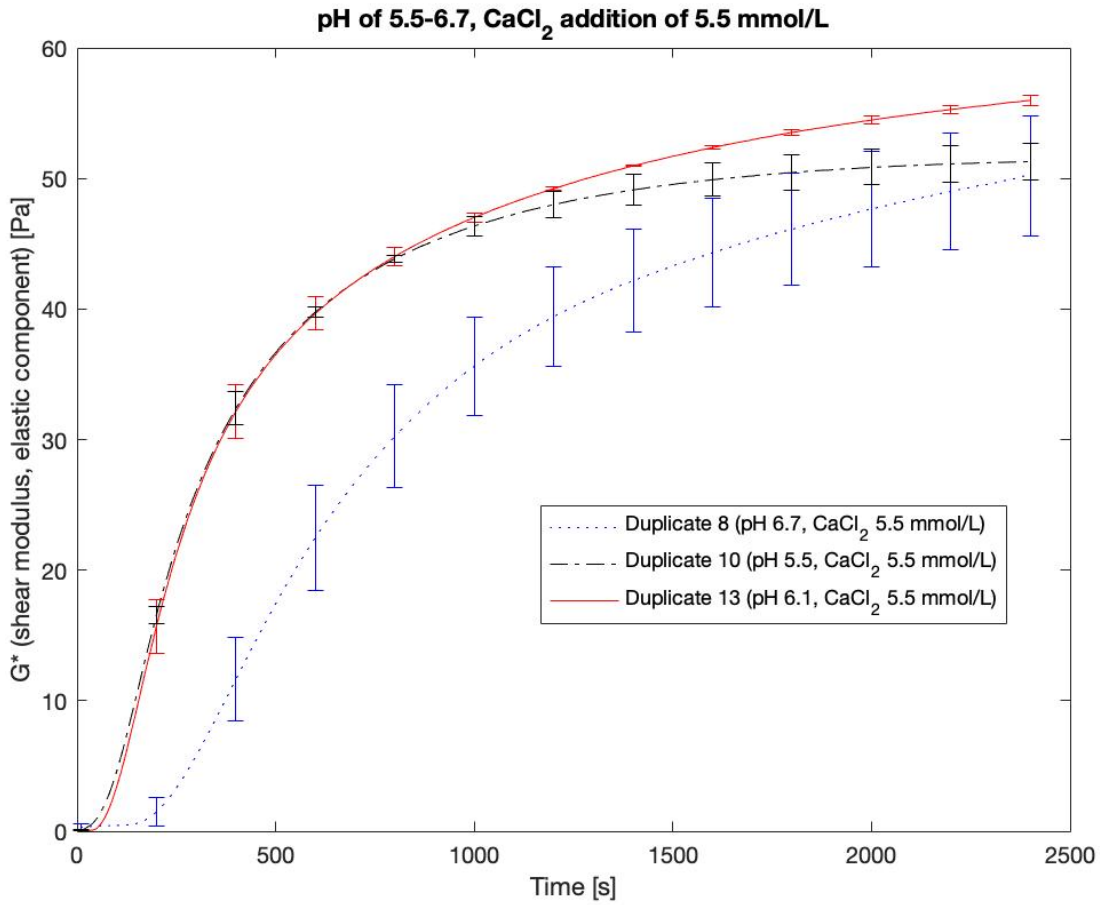

Figure 29 The average G' [Pa] is plotted against Time [s] for duplicate 8 (pH 6.7, $CaCl_2$ 5.5 mmol/L), duplicate 10 (pH 5.5, $CaCl_2$ 5.5 mmol/L) and duplicate 13 (pH 6.1, $CaCl_2$ 5.5 mmol/L) with error bars indicating standard deviation.

When comparing duplicates 2 (pH 6.5, $CaCl_2$ 8.7) and 4 (pH 5.7, $CaCl_2$ 8.7) again and their respective G' 30 min values, it is clear that duplicate 4 with the lower pH also has a higher G' 30 min value, compared to duplicate 2 with a lower pH. The same pattern can be seen when looking at duplicates 3 (pH 6.5, $CaCl_2$ 2.3) and 6 (pH 5.7, $CaCl_2$ 2.3), where duplicate 6 with the lower pH also has higher G' 30 min value compared to duplicate 3. This indicates that a higher pH result in a lower G' 30 min value and that a higher G' 30 min value can be seen at lower pH. This observation is supported by the Pairwise Pearson comparison presented in Table 10 below, where a higher G' 30 min value correlates to a lower pH. Here the p-value is smaller than α (0.05), indicating that the result is statistically significant.

Table 10 Pairwise Pearson Correlation of G' 30 min vs pH

Variable	Factor	N	Correlation	95% CI for ρ	P-Value
G' 30 mins (Pa)	pH	28	-0.478	(-0.722; -0.128)	0.010

4.2.2.3. ΔBS 30 min

In Figure 30, duplicate 8 (pH 6.7, $CaCl_2$ 5.5 mmol/L), duplicate 10 (pH 5.5, $CaCl_2$ 5.5 mmol/L) and duplicate 13 (pH 6.1, $CaCl_2$ 5.5 mmol/L) can be seen, where their respective ΔBS values [%] are plotted against time [s]. The ΔBS is a direct link to the size of particles in the forming gel, as larger particles will result in a higher degree of back scatter to occur. Here, duplicate 13, with the middle pH has a very steep start of its gelation curve compared to that of par 10 and duplicate 8. Duplicate 8 and duplicate 10 are more quite similar at start of gelation but does differentiate at around 600 s. It is also during this period that the standard deviations of duplicate 10 and duplicate 13 makes all duplicates appear in a similar region. Duplicate 10 and duplicate 8 continues to differentiate as time goes and duplicate 8 moves closer to that of duplicate 13. The ΔBS 30 min values of duplicates 8 and 13 are similar at 13.7 % and 14.8 % respectively, while the ΔBS 30 min value of duplicate 10 is much lower at 10.7 %. This result indicates that the lowest pH of 5.5 results in a lowest ΔBS 30 min value, but that the highest pH at 6.7 still has a lower ΔBS 30 min value compared to the lower pH of 6.1.

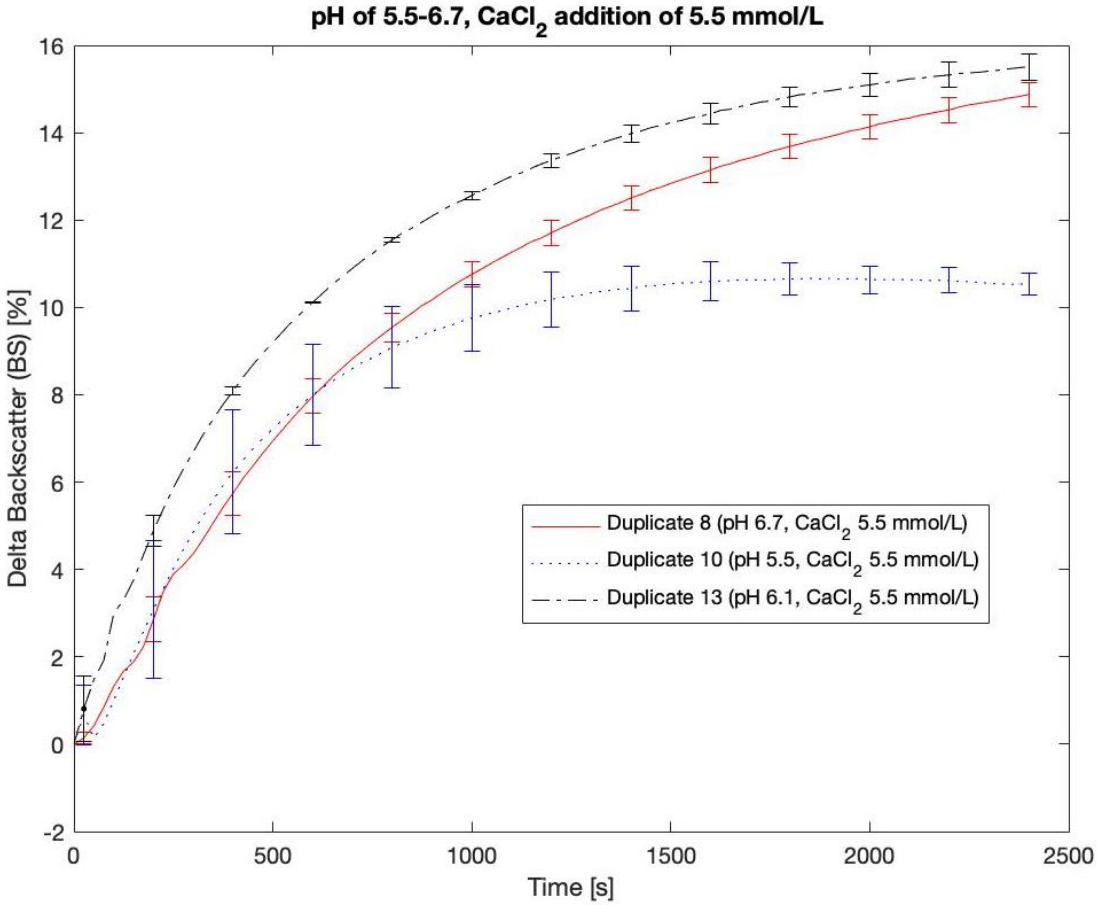

Figure 30 The average ΔBS [%] is plotted against Time [s] for duplicate 8 (pH 6.7, $CaCl_2$ 5.5 mmol/L), duplicate 10 (pH 5.5, $CaCl_2$ 5.5 mmol/L) and duplicate 13 (pH 6.1, $CaCl_2$ 5.5 mmol/L) with error bars indicating standard deviation.

When comparing the ΔBS 30 min value of duplicates 2 (pH 6.5, $CaCl_2$ 8.7) and 4 (pH 5.7, $CaCl_2$ 8.7), duplicate 4 has a higher ΔBS 30 min value, at 12.9 % compared to that of duplicate 2 with a ΔBS 30 min value of 12.0 %. However, as their respective standard deviation is quite large, the averages of both samples fit within both standard deviations. This indicates that a higher pH could result in a higher ΔBS 30 min value and therefore larger particles within the gel network. The same pattern can be seen when looking at duplicates 3 (pH 6.5, $CaCl_2$ 2.3) and 6 (pH 5.7, $CaCl_2$ 2.3), where duplicate 6 with the lower pH also has a lower ΔBS 30 in value compared to duplicate 3. The standard deviation of duplicate 6 is quite large but does not overlap with the standard deviation of

duplicate 3 and therefore, this does also indicate that a higher pH result in a higher ΔBS 30 min value. This is supported by the correlation derived from the Pairwise Pearson Correlations test (Table 11), where an increase in the ΔBS 30 min value results in an increase in pH. Here it is also evident that the result is not statistically significant as the p-value < α (0.05).

Table 11 Pairwise Pearson Correlation of ΔBS 30 min vs pH.

Variable	Factor	N	Correlation	95% CI for ρ	P-Value
ΔBS 30 min	pH	28	0.268	(-0.117; 0.583)	0.168

4.2.3. Effect of $CaCl_2$ on gelation time, G' 30 min and ΔBS 30 min

For this section, the importance of $CaCl_2$ for gelation time, G' 30 min and ΔBS 30 min is presented.

4.2.3.1. Gelation time

When comparing the gelation time of duplicates with the same pH but differentiating addition of $CaCl_2$, it is possible to investigate the role of $CaCl_2$. Duplicates 9 (pH 6.1, $CaCl_2$ 5.5), 11 (pH 6.1, $CaCl_2$ 1.0) and 14 (pH 6.1, $CaCl_2$ 10.0) all have varying gelation times at 65 s, 70 s and 80 s respectively. Duplicate 14 with the highest $CaCl_2$ addition is the duplicate with the longest gelation time, while duplicate 9 with the middle addition has the shortest gelation time. Duplicate 9 has a small standard deviation while both duplicate 11 and duplicate 14 have large standard deviations where the average of all the duplicate fit within these standard deviations. This indicates that an increase in addition of $CaCl_2$ from 1.0 mmol/L to 5.5 mmol/L would shorten the gelation time, but an increase from 5.5 mmol/L to 10.0 mmol/L would increase the gelation time again.

At the pH of 6.5, duplicates 2 (pH 6.5, $CaCl_2$ 8.7) and 3 (pH 6.5, $CaCl_2$ 2.3) have very different gelation times, with the much shorter gelation time of duplicate 2 at 135 s, compared to duplicate 3 at 195 s. The standard deviation of duplicate 3 is however very large and the result does therefore overlap with the average duplicate 2. This would however indicate slightly that a higher amount of added $CaCl_2$ would result in a shorter gelation time. At pH 5.7 with duplicates 4 (pH 5.7, $CaCl_2$ 8.7) and 6 (pH 5.7, $CaCl_2$ 2.3) the revers can be seen in comparison to duplicates 2 and 3, where duplicate 6 with the lower amount of added $CaCl_2$ had a shorter gelation time compared to that of duplicate 4. The duplicates only overlap slightly at the very top and bottom of their standard deviations.

When looking at the Pairwise Pearson Correlation test (table 12), it is evident from the p-value > α (0.05) that the result is not statistically significant. According to the correlation between gelation time and $CaCl_2$, indicates that a small increase in gelation time suggest a reduction in $CaCl_2$. This is consistent with the findings of Walstra [31] in Figure 6. A larger amount of Ca^{2+}, caused by a larger amount of added $CaCl_2$ indicates a shorter clotting time and an increased effect on aggregation.

Table 12 Pairwise Pearson Correlation of Gelation time vs CaCl2.

Variable	Factor	N	Correlation	95% CI for ρ	P-Value
Gelation time (s)	$CaCl_2$	28	-0.050	(-0,415; 0,330)	0.802

4.2.3.2. G' 30 min

In Figure 31 below duplicates 9 (pH 6.1, $CaCl_2$ 5.5), 11 (pH 6.1, $CaCl_2$ 1.0) and 14 (pH 6.1, $CaCl_2$ 10.0) are compared regarding their G' values [Pa] at a certain time [s] interval. The duplicates seem to have very similar starts of gelation, and follows similar patterns throughout their respective gelation curves, with some small differences in G'. At G' 30 min, duplicate 9 has a value of 54.4 Pa, while duplicates 11 and 14 have G' 30 min values of 50.6 Pa and 56.8 Pa respectively. This suggests that the duplicate with the highest addition of $CaCl_2$, duplicate 14, also has the highest G'

30 min value, indicating that an increase in $CaCl_2$ addition might result in a higher G' 30 min value. When looking closer at the error bars indicating the standard deviation at a certain point in time for each gelation curve, duplicate 9 has an incredibly small standard deviation and is positioned between the other duplicates. Duplicate 11 and 14 both have larger standard deviations, where the upper and lower limits respectively almost match the G' value of duplicate 9 towards the end of gelation.

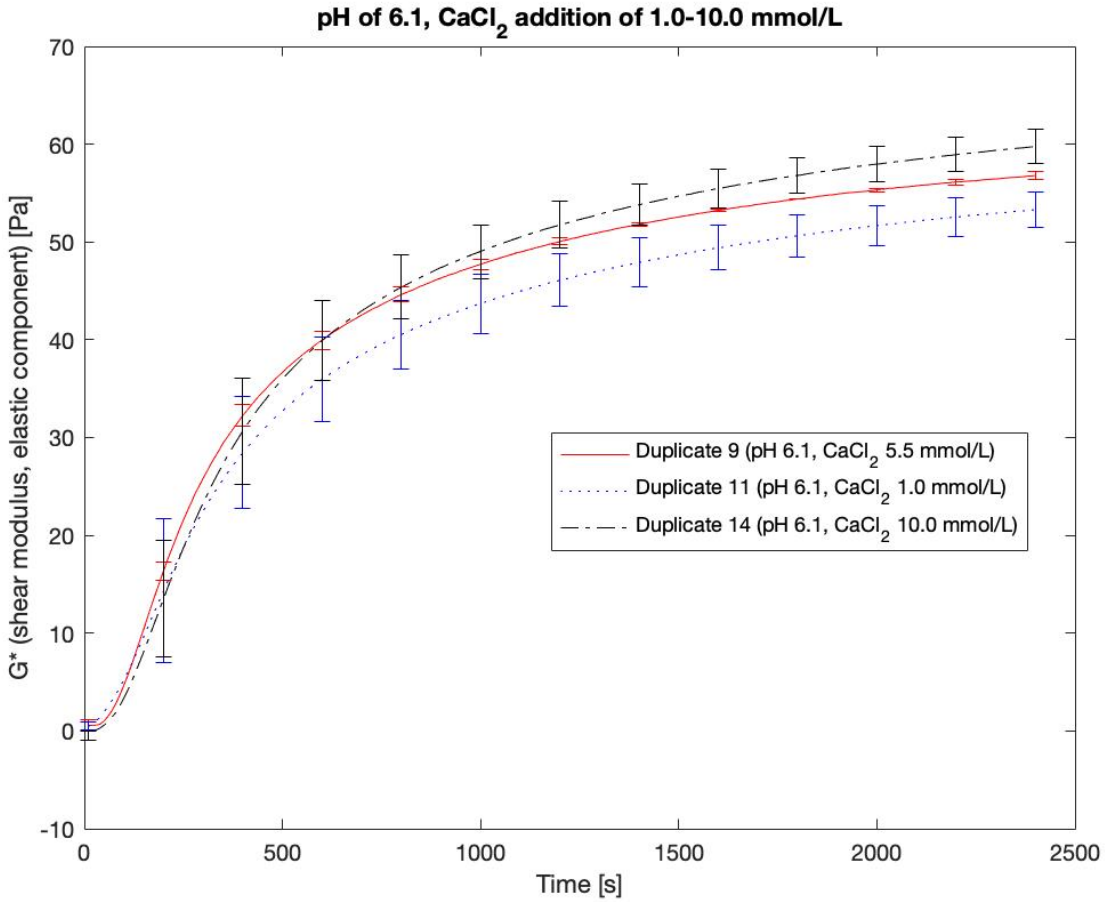

Figure 31 The average G' [Pa] is plotted against Time [s] for duplicate 9 (pH 6.1, $CaCl_2$ 5.5 mmol/L), duplicate 11 (pH 6.1, $CaCl_2$ 1.0 mmol/L) and duplicate 14 (pH 6.1, $CaCl_2$ 10.0 mmol/L) with error bars indicating standard deviation.

At the pH of 6.5, duplicates 2 (pH 6.5, $CaCl_2$ 8.7) and 3 (pH 6.5, $CaCl_2$ 2.3) have very similar G' 30 min values, at 43.5 Pa and 43.1 Pa respectively. Duplicate 3 has on the other hand a quite large standard deviation, so the samples within duplicate 3 presented results with a larger difference compared to samples of duplicate 2. Duplicates 4 (pH 5.7, $CaCl_2$ 8.7) and 6 (pH 5.7, $CaCl_2$ 2.3) have larger differences between the duplicates compared to the previous duplicates, as duplicate 4 have a G' 30 min value of 54.4 Pa and duplicate 6 has a value of 51.8 Pa. This might indicate that a larger addition of $CaCl_2$ results in a higher G' 30 min value, and that a lower amount of added $CaCl_2$ would result in the opposite. This indication is supported by the correlation presented in the Pairwise Pearson Correlation test in Table 13, where the increase in G' 30 min values is correlated to an increase in the addition of $CaCl_2$. However, it is noticeable that this result is not statistically significant, as the p-value > α (0.05).

Table 13 Pairwise Pearson Correlation of G' 30 mins vs $CaCl_2$.

Sample 1	Sample 2	N	Correlation	95% CI for ρ	P-Value
G' 30 mins (Pa)	$CaCl_2$	28	0,220	(-0,167; 0,548)	0,260

4.2.3.3. ΔBS 30 min

In Figure 32, the ΔBS [%] of duplicates 9 (pH 6.1, $CaCl_2$ 5.5), 11 (pH 6.1, $CaCl_2$ 1.0) and 14 (pH 6.1, $CaCl_2$ 10.0), have been plotted against time [s]. It is quite evident from the figure that the three duplicates present very similar behavior regarding their gelation curves up until about 500 s, where they start to differentiate a bit. The ΔBS 30 min values for the duplicates vary only slightly, at 14.2 %, 14.6 % and 13.9 % for duplicate 9, 11 and 14 respectively. The standard deviations of all the duplicates at 30 minutes, but also throughout the entire gelation curve overlap at their highest and lowest values, making it more difficult to really get a get clear image at the effect of $CaCl_2$. It is indicated by these samples that the smallest amount of added $CaCl_2$ would result in a higher ΔBS 30 min value, while the opposite is true for the higher amounts of added $CaCl_2$.

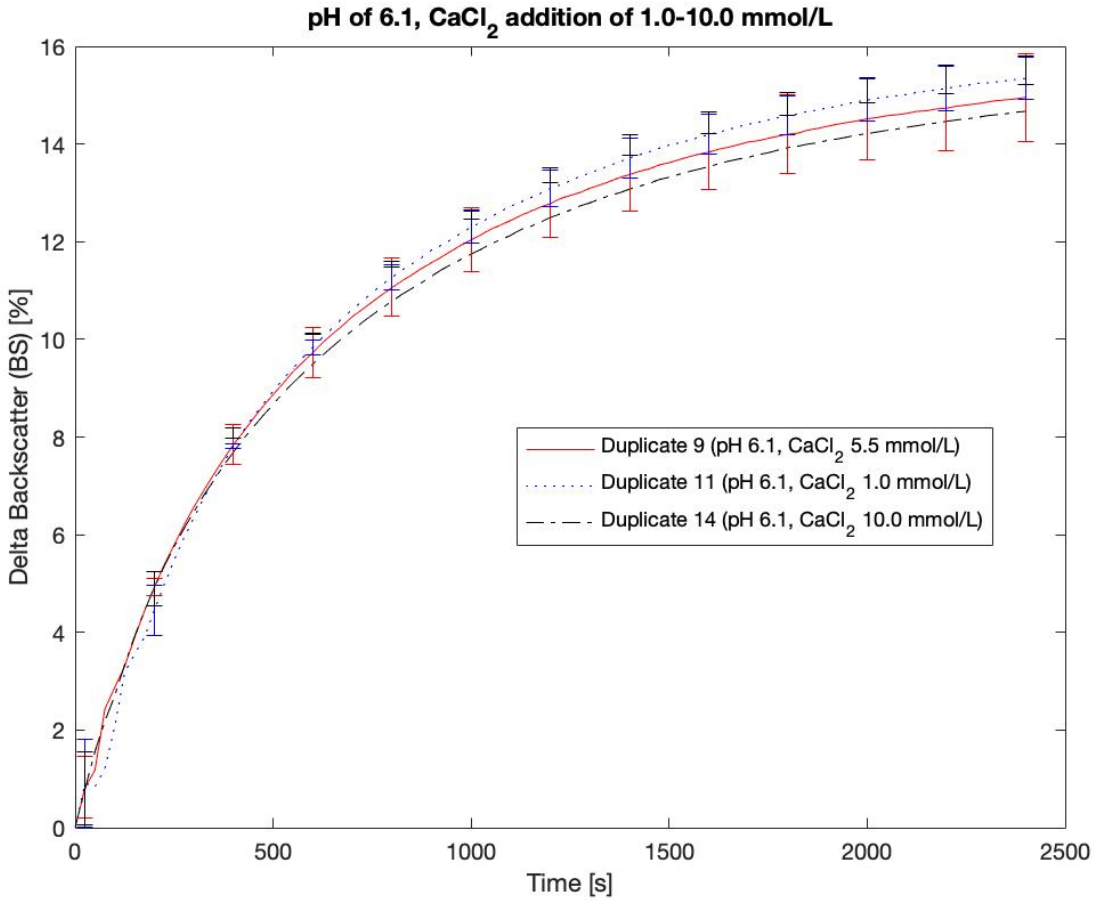

Figure 32 The average ΔBS [%] is plotted against Time [s] for duplicate 9 (pH 6.1, $CaCl_2$ 5.5 mmol/L), duplicate 11 (pH 6.1, $CaCl_2$ 1.0 mmol/L) and duplicate 14 (pH 6.1, $CaCl_2$ 10.0 mmol/L) with error bars indicating standard deviation.

For duplicates 2 (pH 6.5, $CaCl_2$ 8.7) and 3 (pH 6.5, $CaCl_2$ 2.3), the ΔBS 30 min values are similar but not identical, where the larger addition of $CaCl_2$ of duplicate 2 resulted in a lower ΔBS 30 min value, compared to that of duplicate 3. The opposite is however true for duplicates 4 (pH 5.7, $CaCl_2$ 8.7) and 6 (pH 5.7, $CaCl_2$ 2.3), where the larger amount of added $CaCl_2$ resulted in a higher ΔBS 30 min value for duplicate 4 compared to duplicate 6. The standard deviations of these duplicates are however large, making the result of the two duplicates overlap. This makes it harder to draw a strong conclusion about this finding as there is no clear separation between these duplicates. The correlation between ΔBS 30 min and $CaCl_2$, found in Table 14 and derived from the Pairwise Pearson Correlation test supports the observation between duplicates 9, 11 and 14, where an increase in the ΔBS 30 min value indicates a smaller amount of added $CaCl_2$. This result is however not statistically significant as the p-value is > α (0.05).

Table 14 Pairwise Pearson Correlation of ΔBS vs $CaCl_2$.

Variable	Factor	N	Correlation	95% CI for ρ	P-Value
ΔBS 30 min	$CaCl_2$	28	-0,142	(-0,489; 0,244)	0,473

4.2.4. Effect of pH and $CaCl_2$ on gelation time, G' 30 min and ΔBS 30 min

In this section, the influence of both pH and addition of $CaCl_2$ is investigated to potentially find how these factors interact with each other.

4.2.4.1. Gelation time

The average gelation time for each duplicate and their standard deviation is introduced in Table 8 above. As seen in this table, the gelation time between duplicate vary drastically when the pH is varied at the same $CaCl_2$ addition. There are eight duplicates with varying levels of pH (5.5 -6.7) at the same amount of added $CaCl_2$ (5.5 mmol/L). These are duplicate 1 (pH 6.1, $CaCl_2$ 5.5 mmol/L), duplicate 5 (pH 6.1, $CaCl_2$ 5.5 mmol/L), duplicate 7 (pH 6.1, $CaCl_2$ 5.5 mmol/L), duplicate 8 (pH 6.7, $CaCl_2$ 5.5 mmol/L), duplicate 9 (pH 6.1, $CaCl_2$ 5.5 mmol/L), duplicate 10 (pH 5.5, $CaCl_2$ 5.5 mmol/L), duplicate 12 (pH 6.1, $CaCl_2$ 5.5 mmol/L) and lastly duplicate 13 (pH 6.1, $CaCl_2$ 5.5 mmol/L). In this section, the last duplicates with the same pH and added amount of $CaCl_2$ (duplicates 1, 5 ,7 and 12) are compared in order to look closer at differences and similarities that might be present despite the similar starting point.

The gelation time of duplicates 1 (pH 6.1, $CaCl_2$ 5.5 mmol/L), 5 (pH 6.1, $CaCl_2$ 5.5 mmol/L), 7 (pH 6.1, $CaCl_2$ 5.5 mmol/L) and 12 (pH 6.1, $CaCl_2$ 5.5 mmol/L), with the same pH and added amount of $CaCl_2$ differ slightly at 50 s – 65 s. The standard deviation of duplicate 1 is 0 , indicating that both samples had the same gelation time, which strengthens the result of this duplicate. Duplicates 5 and 7 both have a standard deviation of 15 s, which makes these duplicates overlap regarding their averages. Duplicate 12 however has a very large standard deviation at 40 s, overlapping the averages of the other duplicates because of this. Some small differences are expected as the samples are tested at different days and as only 2 significant digits were used to adjust the pH of samples. It is however very likely that another explanation is needed to explain the differences between these duplicates.

The contour plot presented in Figure 33 below was created using the Minitab21 program. Here the impact of pH and $CaCl_2$ on the gelation time is investigated. A lighter color of green represents a shorter gelation time, while the darker shades of green represent a longer gelation time. It is evident that the shorter gelation times can be found at lower amount of added $CaCl_2$ and at lower pH, while the longer gelation times are found at high pH and with little differentiation to amount of added $CaCl_2$. It is observed the statistical significance of pH according to table 15. From the same source, it is observed that pH*pH presents statistical significance suggesting that the model presents curvature. Meanwhile, pH*$CaCl_2$, is almost significant showing the relationship between pH and $CaCl_2$ on effect for the gelation time. The same table shows that neither $CaCl_2$, neither $CaCl_2$*$CaCl_2$ present any statistical significance.

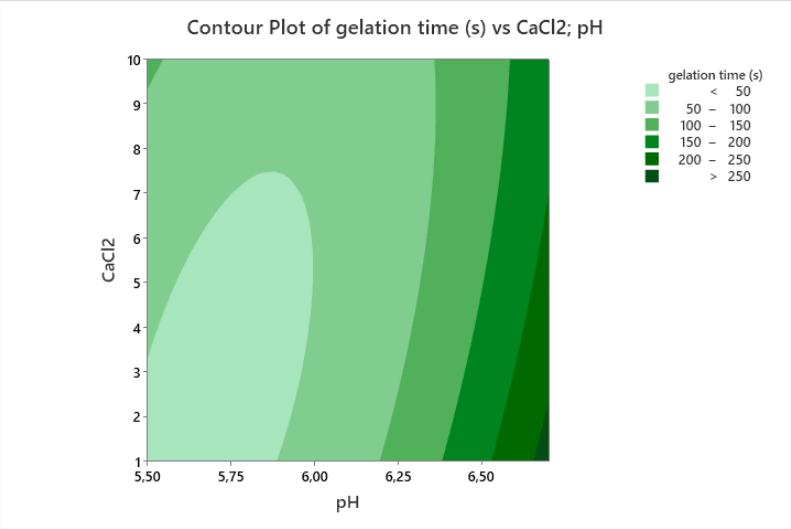

Figure 33 Contour plot of Gelation time [s], where pH is plotted on the x-axis and $CaCl_2$ on the y-axis.

Table 15 Response Surface result of gelation time [s] vs pH; $CaCl_2$.

Term	**P-Value**
pH	0.000
CaCl2	0.557
pH*pH	0.000
CaCl2* CaCl2	0.304
pH* CaCl2	0.053

The following regression equation in uncoded units, was used in order to create the contour plot shown in Figure 32.

$$d(4,3)(nm) = 6782 - 2396\,pH + 75.8\,CaCl_2 + 213.0\,pH * pH + 0.700\,CaCl_2 * CaCl_2 - 13.89\,pH * CaCl_2 \quad (5)$$

From the Table 16, it is visible that the response might not be very well fit, but the model fits the data correctly even if the overfit occurs.

Table 16 Model summary of gelation time [s] vs pH; $CaCl_2$.

S	**R-sq**	**R-sq (adj)**	**R-sq (pred)**
25.8381	85.52%	81.38%	71.30%

4.2.4.2. G' 30 min

The average G' 30 min for each duplicate and their standard deviation is introduced in Table 8 above. Duplicates 1 (pH 6.1, $CaCl_2$ 5.5 mmol/L), duplicate 5 (pH 6.1, $CaCl_2$ 5.5 mmol/L), duplicate 7 (pH 6.1, $CaCl_2$ 5.5 mmol/L), and 12 (pH 6.1, $CaCl_2$ 5.5 mmol/L) all have the same pH (6.1) and added amount of $CaCl_2$ (5.5 mmol/L). This means that all of these duplicates should be considered as the same sample. All of these duplicates vary however in their G' 30 min values between 53.5 Pa - 58.7 Pa. The differences are however much smaller when the duplicate 12, with the highest G' 30 min value and the highest standard deviation is removed. This can clearly be seen in Figure 34, where duplicate 12 has a higher G' at the same point in time compared to the other duplicates. The

standard deviation of duplicate 12 is also large enough to intercept with the gelation curves of the other samples. The duplicates 1, 5 and 7 are very similar throughout their entire gelation curves, something that is expected, with the exception of small inconsistencies.

Duplicate 1, 5 and 7 consists of samples run on day 1 and day 3 with milk coming from the first and second carton of Åsens lantmjölk Gammaldags (2.9-3.1 % fat). Duplicate 12 consists of samples run on day 2 and day 4 with milk coming from the first and second carton of Åsens lantmjölk Gammaldags (2.9-3.1 % fat). There seem to be inconsistencies between day 2 and day 4, as duplicate 12 have a much larger standard deviation than the other duplicates. These inconcinnities are probably not due to the milk, as duplicates 1, 5 and 7 do not suffer large standard deviations. When looking closer at Table A1 in Appendix A, it is clear that sample S5,2, so the 5th run on the second day have a very different G' 30 min ad gelation time compared to all the other samples in these duplicates. Sample S2,4, so the 2nd run on the fourth day, has a G' 30 min value more like the other samples from duplicates 1, 5 and 7 compared to samples S5,2. This indicates that the inconsistency is stemming from day 2. This samples would need a rerun to establish if this inconsistency would persist, or if it was only confined to this specific day and run.

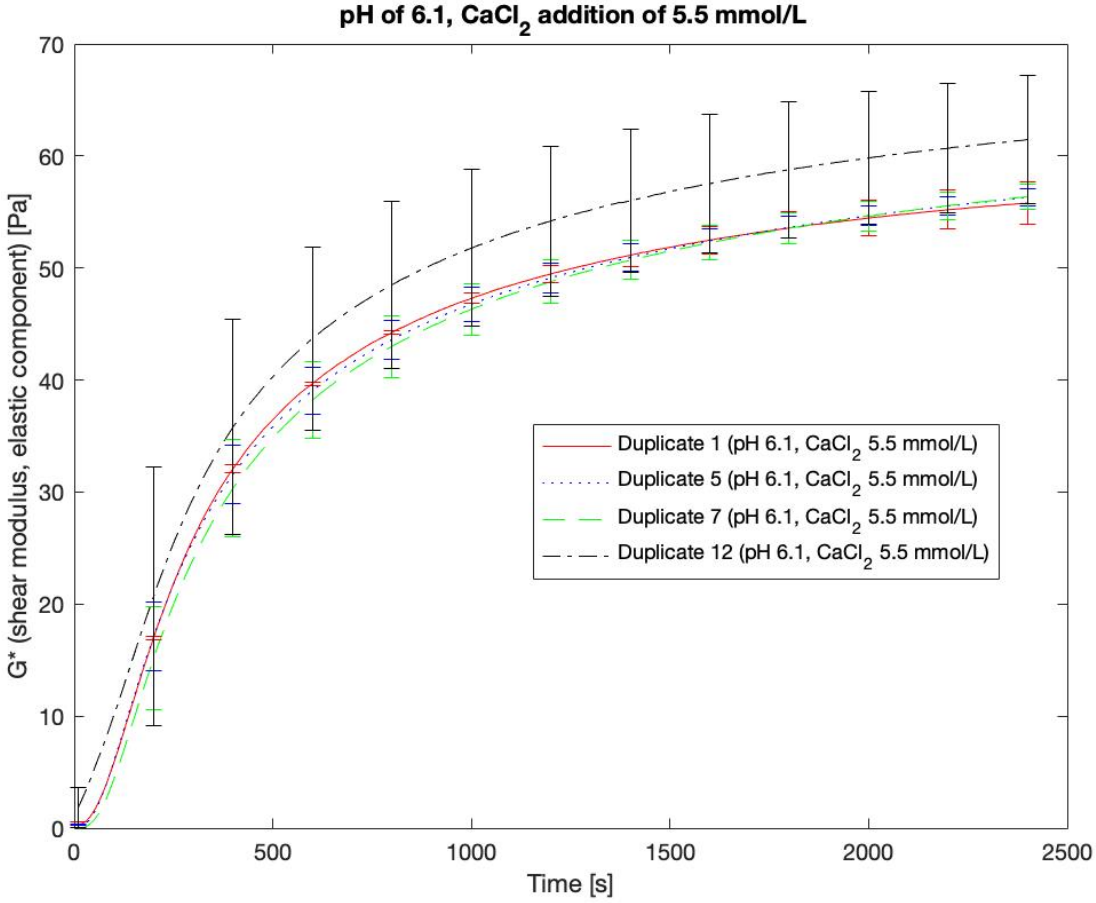

Figure 34 The average G' [Pa] is plotted against Time [s] for duplicate 1 (pH 6.1, $CaCl_2$ 5.5 mmol/L), duplicate 5 (pH 6.1, $CaCl_2$ 5.5 mmol/L), duplicate 7 (pH 6.1, $CaCl_2$ 5.5 mmol/L) and duplicate 12 (pH 6.1, $CaCl_2$ 5.5 mmol/L) with error bars indicating standard deviation.

In Figure 35 below, the contour plot for G' 30 min is presented. A darker shade of green represents a higher G' 30 min value, while a darker shade of blue represents a smaller G' 30 min value. It is clear when looking at this contour plot that the highest values of G' 30 min is present at pH 5.75-6.25 at 6 mmol/L – 10 mmol/L addition of $CaCl_2$. The lowest G' 30 min value can be found at pH above 6.5 where the addition of $CaCl_2$ provided no differentiation. It is shown in table 17 that pH has statistical significance. It is also evident that the plot presents some curvature, which is

corroborated by the significances of pH*pH from the same table. Meanwhile, $CaCl_2$, $CaCl_2$* $CaCl_2$, and pH* $CaCl_2$, are not significant. The addition of $CaCl_2$ is however almost significant and does open up for discussion about the perhaps small impact of $CaCl_2$ on the G' 30 min if the span of pH would not have been as large. This would enable more additions of $CaCl_2$ to be added, both higher and lower compared to current values. It is possible that the effect of $CaCl_2$ is simply overshadowed by the effect of pH, as it was mentioned before, pH has a greater impact on gelling properties generally, but this does not automatically disqualify the contribution of $CaCl_2$.

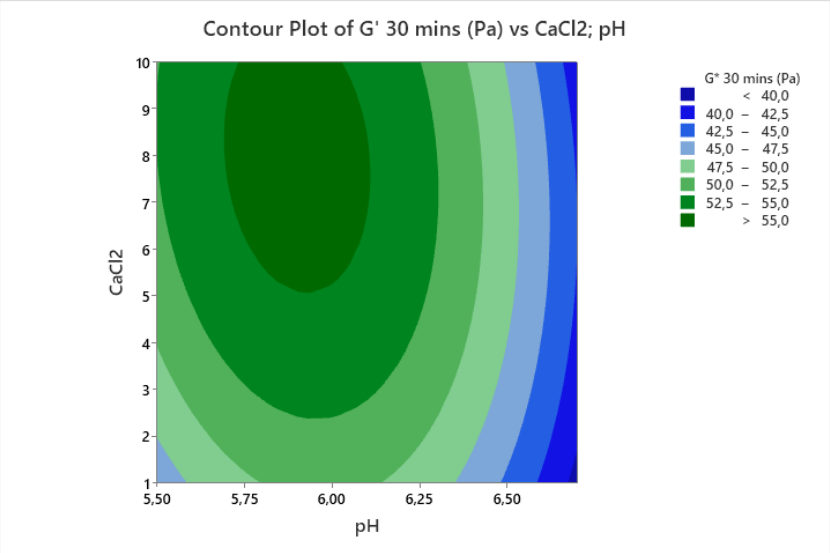

Figure 35 Contour plot of G' 30 min [Pa], where pH is plotted on the x-axis and $CaCl_2$ on the y-axis.

Table 17 Response Surface result of G'30 [Pa] vs pH; $CaCl_2$

Term	**P-Value**
pH	0.001
$CaCl_2$	0.090
pH*pH	0.000
$CaCl_2$* $CaCl_2$	0.209
pH* $CaCl_2$	0.637

The following regression equation in uncoded units, was used in order to create the contour plot shown in Figure 34.

$$d(4,3)(nm) = -715 + 255.8\,pH + 4.24\,CaCl_2 - 21.40\,pH * pH - 0.1111\,CaCl_2 * CaCl_2 - 0.419\,pH * CaCl_2 \quad (6)$$

As it appears in table 18, the model correctly describes the results but doesn't fit very well the data, also the overfit occurs as well.

Table 18 Model summary of G'30 [Pa] vs pH; $CaCl_2$.

S	**R-sq**	**R-sq (adj)**	**R-sq (pred)**
3.33387	67.71%	58.49%	40.69%

4.2.4.3. ΔBS 30 min

The average ΔBS for each duplicate and their standard deviation is introduced in Table 8 above. Like with the gelation time and G' 30 min, the duplicates with the same addition of $CaCl_2$ (5.5 mmol/L) and pH (6.1), duplicates 1, 5, 7 and 12 are compared to each other regarding their ΔBS. The ΔBS of duplicates 1, 5, 7 and 12 are 13.1 %, 15.0 %, 13.9 % and 13.8 % respectively. It is evident that duplicate 12 and duplicate 7 have very similar ΔBS – values, while those of duplicate 1 and duplicate 5 differ more. This can also be seen in Figure 36, where duplicate 1 and duplicate 5 are below and over the other duplicates. Duplicate 7 and 12 seem to have very similar behavior throughout the entirety of the curve. However, when looking closer at the individual samples of these duplicates there are some very large differences. For duplicate 7, consisting of samples S7,1 and S7,3, their individual ΔBS 30 min values are 12.1 % and 15.6 % respectively. A similar but smaller difference can be seen between the samples of duplicate 12, with a ΔBS 30 min value of 12.8 % for sample S5,2 and 14.7 % for sample S2,4. So while the average of the duplicates match, there are big inconsistencies between samples. Duplicate 5, that seem to differ more from the rest of the duplicates, have very small standard deviation. This indicates consistency between samples and the days they were run. Duplicate 1 have similar inconsistencies as duplicates 5 and 7, as the sample S1,1 of duplicate 1 has a ΔBS 20 min value of 11.8 %, while samples S3,3 of the same duplicates has a ΔBS 30 min value of 14.4 %. The big question is, which duplicate is the right one? Is it duplicates 7 and 12, where the averages of each duplicate match, but they both have a large standard deviation? Or is the right one duplicates 5, as even though it stands out from the rest, it has a very low standard deviation, indicating consistency between samples? It is also hard to rule out the different milk and day of analysis as having an impact on these results, as only one duplicate shows consistency throughout both days of analysis.

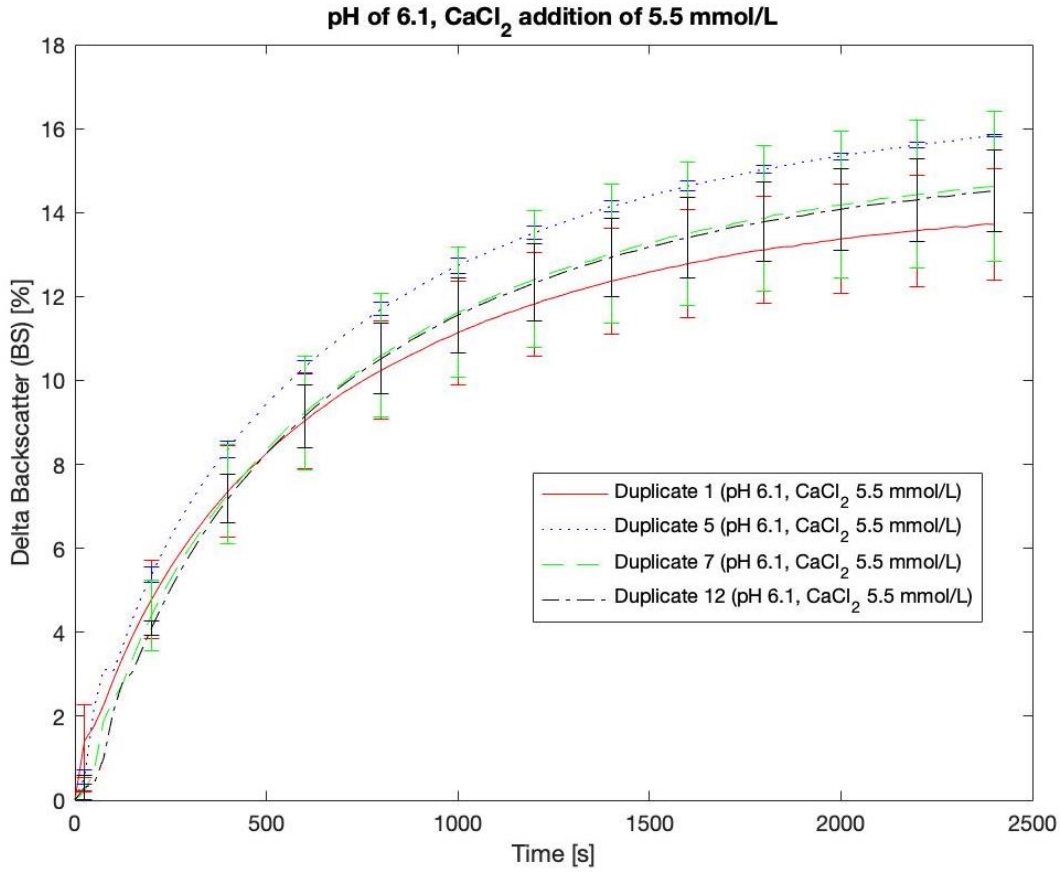

Figure 36 The average ΔBS [%] is plotted against Time [s] for duplicate 1 (pH 6.1, $CaCl_2$ 5.5 mmol/L), duplicate 5 (pH 6.1, $CaCl_2$ 5.5 mmol/L), duplicate 7 (pH 6.1, $CaCl_2$ 5.5 mmol/L) and duplicate 12 (pH 6.1, $CaCl_2$ 5.5 mmol/L) with error bars indicating standard deviation.

The contour plot of ΔBS at 30 min and the effect of pH and $CaCl_2$ is presented in Figure 37. Here the darker green colors represent a higher ΔBS 30 min, while a darker blue represents a lower ΔBS 30 min. It is evident that a higher pH and lower amount of added $CaCl_2$ result in a higher ΔBS 30 min, while lower ΔBS 30 min values can be found at lower pH and at all additions of $CaCl_2$. As it is observed in Table 21, it is clear that none of the terms are significant.

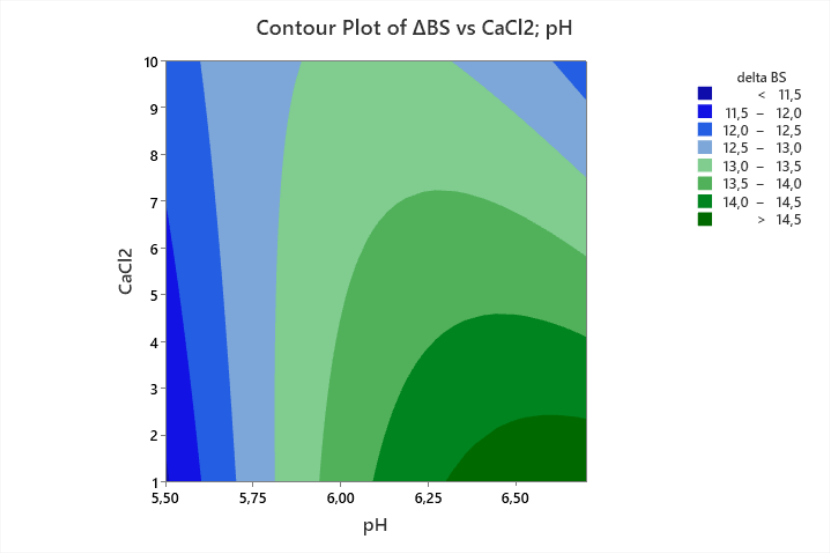

Figure 37 Contour plot of ΔBS [%], where pH is plotted on the x-axis and $CaCl_2$ on the y-axis.

Table 19 Response Surface result of ΔBS [%] at 30 min vs pH; $CaCl_2$.

Term	**P-Value**
pH	0.150
$CaCl_2$	0.438
pH*pH	0.319
$CaCl_2$* $CaCl_2$	0.969
pH* $CaCl_2$	0.466

The following regression equation in uncoded units, was used in order to create the contour plot shown in Figure 37.

$$d(4,3)(nm) = -95.2 + 32.6\,pH + 1.86\,CaCl_2 - 2.41\,pH * pH - 0.0017\,CaCl_2 * CaCl_2 - 0.318\,pH * CaCl_2 \quad (7)$$

Checking the Table 22, the model correctly describes the results but does not fit the data very well and the overfit occurs as well.

Table 20 Model summary of ΔBS [%] at 30 min vs pH; $CaCl_2$.

S	**R-sq**	**R-sq (adj)**	**R-sq (pred)**
1.63614	32.74%	13.52%	0.00%

4.2.3.4. Correlations between variables.

In Table 21 below, the result of the Pairwise Pearson Correlation test is presented, where the variables of Gelation time, G' 30 min, particle size (d[4,3]) before gelation and ΔBS 30 min are compared to investigate potential correlations between variables. As the p-value < α (0.05), the G' 30 min have a strong correlation with gelation time, where an increase in G' 30 min results in a decrease in gelation time. It also evident by the p-value < α (0.05) that the d[4,3] is significant for the ΔBS 30 min value, where an increase in the d[4,3] value would cause a decrease in the ΔBS 30 min value. There are no further statistically significant variable interactions, however, it is interesting to note that the size of casein micelles ahead of gelation does not have a significant effect on the gelation time. As mentioned earlier, a smaller casein micelle size generally results in a faster coagulation, which implies a faster gelation time. This is however, not seen in this correlation, as an increase in particle size causes a decrease in gelation time, but it is not significant.

A correlation between G' 30 min and ΔBS 30 min was very much expected, as both values are taken at the same point in time during gelation and the gelation curves presented in both analyses are very similar. However, according to the Pairwise Pearson correlation, they are not even closely correlated. This indicates that the change in particle size from start of gelation to 30 min does not have a significant effect on the G' at 30 min.

Table 21 Pairwise Pearson Correlation between variables.

Variable 1	Variable 2	N	Correlation	95% CI for ρ	P-Value
G' 30 mins (Pa)	Gelation time (s)	28	-0.807	(-0.907; -0.621)	0.000
ΔBS 30 min (%)	Gelation time (s)	28	0.246	(-0.140; 0.567)	0.206
d[4,3] (nm)	Gelation time (s)	28	-0.134	(-0.483; 0.252)	0.497
ΔBS 30 min (%)	G' 30 mins (Pa)	28	-0.094	(-0.451; 0.290)	0.636
d[4,3] (nm)	G' 30 mins (Pa)	28	0.086	(-0.297; 0.445)	0.663
d[4,3] (nm)	ΔBS 30 min (%)	28	-0.434	(-0.695; -0.073)	0.021

4.3 Effect of fat on gelation-trial

4.3.1. Compilation table

Table 25 presents the average and standard deviation for gelation time, G' at 2x gelation time, G' 30 min, particle size (d[4,3]) and ΔBS 30 min for duplicates A-D of the Effect of fat on gelation-trial. The result for each sample in all 4 duplicates in the Effect of fat on gelation-trial are presented in Table A2 in Appendix A. In Appendix D and E, the samples of each duplicate are plotted against each other, regarding the result derived from the Rheometer and Turbiscan respectively.

Table 22 Compilation table of the average and standard deviation for gelation time, G' at 2x gelation time, G' 30 min, particle size (d[4,3]) and ΔBS 30 min for duplicates A-D of the Effect of fat on gelation-trial.

Sample	Duplicate	Type	Fat content	Gelation time [s]	G' at 2x gelation time [Pa]	G' 30 min [Pa]	d(4,3) [nm]	ΔBS 30 min [%]
SSM3,1 SSM3,2	A	Skim milk	3%	690 ± 150	6.82 ± 0.795	12.9 ± 5.78	128 ± 1	11.2 ± 0.587
SM3,1 SM3,2	B	Full fat milk	3%	385 ± 95	7.41 ± 0.355	25.3 ± 4.57	$4.147 \cdot 10^3 \pm 0.147 \cdot 10^3$	10.3 ± 0.0651
SSM2,1 SSM2,2	C	Skim milk	2%	310 ± 20	6.87 ± 0.224	29.5 ± 1.71	130 ± 0.500	12.4 ± 0.108
SM2,1 SM2,2	D	Full fat milk	2%	445 ± 85	9.41 ± 0.391	25.9 ± 3.55	$4.070 \cdot 10^3 \pm 0.004 \cdot 10^3$	12.2 ± 0.0523

4.3.2. The effect of Fat/non-fat on gelation time, G' at 2x gelation time, G' 30 min and ΔBS 30 min

In this section, skim milk and full fat milk are compared at 3% and 2% fat content.

4.3.2.1. Skim milk and Full fat milk at 3%

Here duplicate A (skim milk) and duplicate B (full fat milk) at 3% fat content is compared.

4.3.2.1.1. Gelation time

In Table 25, the gelation time and standard deviation for duplicates A and B are presented. Duplicate A consists of skim milk samples derived from 3% full fat milk, while duplicate B consists of full fat milk samples at 3%. It is evident by Table 25 that the difference in gelation time between these two duplicates is very large, with a gelation time of 690 s for duplicate A and 385 s for duplicate B. The standard deviation of duplicate A is also considerably large, but not large enough to come close to the gelation time of duplicate B. This is clearly visualized in Figure 38, where a boxplot was created using Minitab21. The two blue boxes represent the two duplicates and their mean gelation time. The box for duplicate A is the skim milk, and the box for duplicate B is the full fat milk. This result would suggest that the presence of fat in the sample causes a longer gelation time. However, when performing a 2- Sample T-test, it was determined that the result was not statistically significant as the p-value of 0.336 > α (0.05).

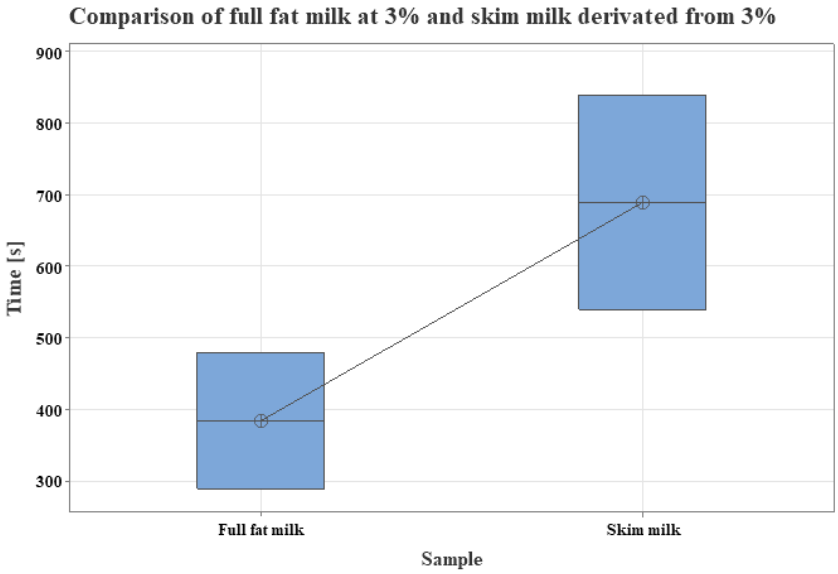

Figure 38 Boxplot comparing the average Gelation time [s] of duplicate A (skim milk, 3%) and duplicate B (Full fat milk, 3%) in the Effect of fat on gelation-trial.

4.3.2.1.2. G' at 2x gelation time

In Table 25, the G' at 2x gelation time and standard deviation for duplicates A and B are presented. Duplicate A consists of skim milk samples derived from 3% full fat milk, while duplicate B consists of full fat milk samples at 3%. It is clear that the G' at 2x gelation time is quite similar between duplicate A and duplicate B, despite the large difference is gelation time. The result was obtained at totally different times in the gelation curves, but at the same point in the gel build up. If there was no difference between samples, despite one duplicate containing fat (duplicate B) and the other one not containing any fat (duplicate B), then there might not be any significant difference between the duplicates. This is confirmed by the p-value derived from the 2- Sample T-test, where the p-value of 0.621 is larger than α (0.05), indicating that there is no statistically significant difference between these duplicates.

In Figure 39, it is evident that the standard deviation is larger for duplicate A (skim milk) than for duplicate B (full fat milk), and does reach the average for duplicate B. Therefore, the similarity at this variable seem to make a bigger impact than the differences and suggests some connection between the duplicates. This strengthen the previous observation made.

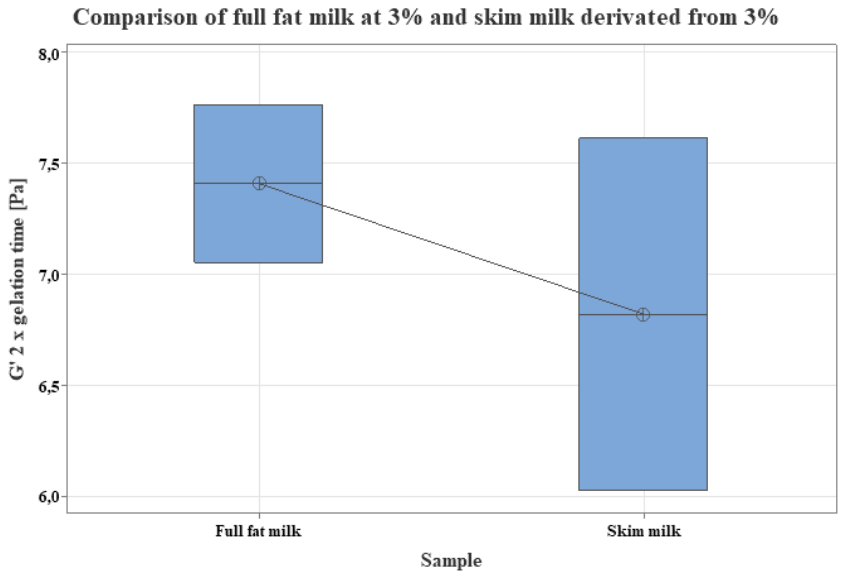

Figure 39 Boxplot comparing the average G' at 2x gelation time [Pa] of duplicate A (Skim milk, 3%) and duplicate B (Full fat milk, 3%) in the Effect of fat on gelation-trial.

4.3.2.1.3. G' 30 min

In Table 25, the G' 30 min and standard deviation for duplicates A and B are presented. Duplicate A consists of skim milk samples derived from 3% full fat milk, while duplicate B consists of full fat milk samples at 3%. The G' 30 min value differ greatly, as the G' 30 min value of duplicate A is 12.9 Pa, while it is 25.3 Pa for duplicate B. The major difference in G' 30 min and at other points in the gelation curve between these duplicates can be seen in Figure 40. Here, like discussed previously, the gelation times of the duplicates do not look remotely similar, which in extension causes some of the differences seen between start of gelation and the G' 30 min, and then for the rest of the gelation curve. Not even the large standard deviations of each duplicate can start to negate the differences between the gelation curves of these duplicates.

During the pH adjustment of all the samples used during this trial, only one sample did not need an adjustment, as their pH according to the pH meter was at 6.74, which was within the accepted range for the pH 6.7 that each sample would have before it was used during analysis. It is unlikely that only this sample, SSM3,1 (duplicate A) would not need its pH adjusted as all of the skim milk samples from the same milk carton needed this adjustment. Therefore, it is likely that the pH meter would have needed more time to settle before it displayed the correct pH of this sample, and the pH of this sample is most likely higher compared to the other samples in this trial. This would affect the entire gelation curve of this sample and is probably the major contributor to the enormous standard deviation that duplicate A is presenting.

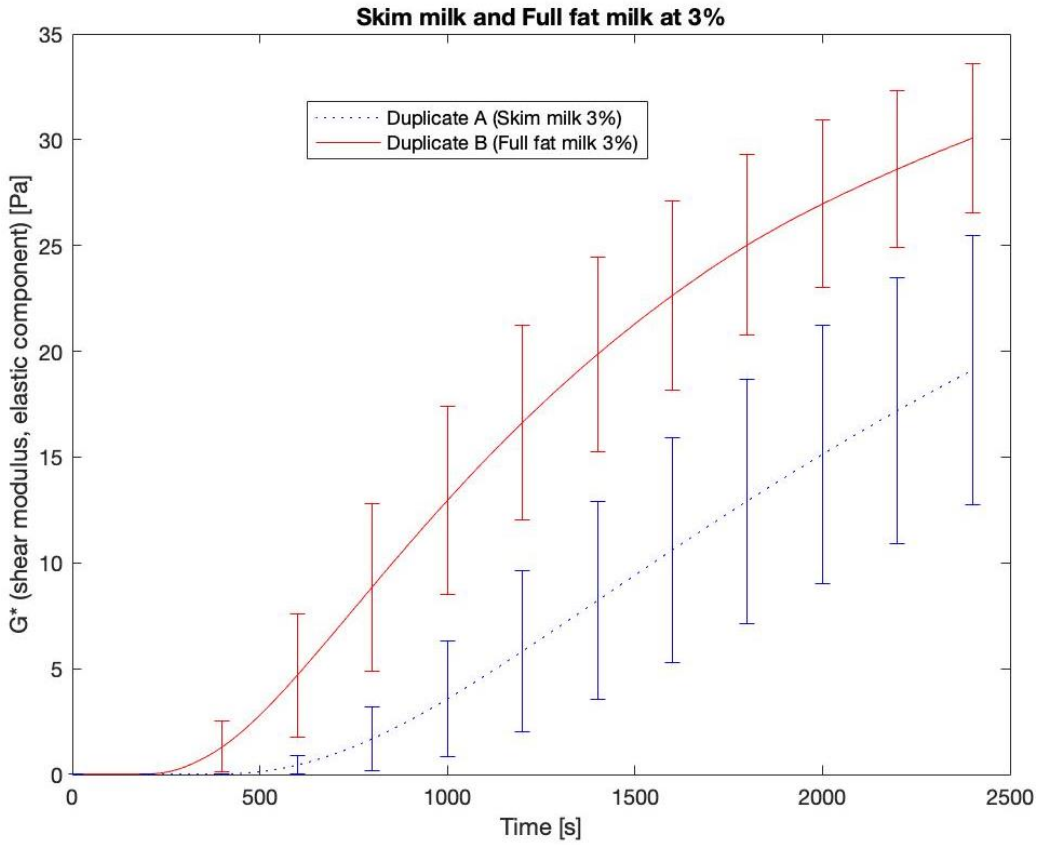

Figure 40 The average G' [Pa] is plotted against Time [s] for duplicate A (Skim milk, 3%) and duplicate B (Full fat milk, 3%) with error bars indicating standard deviation.

These differences are further verified when considering the box plot in Figure 41. It is possible that due to the differences in the gel network created, as there will not be any fat present in the pores in the network when using the skim milk, the gelation curves of duplicate A and duplicate B diverge from each other. When the p-value derived from the 2- Sample T-test is considered, it is clear that the result is not statistically significant as the p-value of 0.341 > α (0.05).

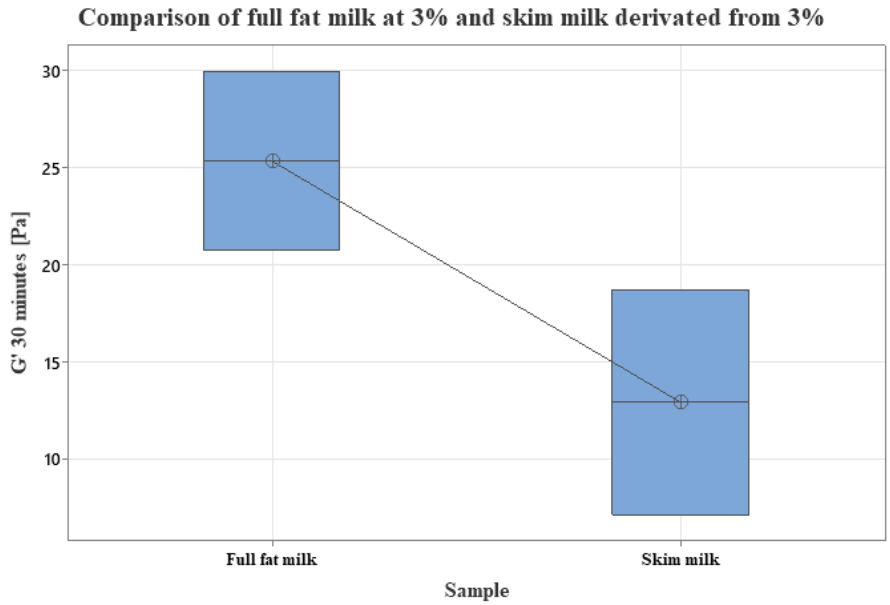

Figure 41 Boxplot comparing the average G' 30 min [Pa] of duplicate A (Skim milk, 3%) and duplicate B (Full fat milk, 3%) in the Effect of fat on gelation-trial.

4.3.2.1.4. ΔBS 30 min

In Table 25, the ΔBS 30 min and standard deviation for duplicates A and B are presented. Duplicate A consists of skim milk samples derived from 3% full fat milk, while duplicate B consists of full fat milk samples at 3%. Here the ΔBS 30 min value for duplicate A is slightly higher at 11.2 % compared to duplicate B at 10.3 %. The standard deviation for duplicate A is also larger compared to that of duplicate B. This is seen quite clearly in the boxplot presented in Figure 42.

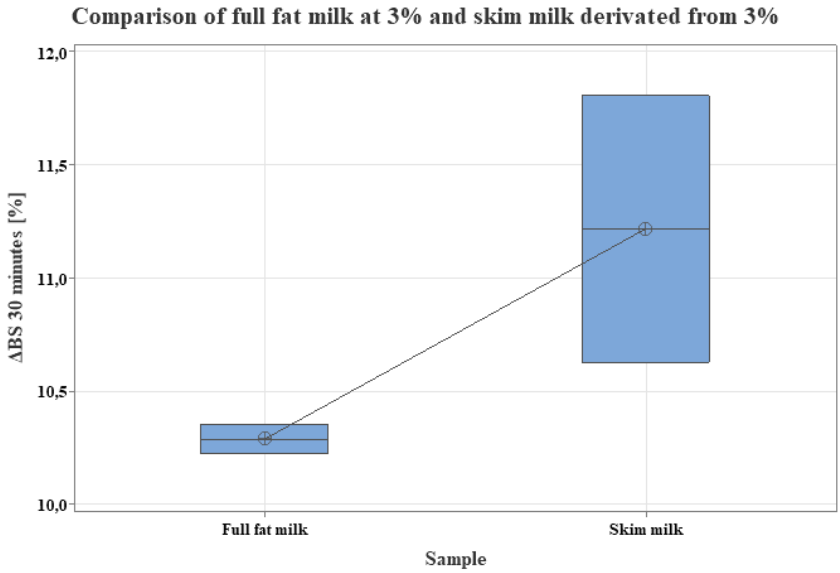

Figure 42 Boxplot comparing the average ΔBS 30 min [%] of duplicate A (Skim milk, 3%) and duplicate B (Full fat milk, 3%) in the Effect of fat on gelation-trial.

In Figure 43, the gelation curve of both duplicate is also presented, as obtained from the Turbiscan analysis. Here, the gelation curves of both duplicates are very similar at start of gelation up until about 1000 s, where they then start to diverge from each other. It is also evident that the standard deviation of duplicate B stays consistently small throughout the entire gelation curve, while the standard deviation of duplicate A increases as the gelation continues, indicating differences between the samples in duplicate A. There is also a small shoulder present at around 500 s, where the increase in ΔBS slows down, to then later increase again. This shoulder seems to coexist with start of gelation, i.e., gelation time. This allows for a better understanding of what happens during the time where the analysis in the Rheometer still have not seen an increase in G' values. A big increase can be seen around 250 s, which indicates that big differences in particle size is happening. This would occur right before the casein micelles start to aggregate. When the p-value derived from the 2-Sample T-test is considered, the result is not statistically significant as the p-value of 0.361 > α (0.05).

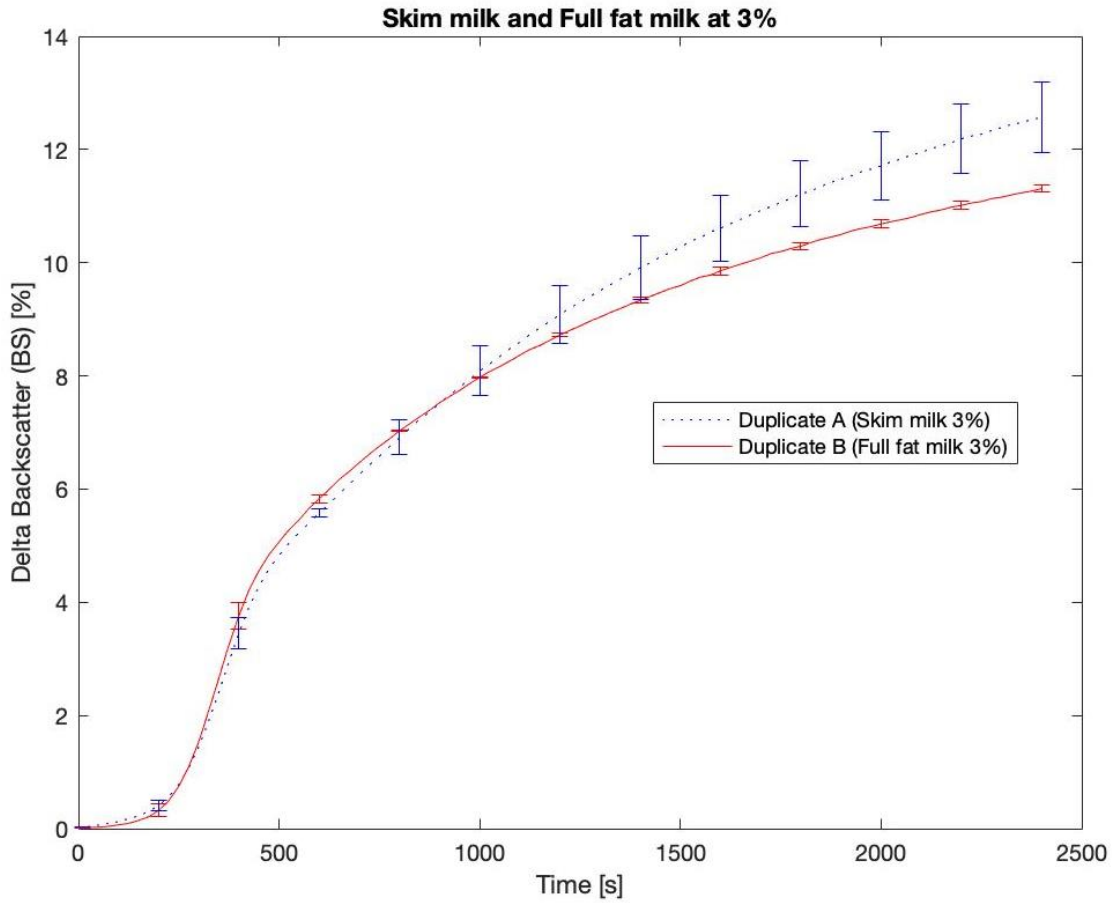

Figure 43 The average ΔBS [%] is plotted against Time [s] for duplicate A (Skim milk, 3%) and duplicate B (Full fat milk, 3%) with error bars indicating standard deviation.

4.3.2.2. Skim milk and Full fat milk at 2%

Here duplicate C (skim milk) and duplicate D (full fat milk) at 2% fat content is compared.

4.3.2.2.1. Gelation time

The gelation time of duplicates C and D, as seen in Table 25, differ from each other, as duplicate C has a shorter gelation time at 310 s comparted to that of duplicate D at 445 s. When looking closer at the boxplot presented in Figure 44, the standard deviation of duplicate C (skim milk) is much smaller compared to that of duplicate D (full fat milk). This contrasts the previous findings between duplicate A and duplicate B, as the skim milk duplicate at 2 % had a shorter gelation time compared to the full fat milk duplicate. However, as the p-value derived from the 2- Sample T-test at 0.366 > α (0.05), this result is not considered statistically significant.

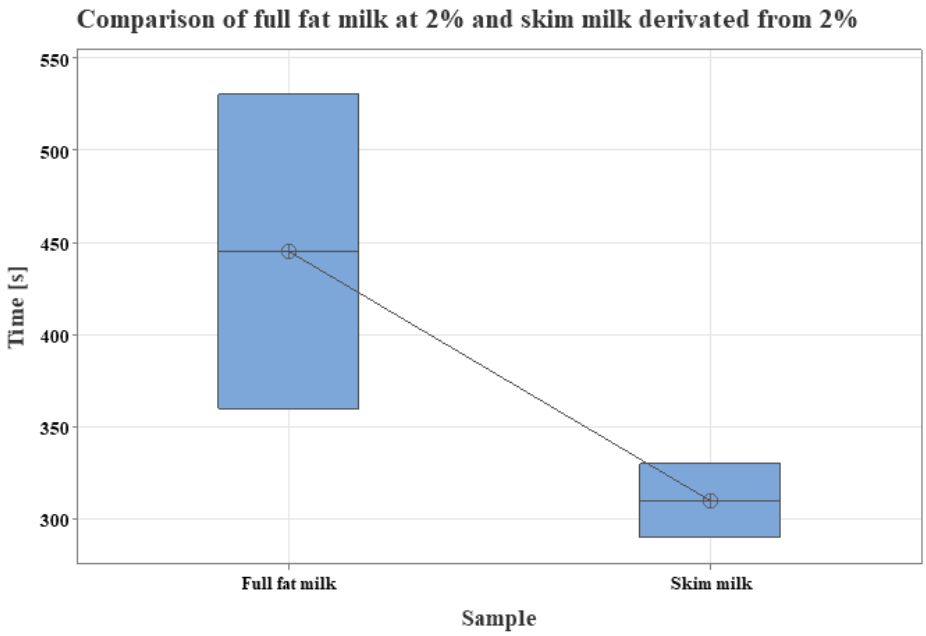

Figure 44 Boxplot comparing the average Gelation time [s] of duplicate C (skim milk, 2%) and duplicate D (Full fat milk, 2%) in the Effect of fat on gelation-trial.

4.3.2.2.2. G' at 2x gelation time

In Table 25, the G' at 2x gelation time and standard deviation for duplicates C and D are presented. Duplicate C consists of skim milk samples derived from 2% full fat milk, while duplicate D consists of full fat milk samples at 2%. When considering the boxplot presented in Figure 45, it is clear that the G' at 2x gelation time between these duplicates are not very similar, as the average of duplicate C is 6.87 Pa (skim milk), while the average for duplicate D is 9.41 Pa (full fat milk). The standard deviations of each duplicate are more similar, but not big enough to bridge the gap between the two averages. When looking at the p-value derived from the 2- Sample T-test, it is clear that the result is not statistically significant as the p-value of 0.112 > α (0.05).

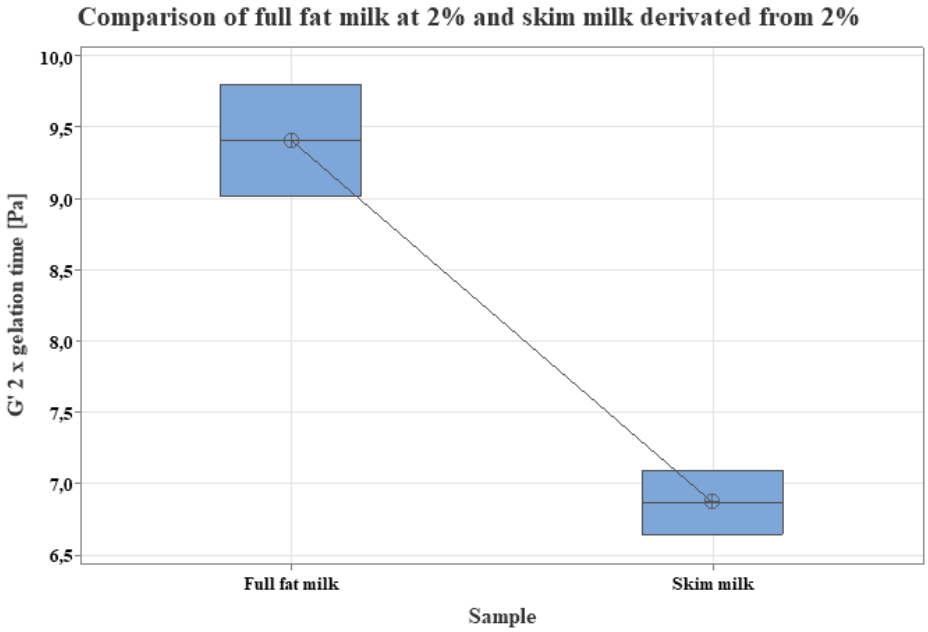

Figure 45 Boxplot comparing the average G' at 2x gelation time [Pa] of duplicate C (Skim milk, 2%) and duplicate D (Full fat milk, 2%) in the Effect of fat on gelation-trial.

4.3.2.2.3. G’ 30 min

The G’ 30 min for duplicates C (skim milk) and D (full fat milk) can be found in Table 25. Duplicates C has a higher G’ 30 min value at 29.5 Pa compared to that of duplicate D at 25.9 Pa. This can be seen clearly in Figure 46. When comparing the gelation curves found in this figure, it is clear that while there are some separation between the two curves, they follow a similar pattern, If the gelation time of duplicate C would have been slightly longer and if the gelation time for duplicate D would have been slightly shorter, the two duplicates would probably have lined up better. When comparing this to the findings between duplicate A and Duplicate B, the conclusions do not align, as the full fat milk have a higher G’ 30 min compared to the skim milk. As the standard deviation of duplicate D is quite large, the upper limit of the standard deviation reaches the average of duplicate C. This can be seen very clearly in the box plot found in Figure 47.

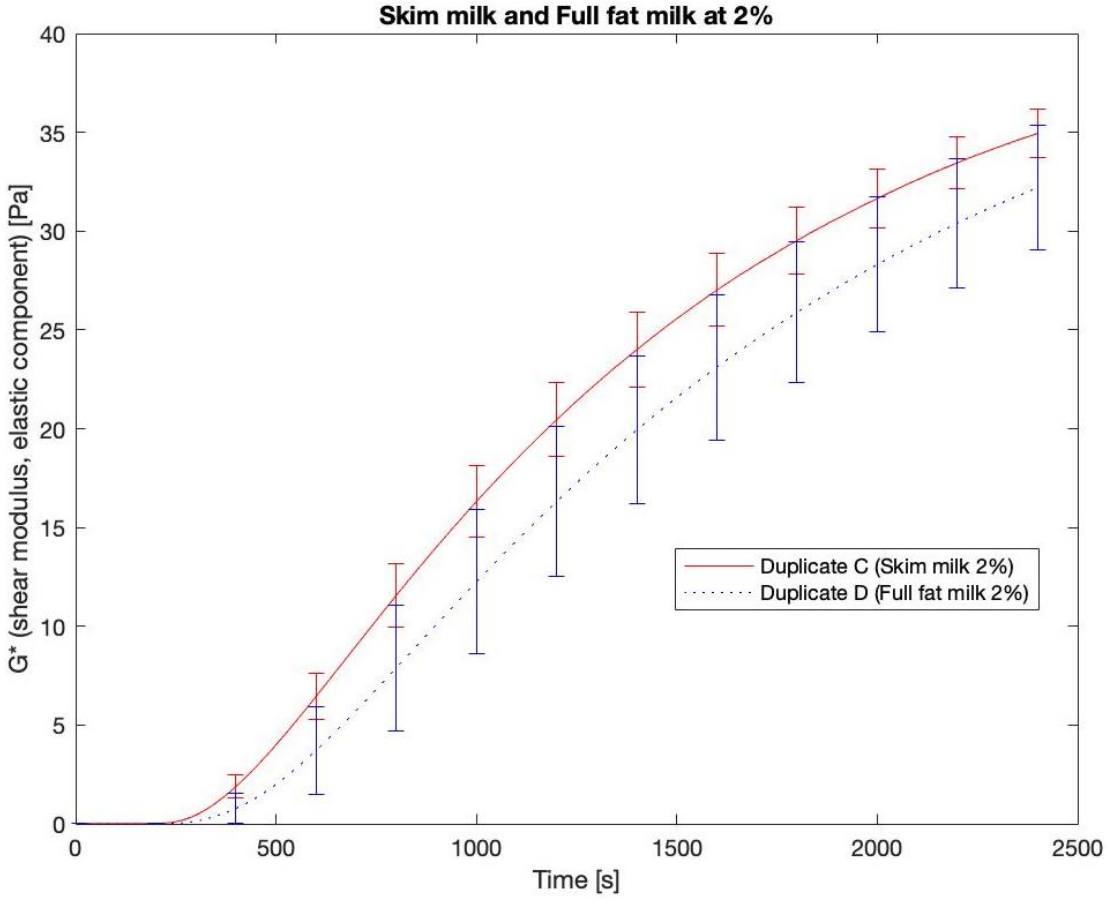

Figure 46 The average G' [Pa] is plotted against Time [s] for duplicate C (Skim milk, 2%) and duplicate D (Full fat milk, 2%) with error bars indicating standard deviation.

As the box plot suggests, the average of duplicate 3 (skim milk) is about the same level as the upper limit of duplicate 4 (full fat milk). This would suggest that the presence of fat reduces the G’ 30 min value, which is also connected to a longer gelation time. This result is however not statistically significant as the p-value of 0.525, derived from the 2-Sample T-test, is larger than α (0.05).

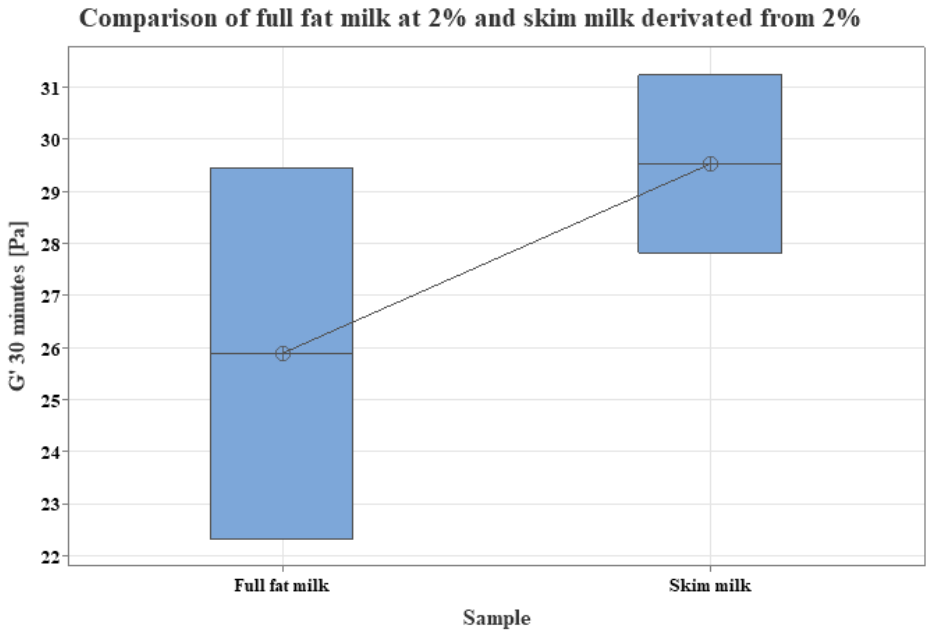

Figure 47 Boxplot comparing the average G' 30 min [Pa] of duplicate C (Skim milk, 2%) and duplicate D (Full fat milk, 2%) in the Effect of fat on gelation-trial.

4.3.2.2.4. ΔBS 30 min

In Table 25, the ΔBS 30 min and standard deviation for duplicates A and B are presented. Duplicate C consists of skim milk samples derived from 3% full fat milk, while duplicate D consists of full fat milk samples at 3%. Here the ΔBS 30 min value for duplicate C is only marginally higher 12.4 % compared to duplicate D at 12.2 %. The standard deviation for duplicate C is also larger compared to that of duplicate D, but the difference is once again very small. This is seen quite clearly in the boxplot presented in Figure 48. The boxplot makes it look like the averages of each duplicate is further apart then they are, as it only ranges from 12.1 % to 12.6 %. Here the standard deviation of neither duplicate is big enough to bridge the gap between the averages, but as the averages are so closely situated, it instead speaks more about the consistency between the four samples that make up duplicate C and duplicate D.

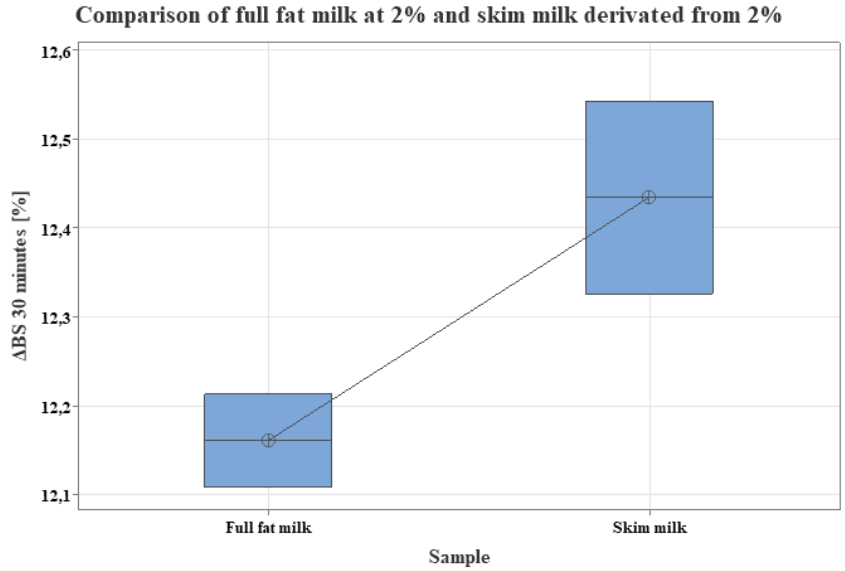

Figure 48 The average ΔBS is plotted against Time [s] for duplicate C (Skim milk, 2%) and duplicate D (Full fat milk, 2%).

The similarities between duplicate C and duplicate D are even more evident when looking closer at Figure 49. The gelation curves of duplicate C and D only present very small differences throughout the entire gelation curve. This would suggest that there are no differences between the full fat milk and the skim milk at the same fat percentage. This does contradict the previous observation regarding the difference between skim milk and full fat milk at 3%, where the skim milk had a higher ΔBS throughout the later part of the gelation curve. Here the shoulder mentioned earlier is also present, and seems to be a bit more pronounced for duplicate C compared to duplicate D. However, the shoulders for both gelation curves occur at the same time, something that suggests that the gelation time should not differ greatly. Regarding the p-value derived from the 2-Sample T-test, as it is larger than $\alpha(0.05)$ at 0.264, the result is not statistically significant.

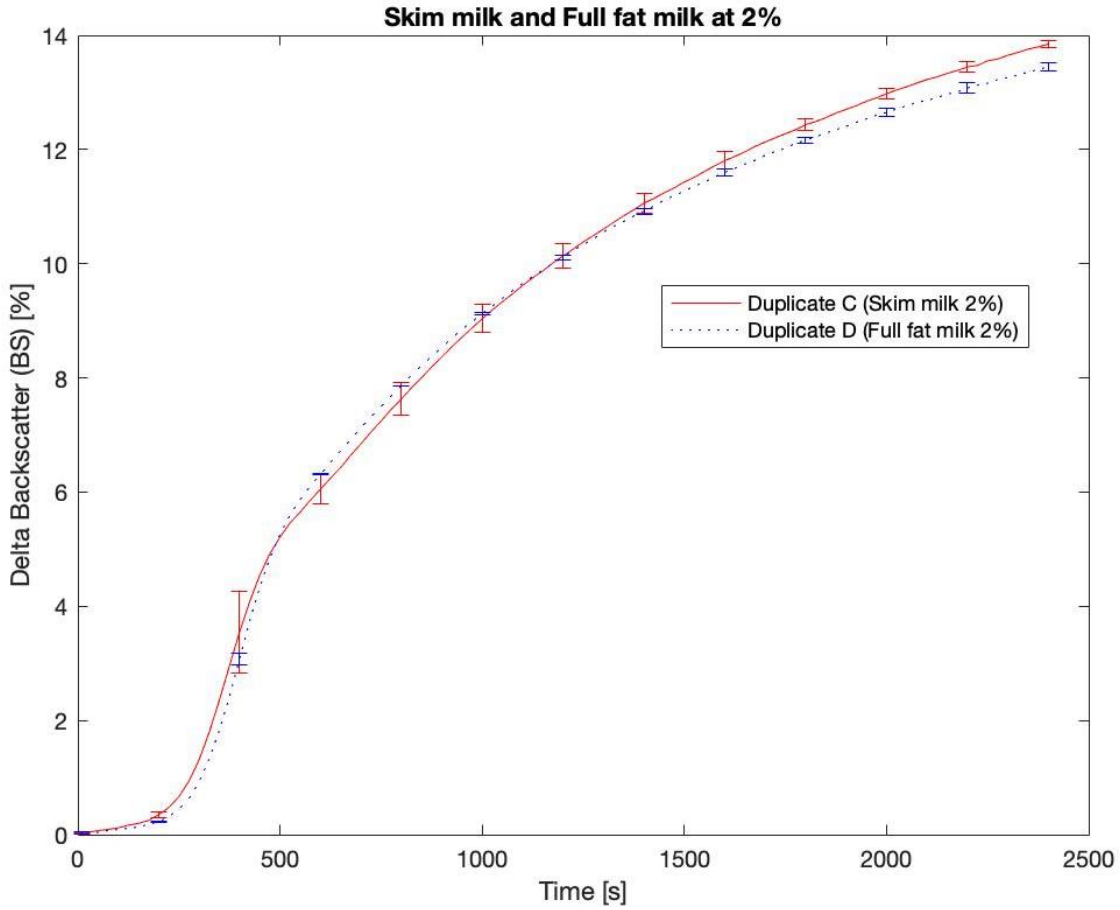

Figure 49 The ΔBS is plotted against Time [s] for duplicate C (Skim milk, 2%) and duplicate D (Full fat milk, 2%).

4.3.3. Effect of Fat content on gelation time, G' at 2x gelation time, G' 30 min and ΔBS 30 min

In this section, skim milk at different fat contents is compared to each other and full fat milk at different fat contents are compared.

4.3.3.1. Skim milk at 3% and skim milk at 2%

Here duplicate A (skim milk) and duplicate C (skim milk) derived from 3% full fat milk is compared.

4.3.3.1.1. Gelation time

The gelation time of duplicate A (skim milk 3%) and duplicate C (skim milk 2%) can be found in Table 25. The averages of each duplicate are as far between each other as possible in this analysis, as the gelation time of duplicate A is 690 s, while the gelation time of duplicate C is 310 s. This is even more evident when looking closer at the boxplot in Figure 50. The standard deviation of duplicate A is very large compared to that of duplicate B, but despite this, duplicate A is nowhere near the average of duplicate C. As mentioned before, duplicate A contains the sample of SSM3,1, which potentially has a much higher pH compared to the other samples in these duplicates and would most likely cause a longer gelation time. However there seems to be differences despite this samples, as the standard deviation of duplicate A is not close the average of duplicate C. Therefore, it could be concluded that a smaller fat content would result in a shorter gelation time. However, as the p-value obtained from the 2-Sample T-test at 0.241 > α(0.05), the result is not significant.

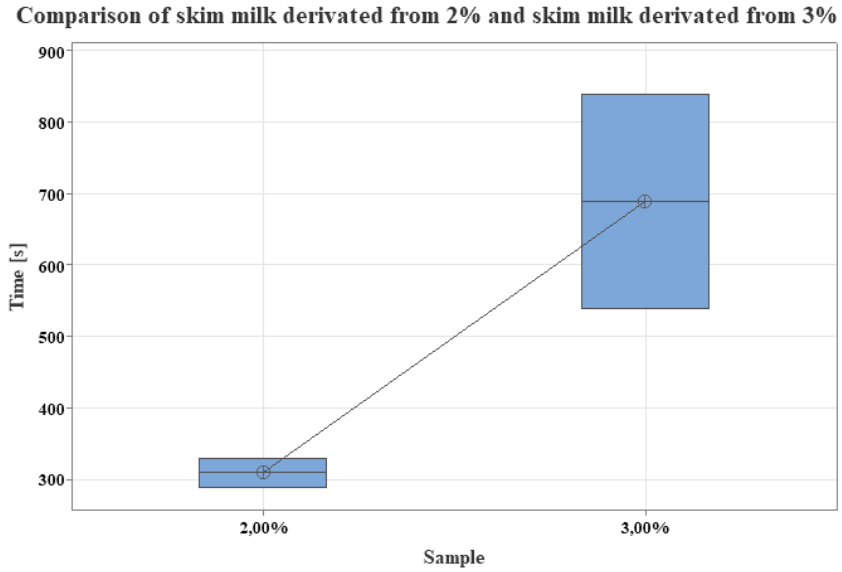

Figure 50 Boxplot comparing the average Gelation time [s] of duplicate A (skim milk, 3%) and duplicate C (Skim milk, 2%) in the Effect of fat on gelation-trial.

4.3.3.1.2. G' at 2x gelation time

In Table 25 above, the G' at 2x gelation time for duplicate A (skim milk 3%) and duplicate C (skim milk 2%) are found. The G' at 2x gelation time for duplicate A is only slightly smaller at 6.82 Pa compared to 6.87 Pa for duplicate C. This result is even more evident when looking closer at the boxplot in Figure 51. The standard deviation for duplicate A (3%) is higher compared to that of duplicate B (2%), but the standard deviation of both duplicates encapsulated the average of the other duplicate. This indicates that there are only small differences between the duplicates, and that there is no difference between the duplicates regardless of their fat content. This is further supported by the p-value obtained from the 2-Sample T-test at 0.960, which is larger than α(0.05). The result is therefore not statistically significant. As both duplicates consist of skim milk, it is possible that the presence of fat is more important compared to the fat content of the milk that the skim milk was derived from.

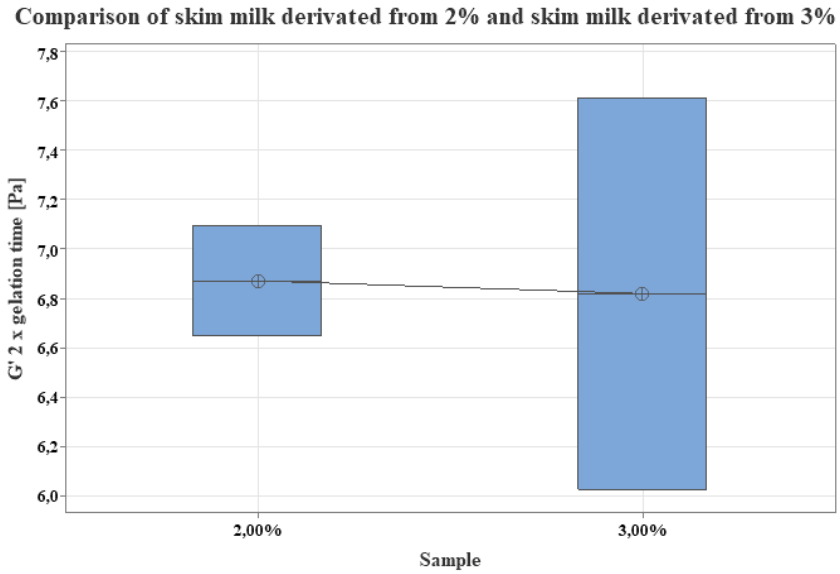

Figure 51 Boxplot comparing the average G' at 2x gelation time [Pa] of duplicate A (skim milk, 3%) and duplicate C (Skim milk, 2%) in the Effect of fat on gelation-trial.

4.3.3.1.3. G' 30 min

G' at 30 minutes

In Table 25 above, the G' 30 min for duplicate A (skim milk 3%) and duplicate C (skim milk 2%) are found. Here some major differences between the different duplicates and their G' 30min values can be seen, as the G' 30 min value of duplicate C is more than double the size of duplicate A. This is visualized in the boxplot in Figure 52. As mentioned earlier, one of the samples (SSM3,1) of duplicate A has most probably a higher pH compared to the other samples in this analysis, which would cause a longer gelation time and most probably cause the smaller G' 30 min. It is possible that the 3% skim milk would cause a longer gelation time and lower G' 30 min value, but it is not possible to determine that from these results.

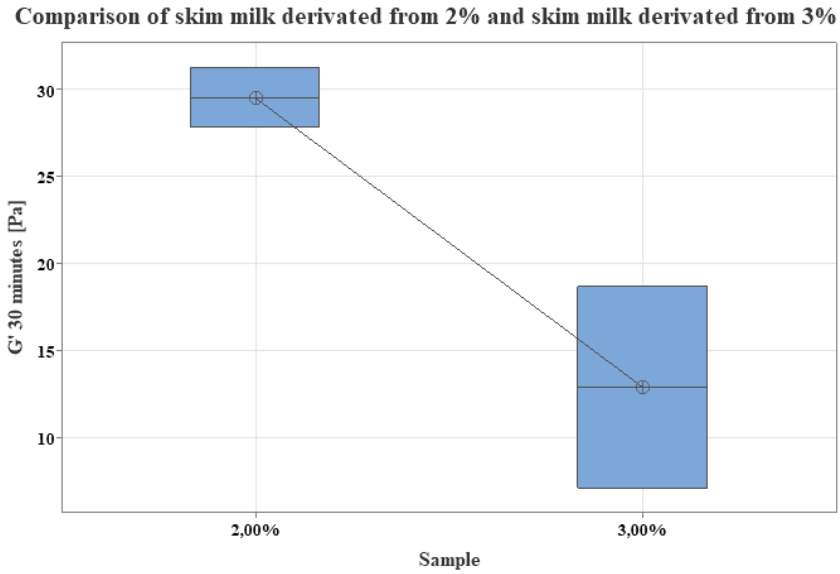

Figure 52 Boxplot comparing the average G' 30 min [Pa] of duplicate A (skim milk, 3%) and duplicate C (Skim milk, 2%) in the Effect of fat on gelation-trial.

The statistical comparison between the skim milk from 2% and the skim milk of 3% showed that the G' after 30 minutes for the skim milk from 2%, as it is seen in Table 25 and the boxplot (figure 51), is higher and had a smaller standard deviation. The test is not significant as the P value is > α (0.05).

The major differences between the two duplicates are even more apparent when the whole gelation curve is considered, as can be seen in Figure 53. Here the separation between the duplicates is clear from the start of gelation and the differences just continue to increase throughout the gelation curve. When looking closer at the gelation curve of duplicate A, it seems like the curve have not stopped its current increase but would continue to increase in its G' value if the gelation would continue for a longer period of time. This contrasts with duplicate C, where the increase in G' is slowly decreasing and would soon reach it maximum. According to the 2-Sample T-test, this result is not statistically significant, as the p-value obtained 0.222 > α(0.05).

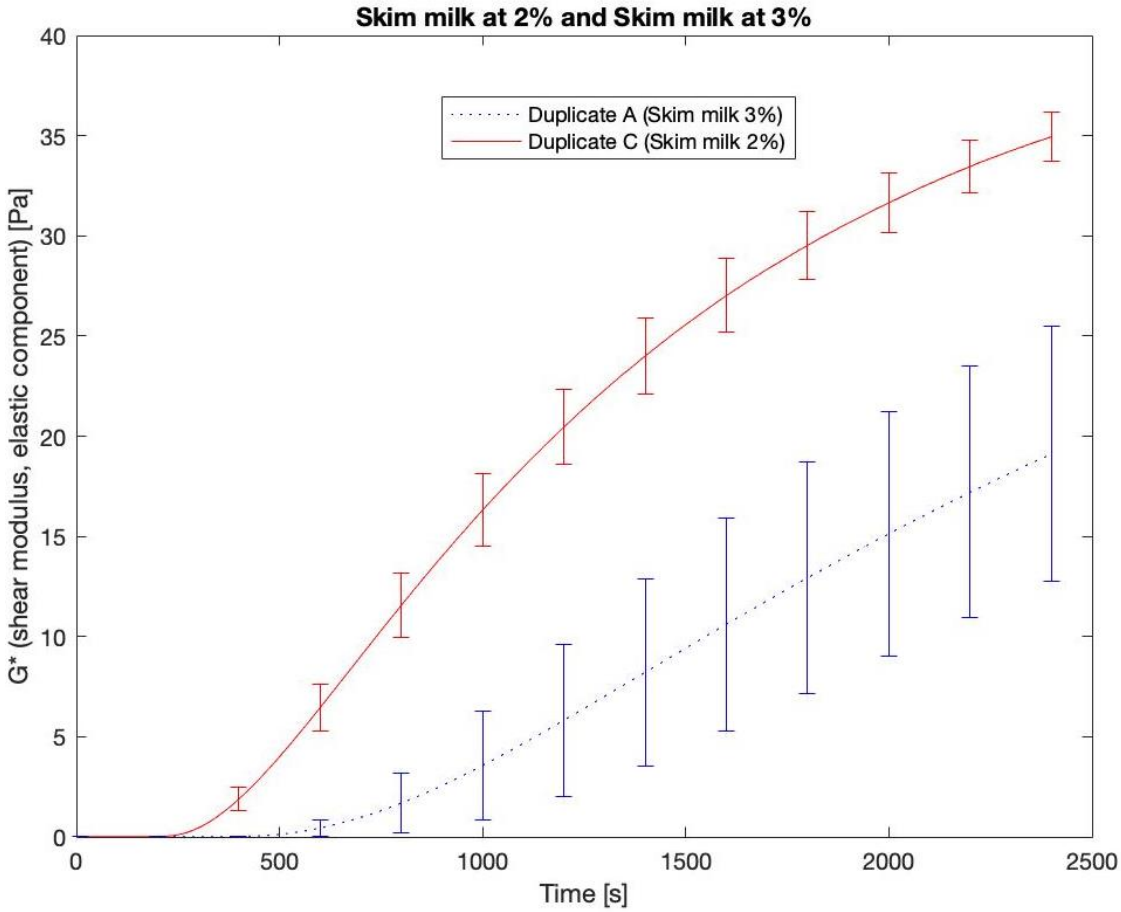

Figure 53 The average G' [Pa] is plotted against Time [s] for duplicate A (Skim milk, 3%) and duplicate C (Skim milk, 2%) with error bars indicating standard deviation.

4.3.3.1.4. ΔBS 30 min

The last comparison between duplicates A (skim milk 3%) and C (skim milk 2%) is regarding the ΔBS 30 min value, which can be found in Table 25. The ΔBS 30 min value for duplicate C is higher compared to that of duplicate A, at 12.4 % and 11.2 % respectively. This is further visualized in the boxplot in Figure 54, where the higher standard deviation of duplicate A do not reach to the average of duplicate C.

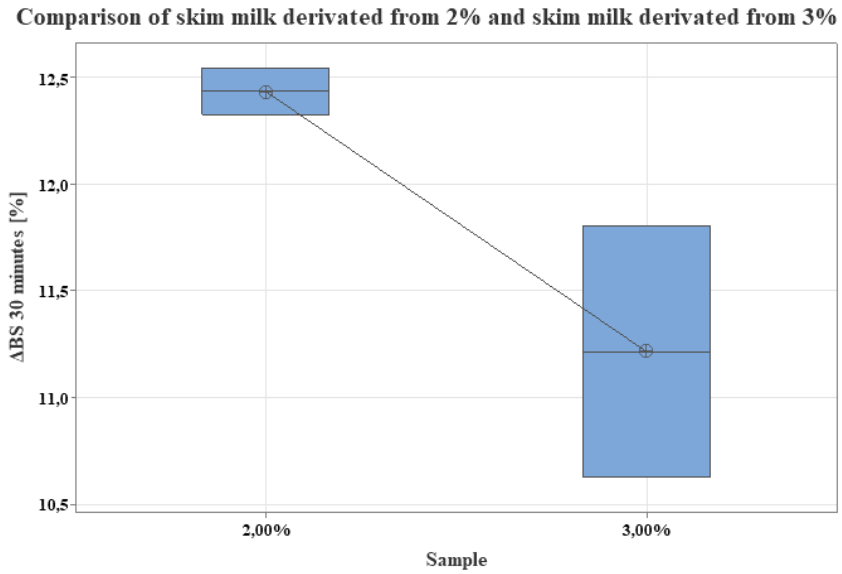

Figure 54 Boxplot comparing the average ΔBS 30 min [Pa] of duplicate A (skim milk, 3%) and duplicate C (Skim milk, 2%) in the Effect of fat on gelation-trial.

Regarding the entire gelation curve of these samples, found in Figure 55, it is possible to see that both duplicates have a very similar start of gelation and follow a very similar pattern up until 500 s. After 500 s, the duplicates diverge, and duplicate C has a higher ΔBS at the same point in time compared to duplicate A. Both duplicates present shoulders at approximately the same time, but at different ΔBS values. These shoulders seem to sometimes coincide with the gelation time, where start of gelation is considered to happen. The increase right before the shoulder explains some of the behavior that is not possible see when the Rheometer analysis is performed. It suggests an increase in the size of particles before they start to aggregate. It is possible that the larger ΔBS of duplicate C after 500 s is due to the small differences in fat content, as duplicate C has a slightly higher fat content at 0.30 % (Table 25) compared to duplicate A at 0.21%. There should therefore be a higher percentage of fat present in the gel network forming, which could have an effect on the ΔBS. This result is however not statistically significant as the p-value, 0.290, obtained from the 2-Sample T-test is larger than α(0.05).

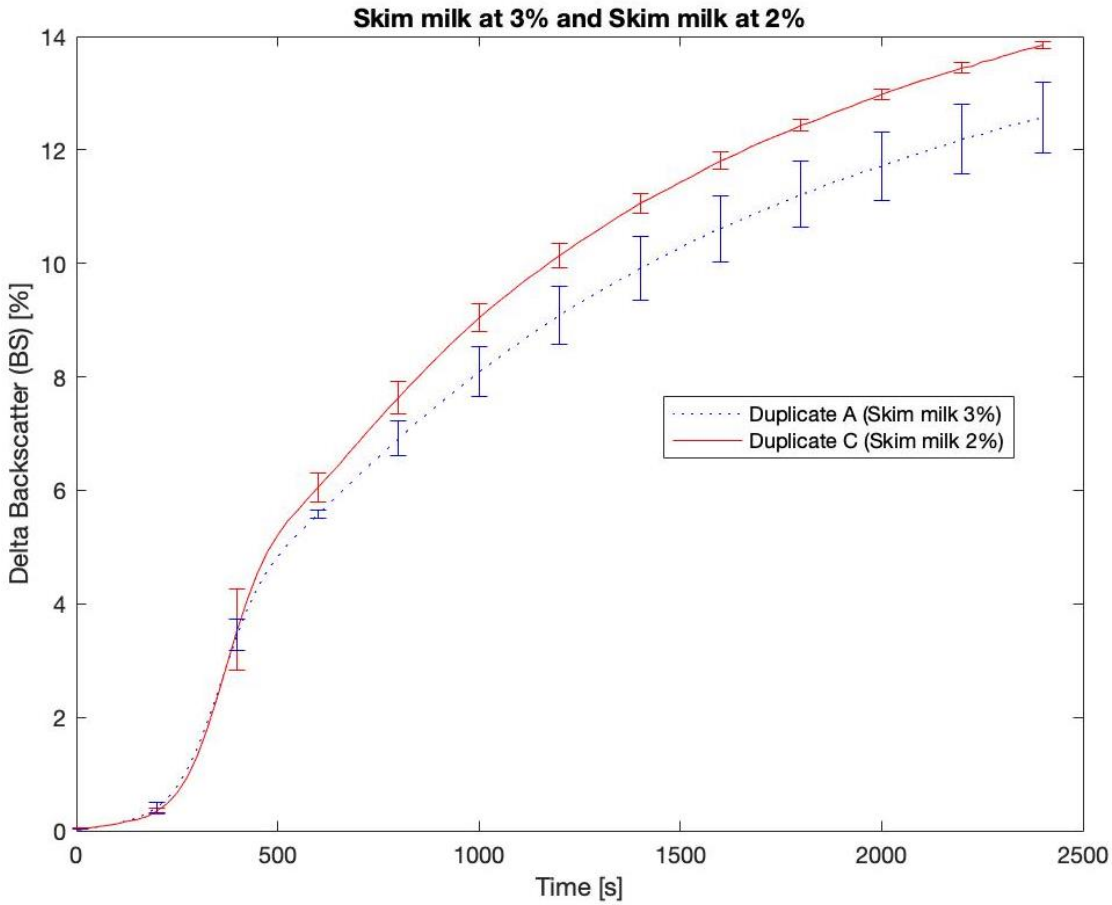

Figure 55 The average ΔBS 30 min [%] is plotted against Time [s] for duplicate A (Skim milk, 3%) and duplicate C (Skim milk, 2%) with error bars indicating standard deviation.

4.3.3.2. Full fat milk at 3% and Full fat milk at 2%

Here duplicate B (full fat milk) and duplicate D (full fat milk) at 2% fat content is compared.

4.3.3.2.1. Gelation time

Here duplicate B (full fat milk 3%) is compared to duplicate D (full fat milk 3%) regarding their gelation time, as seen in Table 25. Here the difference in gelation time between the duplicates is quite large, as the gelation time for duplicate B is shorter at 385 s, compared to duplicate D at 445 s, as can be seen in the boxplot presented in Figure 56. Here the standard deviation for both duplicates are large enough to reach the average of the other duplicates, making it harder to distinguish between them. This suggests that a lower fat content could result in a shorter gelation time, however, as the result is not statistically significant, due to the p-value from the 2-Sample T-test at $0.720 > \alpha(0.05)$.

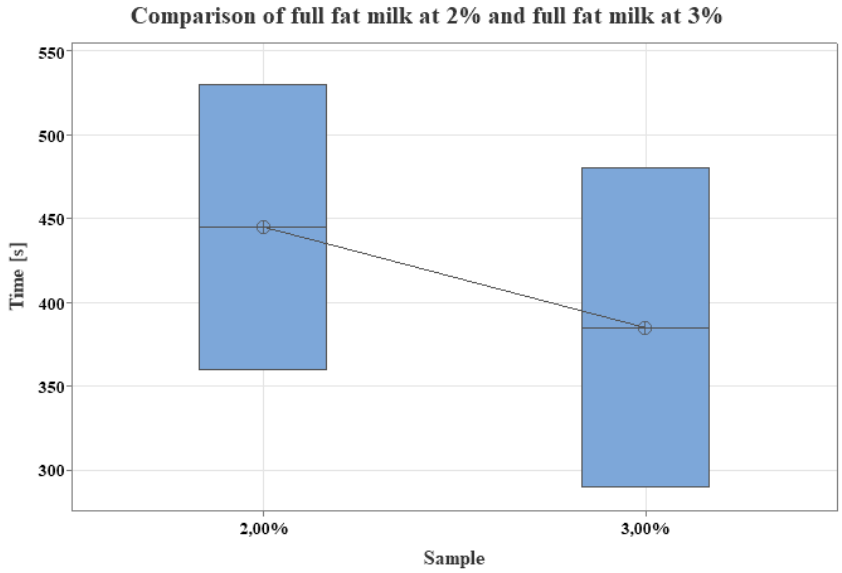

Figure 56 Boxplot comparing the average Gelation time [s] of duplicate B (Full fat milk, 3%) and duplicate D (Full fat milk, 2%) in the Effect of fat on gelation-trial.

4.3.3.2.2. G' at 2x gelation time

In Table 25, the G' at 2x gelation time can be found for duplicate B (full fat milk 3%) and for duplicate C (full fat milk 2%). Here the G' at 2x gelation time for duplicate D is larger compared to that of duplicate B, at 9.41 Pa and 7.41 Pa respectively. The standard deviation of each duplicate is about the same size and is visualized in the boxplot found in Figure 57. There are some distinct differentiations between these duplicates, which suggests that there is an effect on the G' at2x gelation time due to fat content. The p-value derived from the 2-Sample T-test does however as state that the result is not statistically significant, as it is larger than $\alpha(0.05)$ at 0.165. This however a smaller p-value compared to other p-values mentioned in this report, which does give this result some more credibility, even though it is not significant.

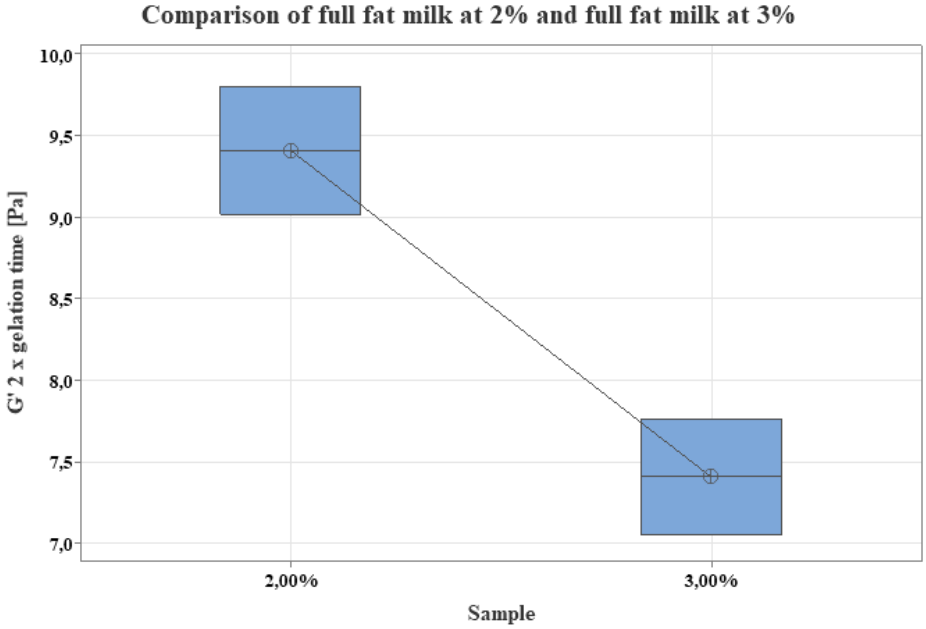

Figure 57 Boxplot comparing the average G' at 2x gelation time [Pa] of duplicate B (Full fat milk, 3%) and duplicate D (Full fat milk, 2%) in the Effect of fat on gelation-trial.

4.3.3.2.3. G’ 30 min

The G’ 30 min values obtained for duplicate B (full fat milk 3 %) and duplicate D (full fat milk 2%) can be found in Table 25. The G’ 30 min value for duplicate B is only slightly smaller at 25.3 Pa, compared to 25.9 Pa for duplicate D. The standard deviations of these duplicate are very large, as seen in the boxplot presented in Figure 58. As the averages of these duplicates are so much alike, coupled with a large standard deviation, no real distinct difference can be seen between these duplicates. This is further supported when looking closer at the plotted gelation curve in Figure 59.

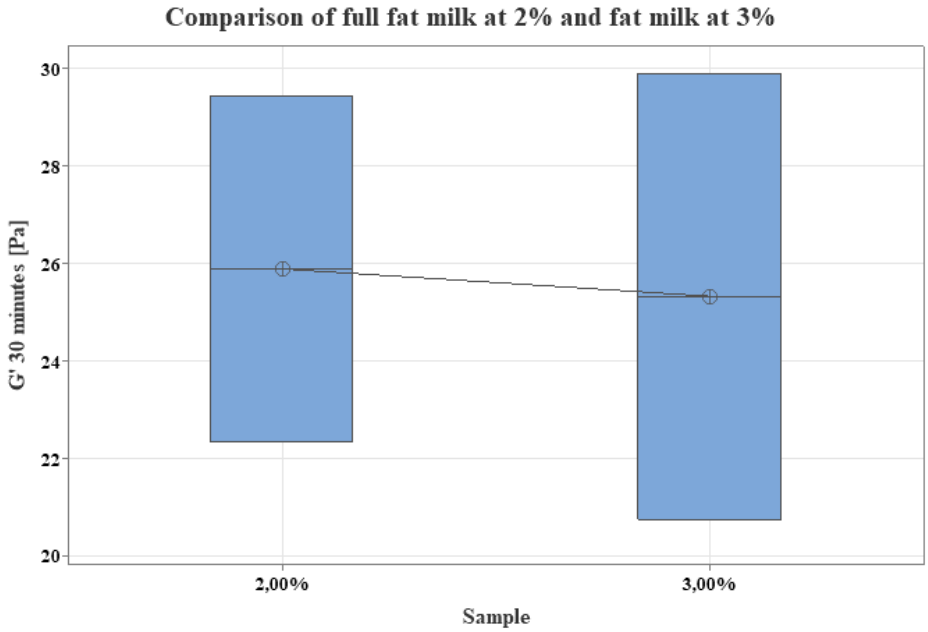

Figure 58 Boxplot comparing the average G’ 30 min [Pa] of duplicate B (Full fat milk, 3%) and duplicate D (Full fat milk, 2%) in the Effect of fat on gelation-trial.

Duplicate B has a shorter gelation time compared to duplicate D, as mentioned before. Due to the shorter gelation time, duplicate B stops increasing earlier compared to duplicate D, resulting in a slightly lower G’ 30 min value and a lower G’ value at the very end of gelation. As the differences between the duplicates during gelation is small and the standard deviations are big, there is no surprise that the result according to the 2-Sample T-test is not statistically significant. This is due to the p-value obtained 0.939 is much larger than $\alpha(0.05)$. This indicates that the fat content of the milk has no effect on the G’ 30 min value obtained.

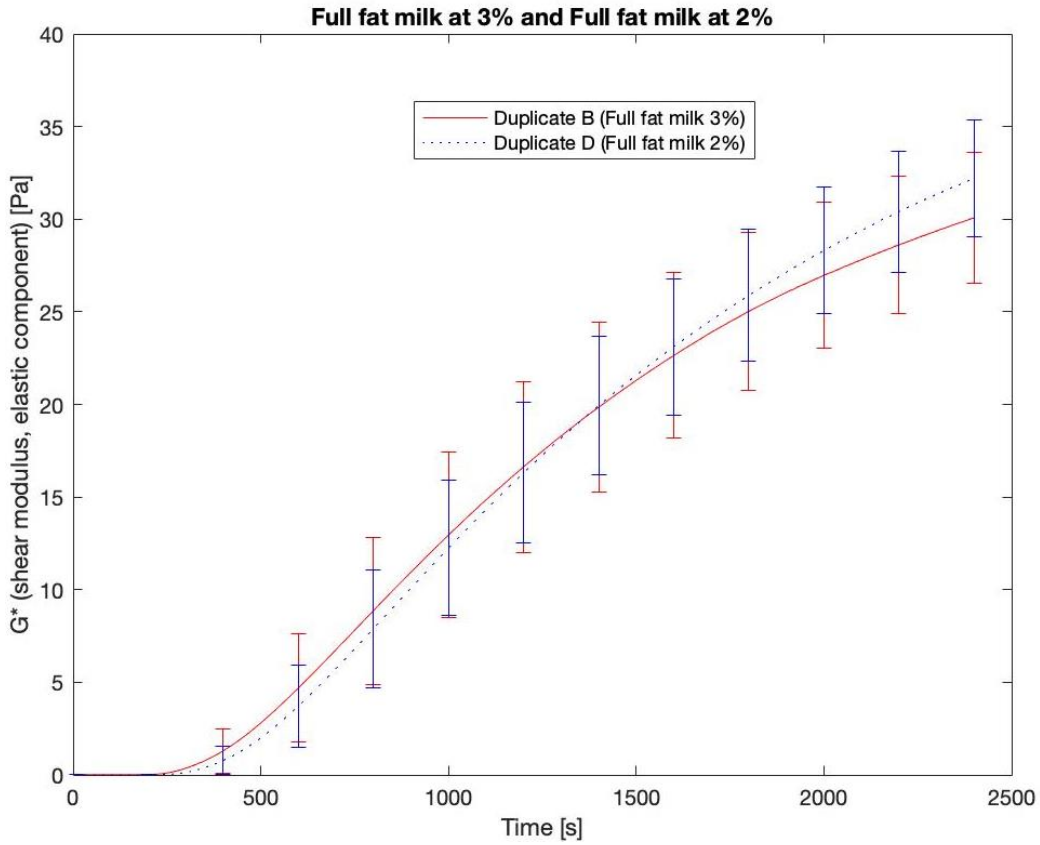

Figure 59 The average G' [Pa] is plotted against Time [s] for duplicate B (Full fat milk, 3%) and duplicate D (Full fat milk, 2%) with error bars indicating standard deviation.

4.3.3.2.4. ΔBS 30 min

The last comparison made between duplicates B and D is of their respective ΔBS 30 min values, which can be found in Table 25. Duplicate B has a smaller ΔBS 30 min value at 10.3 %, compared to that of duplicate D at 12.2. The standard deviation of these duplicates is very small, indicating consistent result between the samples of each duplicate. This is further visualized in the boxplot found in Figure 60.

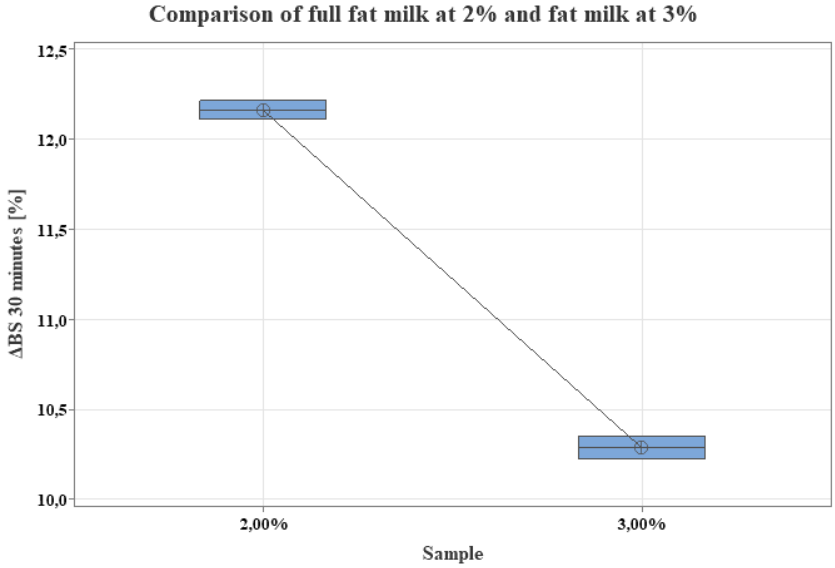

Figure 60 Boxplot comparing the average ΔBS 30 min [Pa] of duplicate B (Full fat milk, 3%) and duplicate D (Full fat milk, 2%) in the Effect of fat on gelation-trial.

In Figure 61, the entirety of the gelation curve is seen for both duplicates. Here the duplicates differentiate slightly in the beginning of the gelation curve to then intersect at about 500 s, where the shoulders of duplicates occur as well. From there duplicate B has consistently lower ΔBS values compared to that of duplicate D. Throughout most of the gelation curve, the standard deviation of both duplicates is very small, and inhibits any interaction between the gelation curves, except at very similar ΔBS values.

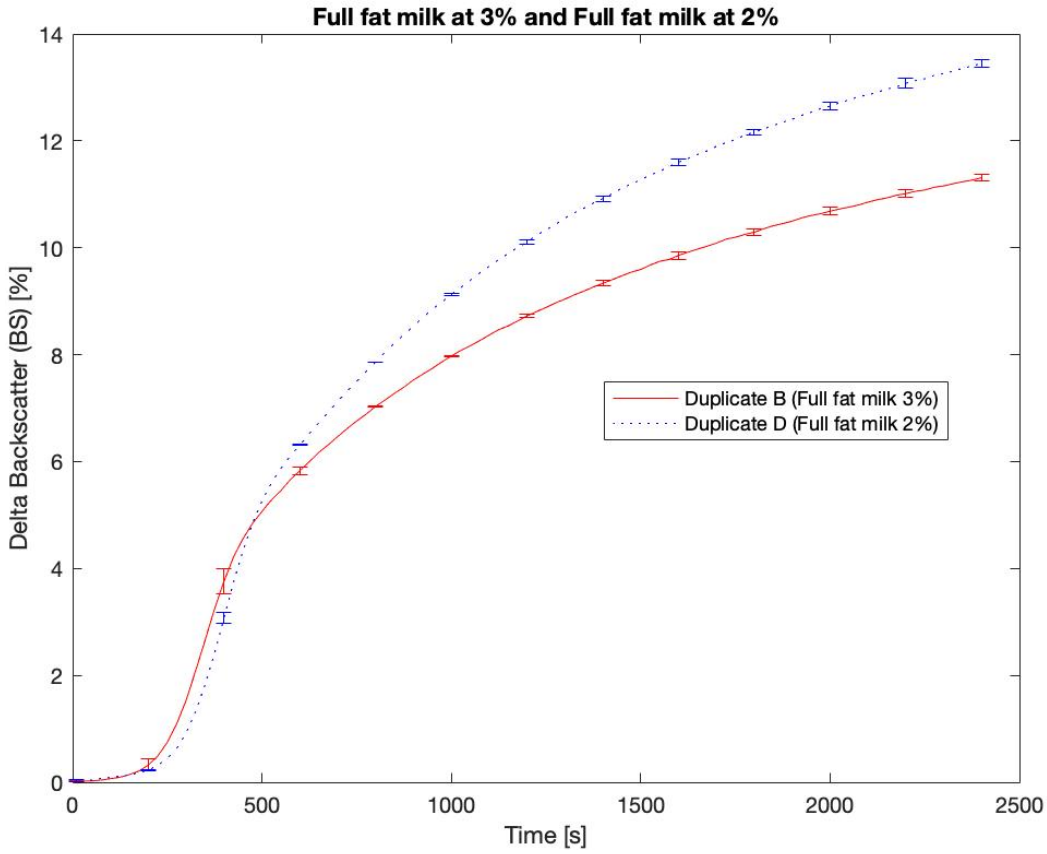

Figure 61 The average G' [Pa] is plotted against Time [s] for duplicate B (Full fat milk, 3%) and duplicate D (Full fat milk, 2%) with error bars indicating standard deviation.

There seem to be some distinct differences between these duplicates, which is verified by the 2-Sample T-test. According to the 2-Sample T-test, the result is significant as the p-value obtained $0.028 < \alpha(0.05)$. This indicates that the fat content of the milk does impact the ΔBS 30 min. This suggests that there is a difference in the gel formation between these duplicates. There is a higher amount of backscattering for duplicate D compared to duplicate B, even though duplicate B has a higher fat content than that of duplicate D. This could suggest that duplicate B has a denser protein network, that might be caused by the lower quantity of fat. Duplicate D has a less dense protein network, perhaps due to a higher amount of fat situated in between the aggregated casein micelles strands in the protein network.

5. General discussion

During this general discussion, the result mentioned above in the result and discussion is summarized to give a clearer picture of the overall result.

Properties of the milk used during both the Response Surface Method trial and the Effect of fat on gelation-trial, were investigated to determine the milk content (fat, protein, lactose, SNF and TS) and particle size of the casein micelles and fat globules. The milk content of the two cartons (carton 1 and carton 2 of Åsens lantmjölk Gammaldags (2.9-3.1 % fat)) of milk used for the Response Surface Method trial had very similar contents, and except for two instances, differed very little regarding the size of the casein micelles. Here the pH had an impact on the size of the casein micelles, which is expected. However, an increase in casein micelles size at a decrease in pH, as found in these results, contradicts other sources stating that the size of casein micelles should decrease with a decreasing pH. Larger differentiation of particle size was expected and seem to contribute to overall consensus that this result is, for a lack of a better word, weird and nonsensical. These results could possibly be due to the change in pH, when the milk samples are added to the Mastersizer, as the Milli-Q water used has a higher pH compared to that of the milk. The casein micelles could possibly then revert back to a different size closer to their original size. A buffer should be added to the Milli-Q water, bringing the water to a pH level that is consistent with the pH of the milk samples, when using this method in the future.

The milk used in the Effect of fat on gelation-trial presented larger differences regarding the contents of the milk, especially regarding the fat and protein content of the two skim milks used (carton 3 of Åsens lantmjölk Gammaldags (2.9-3.1 % fat), and carton 1 of Åsens lantmjölk Orginal (1.7-1.9 % fat)). Differences in fat and TS content and between the full fat versions of these cartons of milk was expected due to the difference in original fat content. The size of the casein micelles is very similar between cartons of milk and the same can be seen for the fat globule size. Lastly, it was noted that an increased addition of $CaCl_2$ up to 10.0 mmol/L caused an increase in the concentration of free calcium ions (Ca^{2+}) found in the milk. This response did however not seem linear, as the increase Ca^{2+} concentration did not increase between the 8.7 mmol/L and 10.0 mmol/L additions. This could possibly be due to that not all $CaCl_2$ added will be as Ca^{2+} in the milk but could be found bound to casein micelles or in other complexes.

The factor of pH is according to the result represented above significant for gelling properties such as gelation time, G' 30 min, but not for ΔBS 30 min. Regarding gelation time and G' 30 min, the pH adjustment did not result in a linear response, suggesting that lowering or raising the pH might not result in a linear decrease or increase of these gelling properties. Gelation time is decreased by the addition of pH, which was expected according to established by Walstra [31]. The addition of $CaCl_2$ does not seem to have any statistically significant effect on these gelling properties, however. As stated earlier, there is a stronger correlation between pH compared to $CaCl_2$ and gelling properties, but there is a connection regarding $CaCl_2$ that cannot be seen in these results that was expected. The connection between gelation time and $CaCl_2$ was clear according to Walstra [31]. There also seem to have been some large inconsistencies between days of analysis as large standard deviations within duplicates, especially regarding the gelation time and G' 30 min, suggests inconsistencies between samples of these duplicates.

Large inconsistencies were also noticed during the Effect of fat on gelation-trial, were some duplicates had major differences between samples, as evident by their large standard deviation. From these results, only the fat content of full fat milk seemed to have a significant impact of the ΔBS 30 min. This could possibly be due to a tighter network being created when smaller quantities of fat is present in the gel network. However, it was most surprising that a similar effect was not

noticed when the full fat versions of each milk (Åsens lantmjölk Gammaldags (2.9-3.1 % fat), and Åsens lantmjölk Orginal (1.7-1.9 % fat)) were compared to their respective skim milk versions, as the differences in fat content is even larger there. It was also unexpected that neither the presence of fat nor the fat content had any significant effect on the gelation time, G' at 2x gelation time or the G' 30 min. This could possibly be due to the very small samples size of this trial, where only 4 duplicates were included, or fat as a factor does not contribute to these gelling properties.

6. Conclusion

The properties of the milk used during the two trials were investigated to establish a baseline ahead of gelation. The differences in fat, protein, lactose, SNF and TS content for milk carton 1 (3%fat) and 2 (3% fat) used during the Response Surface method trial are minimal. Milk carton 3 (3% fat) and milk carton 1 (2% fat) used during the Effect of fat on gelation-trial differed more regarding the protein, lactose, SNF and TS content. Some differences were due to the handling of the milk during centrifugation and subsequent removal of fat. Carton 3 (3%fat) differs from carton 1 (3% fat) and carton 2 (3% fat) regarding some of its content. This is possibly due to seasonal changes, as the milk cartons were bought between February and April.

As expected, a higher concentration of free Ca^{2+} ions were observed during the Response Surface method trial as a higher concentration of $CaCl_2$ was added.

Regarding the particle size, only small differences could be seen between milk samples at different pH and addition of $CaCl_2$. However, the factor of pH has a statistically significant impact on the particle size, as an increase in particle size would be caused by a decrease in pH. This contradicts already established findings regarding the effect of pH on casein micelle size. This could be due to a difference in pH between the milk samples and the Milli-Q water used during the particle size analysis. The addition of $CaCl_2$ does not have a statistically significant effect on particle size. The particle size of skim milk samples used in the Effect of fat on gelation-trial presented similar dimension. Similarly, the particle size between samples of full fat milk only differed slightly. As expected, the presence of fat in the milk samples increased the particle size, due to the much larger dimension of the fat globules compared to the casein micelles.

The impact of pH on the gelling properties of skim milk was investigated during the Response Surface method trial. It was noted that the pH was statistically significant for the gelation time and G' 30 min, but not for the ΔBS 30 min. This is in contrast to the other factor during this trial, the addition of $CaCl_2$. The addition of $CaCl_2$ did not have a statistically significant effect on gelation time, G' 30 min or ΔBS 30 min, even though there is a proven effect of Ca^{2+} on gelation time. The gelation time of the skim milk samples were significantly affected by the combination pH*pH, suggesting that a curvature is present in the response to gelation time by the addition of pH. The combination of pH*$CaCl_2$ almost has a statistically significant effect on the gelation time, while the $CaCl_2$*$CaCl_2$ does not. For the G' 30 min, only the combination of pH*pH is statistically significant, indicating once again that the response of G' 30 min is not linear regarding the pH. Regarding the ΔBS 30 min, neither combination of the factors, i.e., pH*pH, pH*$CaCl_2$ nor $CaCl_2$*$CaCl_2$ are statistically significant.

In the Effect of fat on gelation-trial, the presence of fat and the fat content of the milk samples were investigated. For the gelation time, neither the fat content nor presence of fat had a statistically significant impact. This was also observed for the G' at 2x gelation time and G' 30 min. The fat content was however statistically significant for the ΔBS 30 min. As the ΔBS is closely related to the particle size, it is reasonable to find significant difference between the fat contents. However, a similar difference was expected regarding the presence of fat or not, as the size of the fat globules are much larger compared to that of the casein micelles.

In conclusion, the pH is an important factor regarding gelling properties of rennet milk gels, while the $CaCl_2$ does not have any effect on the variables of gelation time, G' 30 min and ΔBS 30 min. The fat content and the presence of fat had no significant effect on the gelation time, G' at 2x gelation time and G' 30 min, while the fat content had a significant effect on the ΔBS 30 min.

7. Future aspects

As future aspects, more trials are important in order to establish the statistical significance of the factors of pH, $CaCl_2$ and fat. This is of importance, especially for the fat factor, as the number of duplicates used in this master thesis was very low and large inconsistencies were noticed between samples of these duplicates. The trials that were performed during this master thesis should probably be done again to verify the validity of the results presented. The time constrain was a serious factor in the lower number of samples tested, and a longer time period would enable a larger samples size to be used.

The effect of $CaCl_2$ would need to be further investigated. Perhaps the significant effect of $CaCl_2$ was lost due to the large span of pH used. If a smaller span of pH was used, for example 6.7-6.0 or 6.0-5.5, a larger number of different additions of $CaCl_2$ could be tested. It is also possible use multiple additions of $CaCl_2$ at the same pH in order to really study the effect of $CaCl_2$ or to study a large number of samples at the same pH and $CaCl_2$ additions to further investigate how the content of the milk, different trial days and small differences in pH and $CaCl_2$ would affect the reproducibility of these results.

When using the Mastersizer 2000 to determine the particle size for casein micelles at a certain pH, the Milli-Q water used for the analysis should be adjusted to have the same pH as the milk sample. This would ensure that the particle size is the correct one, as the size will revert back to what it was initially when introduced to the neutral pH of the Milli-Q water.

Another interesting aspect for further research would be to incorporate the fat content and the presence of fat into the analysis of pH and $CaCl_2$, to investigate if these four factors correlate. A very good tool to use for performing these trials would be the response surface method, as it allows for minimization of sample size while still enabling accurate and significant results to be produced. Trying other coagulation agents such as guar gum in a similar trial with these factors could prove interesting and would expand on the difference between rennet and alternative coagulation agents.

The trials that were performed during this master thesis should probably be done again to verify the validity of the results presented. In addition, starting from this research question, the gelling properties can be investigated as well using different coagulation agents as guar gum. Also, another idea to continue the research can be to look closer at the effects of gelling properties on the yield of production. A more efficient production process coupled with the usage of less resources could help make a more sustainable cheese industry.

6. References

[1] J. Vigne and D. Helmer, “Was milk a “secondary product” in the Old World Neolithisation process? Its role in the domestication of cattle, sheep and goats,” *Anthropozoologica,* vol. 42, no. 2, pp. 9-40, 2007.

[2] P. Kindstedt, Cheese and Culture: A History of Cheese and its Place in Western Civilization, White River Junction, VT, USA: Chelsea Green Publishing, 2012.

[3] P. McSweeney, P. Fox, P. Cotter and D. Everett, Cheese: Chemistry, Physics and Microbiology, Fourth Edition, London, UK: Academic Press, 2017.

[4] J. Choi, D. Horne and J. Lucey, "Effect of Insoluble Calcium Concentration on Rennet Coagulation," *Journal of Dairy Science,* vol. 90, no. 6, pp. 2612-2623, 2007.

[5] E. Farnworth, Handbook of Fermented Functional Foods Second Edition, Taylor & Francis: Boca Raton, FL, USA, 2013.

[6] P. Fox and P. McSweeney, “Cheese Chemistry, Physics & Microbiology,” in *Cheese: An Overview*, London, UK, Academic Press, 2017, pp. 5-21.

[7] P. Fox, “Milk Proteins: General and Historical Aspects,” in *Advanced Dairy Chemistry—1 Proteins*, Boston, MA, USA, Springer, 2003, pp. 1-48.

[8] G. Bylund, Dairy Processing Handbook, Lund : Tetra Pak Processing Systems AB, 2015.

[9] P. F. Fox, T. Uniacke-Lowe, P. L. H. McSweeny and J. A. O'Mahony, Dairy Chemistry and Biochemistry, London: Springer International Publishing Switzerland , 2015.

[10] H. Swaisgood, “Chemistry of the Caseins,” in *Advanced Dairy Chemistry—1 Proteins*, Boston, MA, USA, Springer, 2003, pp. 139-201.

[11] UniProt, “UniProt,” [Online]. Available: https://www.uniprot.org/uniprot/P02662. [Accessed 16 05 2022].

[12] UniProt, “UniProt,” [Online]. Available: https://www.uniprot.org/uniprot/P02663. [Accessed 16 05 2022].

[13] UniProt, “UniProt,” [Online]. Available: https://www.uniprot.org/uniprot/P02666. [Accessed 16 05 2022].

[14] UniProt, “UniProt,” [Online]. Available: https://www.uniprot.org/uniprot/P02668. [Accessed 16 05 2022].

[15] P. Walstra, “Casein sub-micelles: do they exist?,” *International Dairy Journal,* vol. 9, no. 3-6, pp. 189-192, 1999.

[16] C. Holt, The biological function of casein: Research reviews, In Hannah Research Yearbook, Glasgow, UK: Hannah Research Institute, 1994.

[17] D. Horne, “Casein Interactions: Casting Light on the Black Boxes, the Structure in Dairy Products,” *International Dairy Journal,* vol. 8, no. 3, pp. 171-177, 1998.

[18] C. Phadungath, "Casein micelle structure: a concise review," *Songklanakarin Journal of Science and Technonlogy,* vol. 27, no. 1, pp. 210-212, 2005.

[19] D. Dalgleish, P. Spagnuolo and D. Goff, “A possible structure of the casein micelle based on high-resolution field-emission scanning electron microscopy,” *International Dairy Journal,* vol. 14, no. 12, pp. 1025-1031, 2004.

[20] R. Panthi, K. Jordan, A. Kelly and J. Sheehan, “Chapter 2 - Selection and Treatment of Milk for Cheesemaking,” in *Cheese (Fourth edition)*, Cambridge, MA, USA, Academic Press, 2017, pp. 23-50.

[21] D. Smith and A. Bakshi, “Effect of Fat Content and Temperature on Viscosity in Relation to Pumping Requirements of Fluid Milk Products,” *Journal of Dairy Science,* vol. 67, no. 6, pp. 1157-1160, 1984.

[22] A. Haug, A. Høstmark and O. Harstad, “Bovine milk in human nutrition – a review,” *Lipids in Health and Disease,* vol. 6, no. 25, 2007.

[23] H. Heid and T. Keenan, “Intracellular origin and secretion of milk fat globules,” *European Journal of Cell Biology,* vol. 84, no. 2-3, pp. 245-258, 2005.

[24] G. Schaafsma, “Lactose and lactose derivatives as bioactive ingredients in human nutrition,” *International Dairy Journal,* vol. 18, no. 5, p. 2008, 458-465.

[25] M. C. Neville and C. D. Watters, "Secretion of calcium into milk: review," *Journal of Dairy Science,* vol. 66, no. 3, pp. 371-380, 1983.

[26] M. Ridder, "Production volume of cheese in Sweden from 2010 to 2020," Statista, 06 September 2021. [Online]. Available: https://www.statista.com/statistics/558503/production-volume-of-cheese-in-sweden/. [Accessed 24 February 2022].

[27] Alfa Laval, "How does a plate heat exchanger work," 2022. [Online]. Available: https://www.alfalaval.my/products/heat-transfer/plate-heat-exchangers/gasketed-plate-and-frame-heat-exchangers/heat-exchanger/how-plate-heat-exchanger-work/. [Accessed 30 March 2022].

[28] T. Uniacke-Lowe and P. F. Fox, "Chymosin, Pepsins and Other Aspartyl Proteinases: Structures, Functions, Catalytic Mechanism and Milk-Clotting Properties," in *Cheese: Chemistry, Physics and Microbiology*, London, Academic Press, 2017, pp. 69-113.

[29] D. Jaros and H. Rohm, “Rennets: Applied Aspects,” in *Cheese: Chemistry, Physics and Microbiology*, London, Academic Press, 2017, pp. 53-67.

[30] I. N. Kugelmass, "The mechanism of milk clotting," *American Journal of Digestive Diseases and Nutrition,* vol. 4, pp. 523-525, 1937.

[31] P. Walstra, J. T. Wouters and T. J. Geurts, “Cheese Manufacture,” in *Dairy Science and Technology*, Boca Raton, FL, Taylor & Francis Group, LLC, 2005, pp. 583-640.

[32] L. Ong, R. R. Dagastine, S. E. Kentish and S. L. Gras, “The effect of calcium chloride addition on the microstructure and composition of Cheddar cheese,” *International Dairy Journal,* vol. 33, no. 2, pp. 135-141, 2013.

[33] T. Janhøj and K. B. Qvist, “Formation of Cheese Curd,” in *Technology of Cheesemaking*, Singapore, Wiley-Blackwell, 2010, pp. 130-165.

[34] J. Tarapata, M. Smoczyński, M. Maciejczyk and J. Zulewska, "Effect of calcium chloride addition on properties of acid-rennet gels," *International Dairy Journal,* vol. 106, 2020.

[35] J. A. Lucy, “Formation, Structural Properties, and Rheology of Acid-Coagulated Milk Gels,” in *Cheese: Chemistry, Physics and Microbiology*, London, United Kingdom, Elsevier Academic Press, 2017, pp. 179-197.

[36] H. Sinaga, N. Bansal and B. Bhandari, "Effects of milk pH alteration on casein micelle sizeand gelation properties of milk," *International Journal of food Properties,* vol. 20, no. 1, pp. 179-197, 2017.

[37] M. Glantz, T. G. Devold, G. E. Vegarud, H. Lindmark Månsson, H. Stålhammar and M. Paulsson, "Importance of casein micelle size and milk composition for milk gelation," *Journal of Dairy Science,* vol. 93, no. 4, pp. 1444-1451, 2009.

[38] C. L. C. Esteves, J. A. Lucey, T. Wang and E. M. V. Pirest, "Effect of pH on the Gelation Properties of Skim Milk GelsMade From Plant Coagulants and Chymosin," *Journal of Dairy Science,* vol. 86, no. 8, pp. 2558-2567, 2003.

[39] K. B. Qvist, M. Harboe and M. L. Broe, “The Production, Action and Application of Rennet and Coagulants,” in *Technology of Cheesemaking*, Singapore, Wiley-Blackwell, 2010, pp. 98-129.

[40] E. Parente, T. M. Cogan and I. B. Powell, "Starter Cultures: General Aspects," in *Cheese Chemistry, Physics and Microbiology*, Amsterdam, Academic Press, 2017, pp. 201-226.

[41] T. Bintsis, “Lactic acid bacteria as starter cultures: An update in their metabolism and genetics,” *AIMS Microbiology,* vol. 4, no. 4, pp. 665-684, 2018.

[42] L. Ong, S. L. Gras, R. R. Dagastine, M. A. Auty and S. E. Kentish, “Coagulation temperature a ects the microstructure and composition of full fat Cheddar cheese,” *Dairy Science and Technology,* vol. 91, pp. 739-758, 2011.

[43] J. M. Kongo, “Lactic Acid Bacteria as Starter-Cultures for Cheese Processing: Past, Present and Future Developments,” in *Lactic Acid Bacteria - R & D for Food, Health and Livestock Purposes*, Janeza Trdine 9, 51000 Rijeka, Croatia , InTech, 2013, pp. 3-22.

[44] P. Guinee, “Advanced Dairy Chemistry,” in *Protein in Cheese and Cheese Products: Structure-Function Relationships*, New York, NY, USA, Springer, 2016, pp. 347-415.

[45] E. Feeney, P. Lamichhane and J. Sheehan, “The cheese matrix: Understanding the impact of cheese structure on aspects of cardiovascular health – A food science and a human nutrition perspective,” *International Journal of Dairy Technology,* vol. 74, no. 4, pp. 656-670, 2021.

[46] L. Ong, R. Dagastine, S. Kentish and S. Gras, “Microstructure and Composition of Full Fat Cheddar Cheese Made with Ultrafiltered Milk Retentate,” *MDPI Foods,* vol. 2, no. 3, pp. 310-331, 2013.

[47] K. Soodam, L. Ong, P. Ian, S. Kentish and S. Gras, “Effect of rennet on the composition, proteolysis,” *Dairy Science & Technology, EDP sciences/Springer,* vol. 95, no. 5, pp. 665-686, 2015.

[48] H. Barnes, J. Hutton and K. Walters, An Introduction to Rheology, Amsterdam, The Netherlands: Elsevier, 1993.

[49] J. Vélez-Ruiz, G. Barbosa Cánovas and M. Peleg, “Rheological properties of selected dairy products,” *Critical Reviews in Food Science & Nutrition,* vol. 37, no. 4, pp. 311-359, 1997.

[50] Anton Paar, “Basics of rheology,” Anton Paar GmbH, [Online]. Available: https://wiki.anton-paar.com/se-en/basics-of-rheology/. [Accessed 23 02 2022].

[51] Z. Miloradovic, N. Kljajevic, J. Miocinovic, S. Levic, V. Pavlovic, M. Blažić and P. Pudja, “Rheology and Microstructures of Rennet Gels from Differently Heated Goat Milk,” *MDPI Open Access,* vol. 9, no. 3, p. 283, 2020.

[52] Malvern Instruments Ltd, Kinexus Series User Manual, Worcestershire, UK: Malvern Instruments Ltd, 2014.

[53] Formulaction SA, Turbiscan Lab User Guid, Toulouse, France: Formulaction SA, 2006.

[54] M. Wedd, Encyclopedia of Analytical Science (Second Edition), Amsterdam, Netherlands: Elsevier, 2005.

[55] Malvern Instruments Ltd., Mastersizer 2000 User Manual, Worcestershire, UK: Malvern Instruments Ltd., 2007.

[56] N. Nicolaou, Y. Xu and R. Goodacre, “Fourier transform infrared spectroscopy and multivariate analysis for the detection and quantification of different milk species,” *Journal of Dairy Science,* vol. 93, no. 12, pp. 5651-5660, 2010.

[57] R. Pralle, K. Weigel and H. White, “Predicting blood β-hydroxybutyrate using milk Fourier transform infrared spectrum, milk composition, and producer-reported variables with multiple linear regression, partial least squares regression, and artificial neural network,” *Journal of Dairy Science,* vol. 101, no. 5, pp. 4378-4387, 2018.

[58] FOSS A/S, MilkoScan Mars solution Brochure EN, Hillerød, Denmark: FOSS A/S, 2018.

[59] T. T. Allen, Introduction to Engineering Statistics and Lean Sigma, London: Springer, 2010.

[60] F. Gustavsson, A. J. Buitenhuis, M. Glantz, H. Stålhammar, H. Lindmark-Månsson, N. A. Poulsen, L. B. Larsen, A. Andrén and M. Paulsson, "Impact of genetic variants of milk proteins on chymosin-inducedgelation properties of milk from individual cows of Swedish Red dairycattle," *International Dairy Journal,* vol. 39, no. 1, pp. 102-107, 2014.

[61] HORIBA Scientific, " www.horiba.com/scientific," [Online]. Available: https://static.horiba.com/fileadmin/Horiba/Products/Scientific/Particle_Characterization/Downloads/Technical_Notes/TN156_Understanding_and_Interpreting_PSD_Calculations.pdf. [Accessed 02 05 2022].

[62] Malvern Instruments Limited, "https://www.atascientific.com.au/," 02 2017. [Online]. Available: https://www.atascientific.com.au/wp-content/uploads/2017/02/AN020710-Basic-Principles-Particle-Size-Analysis.pdf. [Accessed 02 05 2022].

[63] Minitab LLC, "Regression equation table for Analyze Factorial Design," Minitab LLC, [Online]. Available: https://support.minitab.com/en-us/minitab/18/help-and-how-to/modeling-statistics/doe/how-to/factorial/analyze-factorial-design/interpret-the-results/all-statistics-and-graphs/regression-equation/. [Accessed 26 05 2022].

[64] Minitab LLC, "Specify display design options for Display Design," Minitab LLC, [Online]. Available: https://support.minitab.com/en-us/minitab/18/help-and-how-to/modeling-statistics/doe/how-to/factorial/display-and-modify-design/perform-the-analysis/specify-display-design-options/#units-for-factors-for-screening-factorial-and-response-surface-designs. [Accessed 26 05 2022].

[65] Minitab LLC, "Coefficients table for Analyze Response Surface Design," Minitab, 2022. [Online]. Available: https://support.minitab.com/en-us/minitab/18/help-and-how-to/modeling-statistics/doe/how-to/response-surface/analyze-response-surface-design/interpret-the-results/all-statistics-and-graphs/coefficients-table/. [Accessed 04 05 2022].

[66] Minitab LLC, "Interpret the key results for Analyze Response Surface Design," Minitab LLC, 2022. [Online]. Available: https://support.minitab.com/en-us/minitab/21/help-and-how-to/statistical-modeling/doe/how-to/response-surface/analyze-response-surface-design/interpret-the-results/key-results/?SID=129050. [Accessed 04 05 2022].

[67] Minitab Blog, "Learning to Love Correlograms in the Latest Minitab Release," Minitab LLC, 20 04 2021. [Online]. Available: https://blog.minitab.com/en/learning-correlograms-latest-minitab-release. [Accessed 09 05 2022].

[68] Minitab LLC, "Interpret all statistics and graphs for Correlation," Minitab LLC, 2022. [Online]. Available: https://support.minitab.com/en-us/minitab/19/help-and-how-to/statistics/basic-statistics/how-to/correlation/interpret-the-results/all-statistics-and-graphs/#confidence-intervals-for-correlation. [Accessed 09 05 2022].

Appendix A

Table 1A presents the results obtained from Response Surface method trial regarding gelation time, G' 30 min, particle size (d[4,3]) and ΔBS 30 min for all samples.

Table 1A: Results obtained from the Response Surface method trial regarding gelation time, G' 30 min, particle size (d[4,3]) and ΔBS 30 min for all samples of the 14 duplicates.

Sample	**Duplicate**	**Gelation time [s]**	**G' 30 min [Pa]**	**d[4,3] [nm]**	**ΔBS 30 min [%]**
S1,1	1	50	52.1	126	11.8
S3,3		50	55.0	129	14.4
S2,1	2	110	43.8	128	11.7
S5,3		160	43.3	128	14.0
S3,1	3	120	46.5	132	14.3
S4,3		270	39.7	129	13.3
S4,1	4	50	54.9	141	10.4
S2,3		60	54.0	129	13.6
S5,1	5	40	54.6	129	14.9
S6,3		70	52.7	128	15.1
S6,1	6	30	51.4	130	8.25
S1,3		50	52.1	128	12.7
S7,1	7	50	55.0	129	12.1
S7,3		80	52.1	129	15.6
S1,2	8	180	50.4	128	14.0
S4,4		230	41.8	128	13.4
S2,2	9	70	54.4	128	13.4
S1,4		60	54.4	129	15.0
S3,2	10	60	51.8	144	10.3
S6,4		80	49.1	128	11.1
S4,2	11	30	52.8	127	14.2
S7,4		110	48.5	131	15.0
S5,2	12	10	64.9	129	12.8
S2,4		100	52.7	129	14.7
S6,2	13	70	53.3	129	14.6
S3,4		80	53.8	129	15.1
S7,2	14	50	58.7	120	13.6
S5,4		110	55.0	129	14.2

Table 2A presents the results obtained from Effect of fat on gelation-trial method trial regarding gelation time, G' at 2x gelation time, G' 30 min, particle size (d[4,3]) and ΔBS 30 min for all samples.

Table 2A: Results obtained from Effect of fat on gelation-trial method trial regarding gelation time, G' at 2x gelation time, G' 30 min, particle size (d[4,3]) and ΔBS 30 min for all samples.

Sample	**Duplicate**	**Gelation time [s]**	**G' at 2x gelation time [Pa]**	**G' 30 min [Pa]**	**d(4,3) [nm]**	**ΔBS 30 min [%]**
SSM3,1	A	840	6.03	7.15	129	10.6
SSM3,2		540	7.61	18.7	127	11.8
SM3,1	B	290	7.06	29.9	6323	10.2
SM3,2		480	7.77	20.8	4358	10.4
SSM2,1	C	330	6.65	27.8	130	12.5
SSM2,2		290	7.10	31.2	129	12.3
SM2,1	D	360	9.02	29.4	3401	12.2
SM2,2		530	9.80	22.3	3443	12.1

Appendix B

In this appendix, the G’ [Pa] is plotted against Time [s] for the two samples of each duplicate in the Response Surface Method trial. This result was obtained using the Rheometer.

In Figure B1, the G’ [Pa] is plotted against Time [s] for duplicate 1 (samples S1,1 and S3,3).

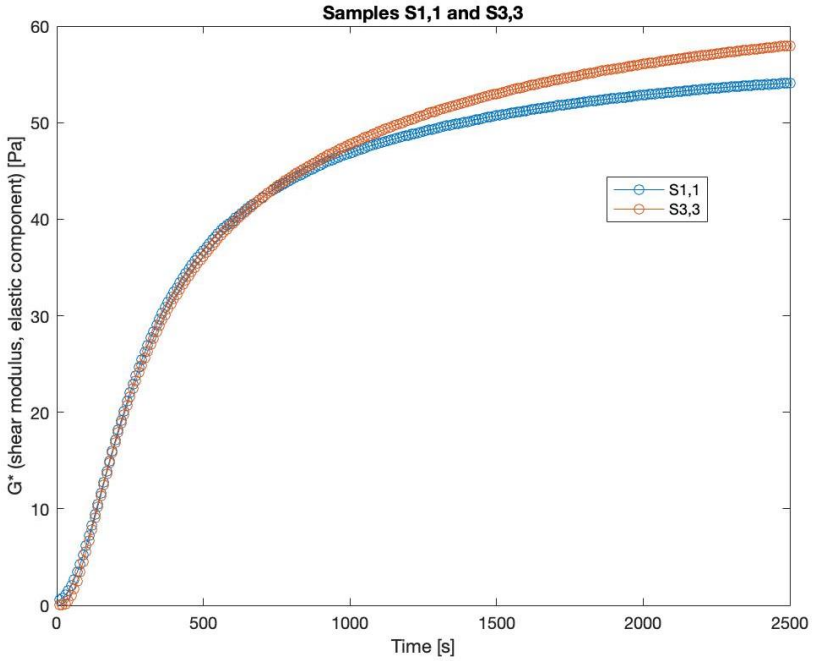

Figure B1 G' [Pa] plotted against time [s] for duplicate 1 (samples S1,1 and S3,3).

In Figure B2, the G’ [Pa] is plotted against Time [s] for duplicate 2 (samples S2,1 and S5,3).

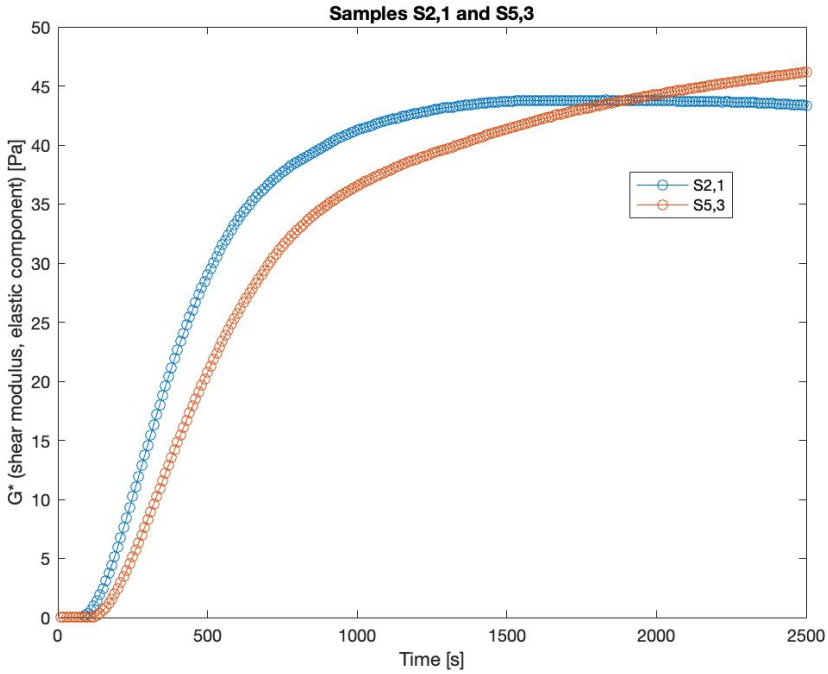

Figure B2 G’ [Pa] is plotted against Time [s] for duplicate 2 (samples S2,1 and S5,3).

In Figure B3, the G’ [Pa] is plotted against Time [s] for duplicate 1 (samples S3,1 and S4,3).

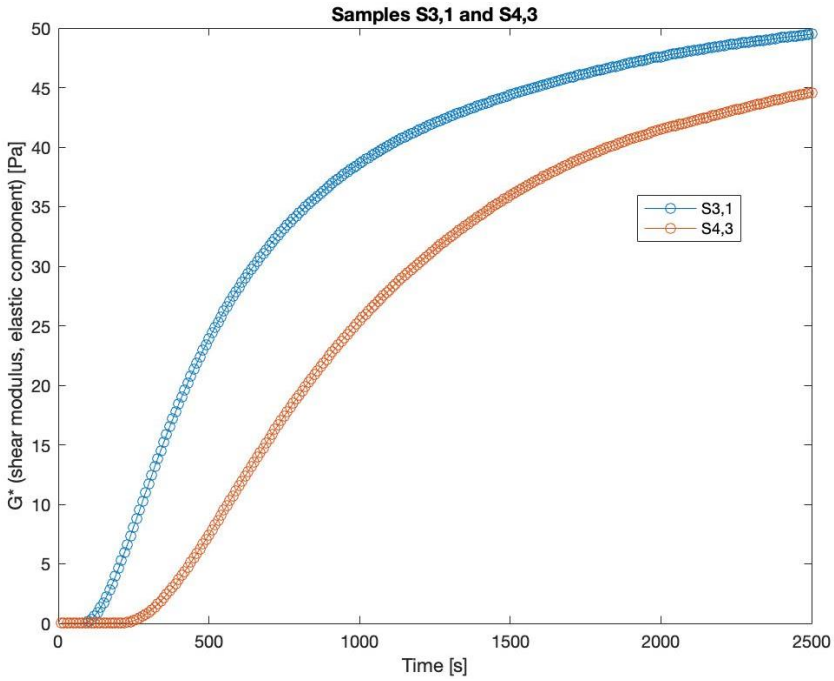

Figure B3 G' [Pa] is plotted against Time [s] for duplicate 3 (samples S3,1 and S4,3).

In Figure B4, the G' [Pa] is plotted against Time [s] for duplicate 1 (samples S4,1 and S2,3).

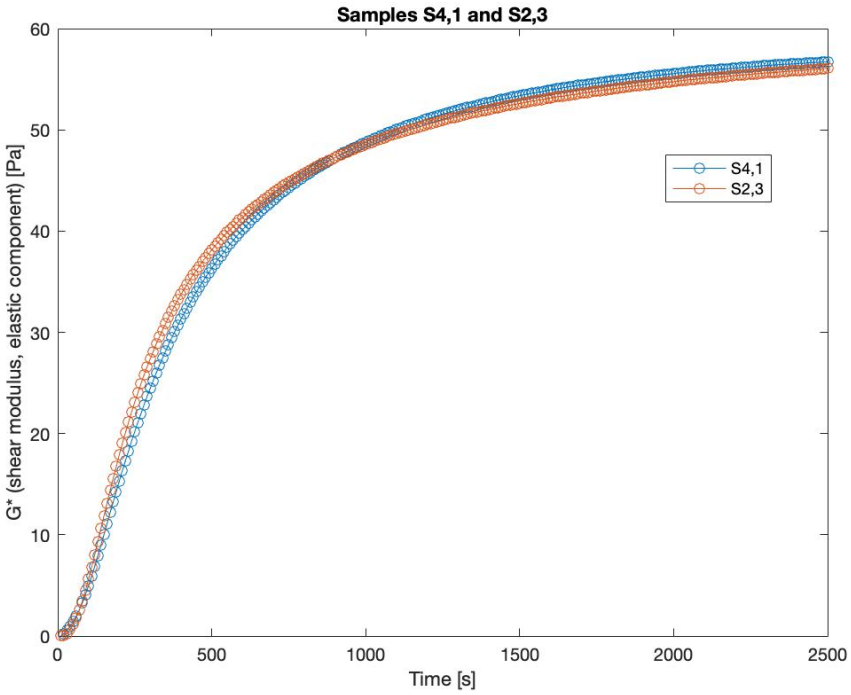

Figure B4 G' [Pa] is plotted against Time [s] for duplicate 4 (samples S4,1 and S2,3).

In Figure B5, the G' [Pa] is plotted against Time [s] for duplicate 5 (samples S5,1 and S6,3).

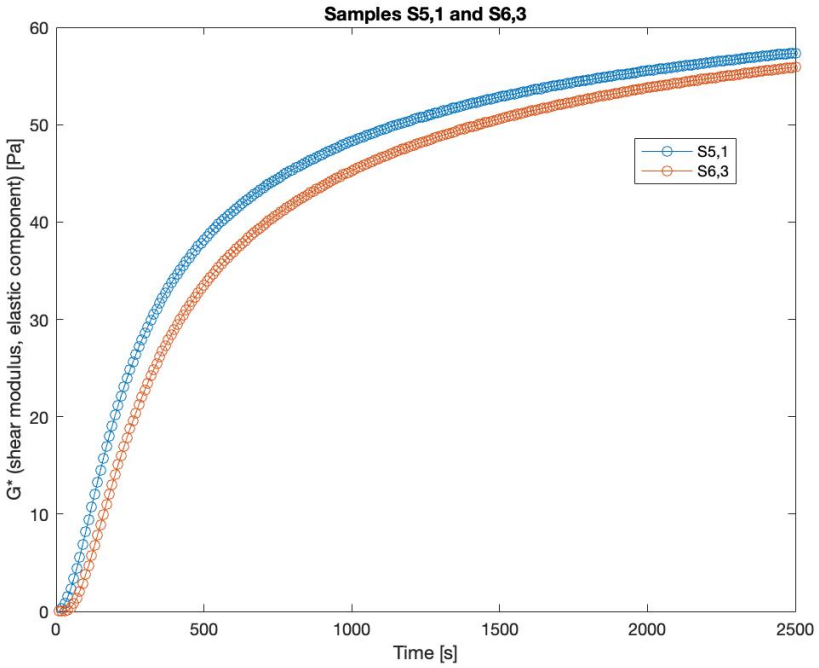

Figure B5 G' [Pa] plotted against time [s] for duplicate 5 (samples S5,1 and S6,3).

In Figure B6, the G’ [Pa] is plotted against Time [s] for duplicate 6 (samples S6,1 and S1,3).

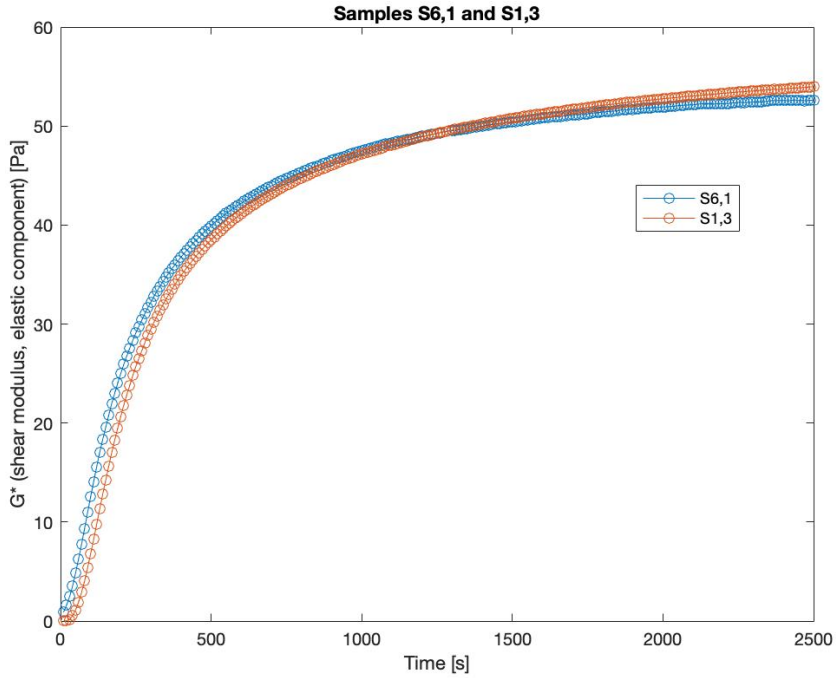

Figure B6 G' [Pa] plotted against time [s] for duplicate 6 (samples S6,1 and S1,3).

In Figure B7, the G’ [Pa] is plotted against Time [s] for duplicate 7 (samples S7,1 and S7,3).

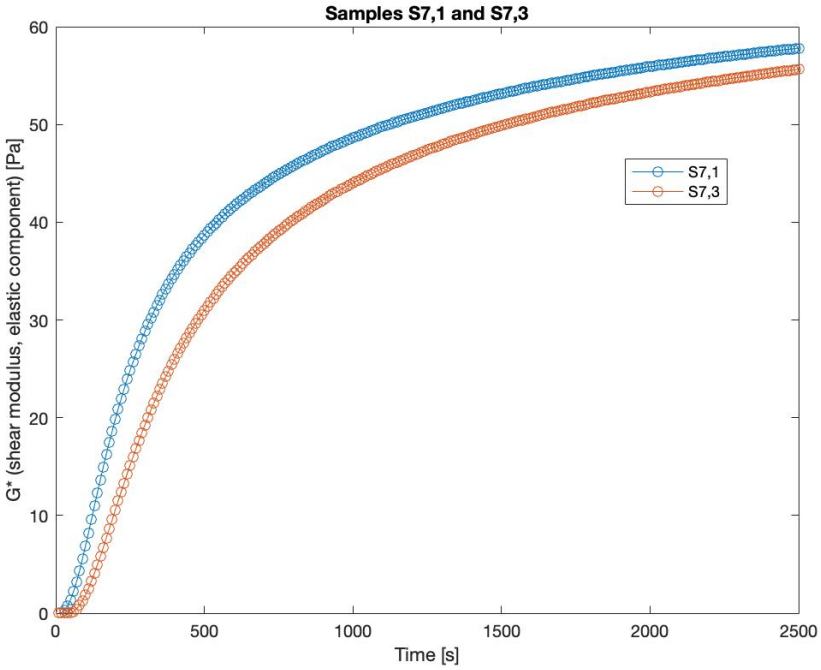

Figure B7 G' [Pa] plotted against time [s] for duplicate 7 (samples S7,1 and S7,3).

In Figure B8, the G’ [Pa] is plotted against Time [s] for duplicate 8 (samples S1,2 and S4,4).

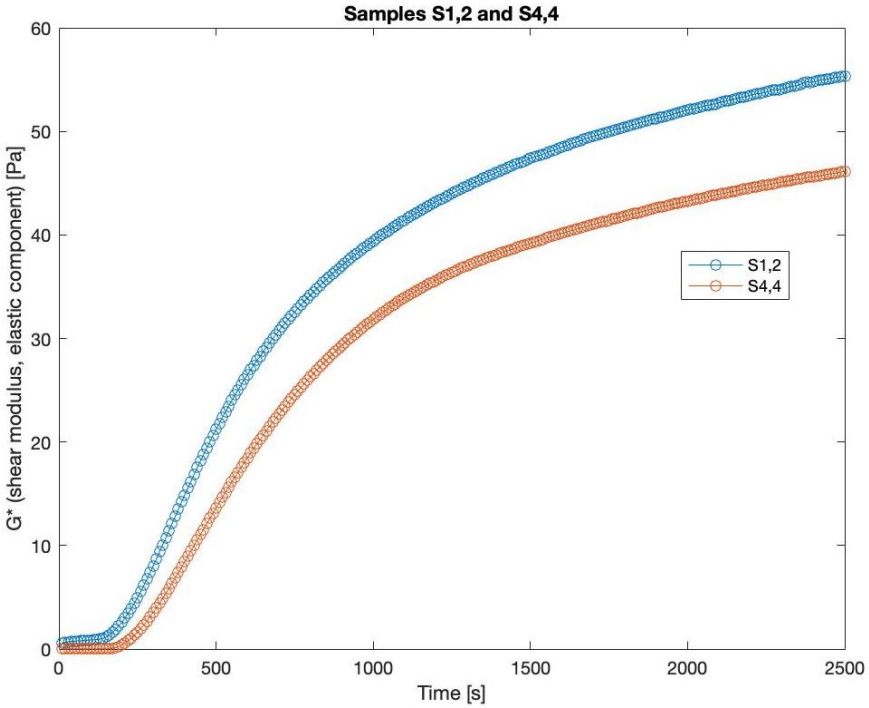

Figure B8 G' [Pa] plotted against time [s] for duplicate 8 (samples S1,2 and S4,4).

In Figure B9, the G’ [Pa] is plotted against Time [s] for duplicate 9 (samples S2,2 and S1,4).

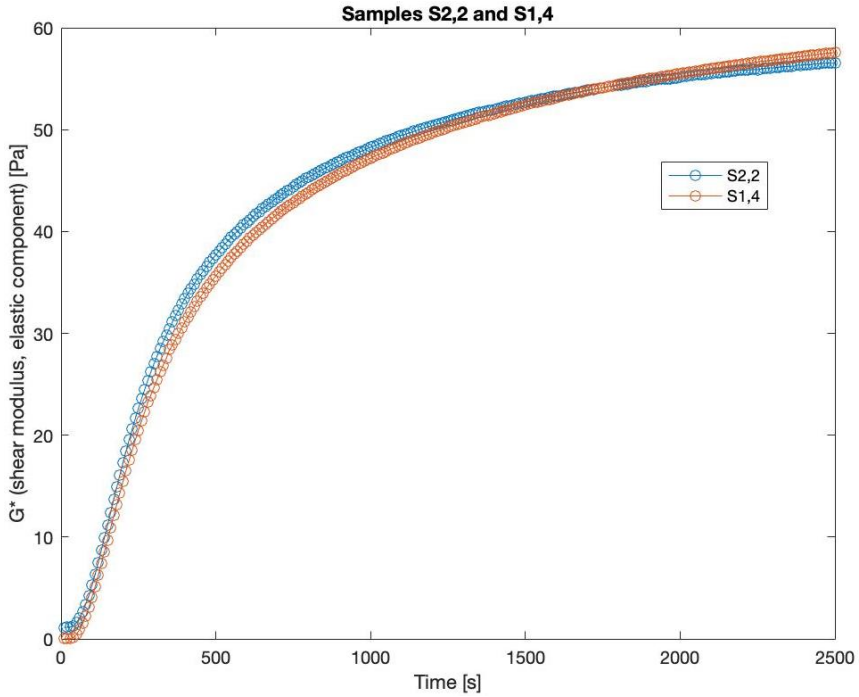

Figure B9 G' [Pa] plotted against time [s] for duplicate 9 (samples S2,2 and S1,4).

In Figure B10, the G’ [Pa] is plotted against Time [s] for duplicate 10 (samples S3,2 and S6,4).

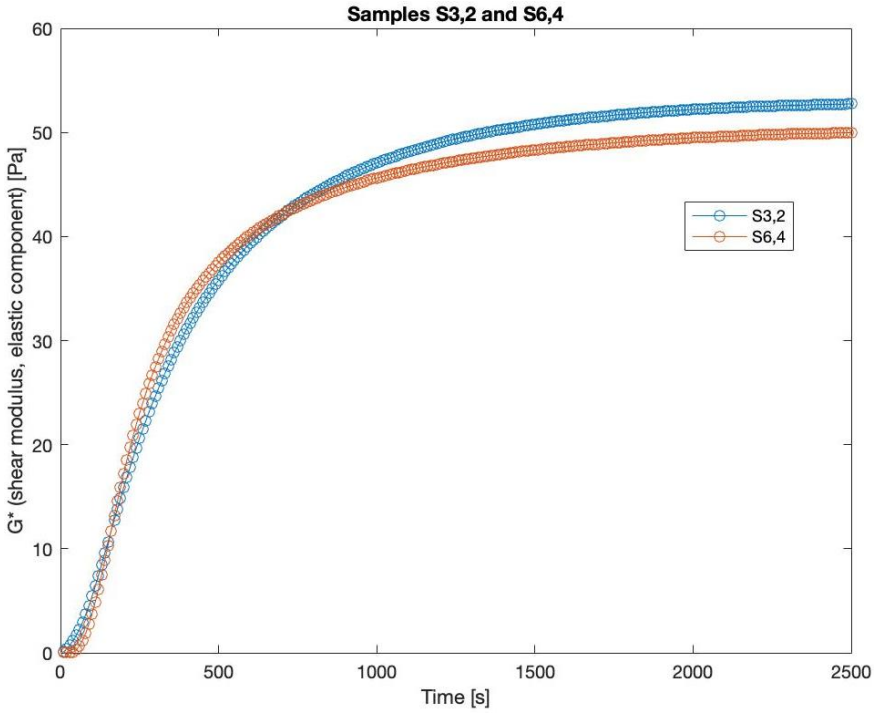

Figure B10 G' [Pa] plotted against time [s] for duplicate 10 (samples 3,2 and S6,4).

In Figure B11, the G’ [Pa] is plotted against Time [s] for duplicate 11 (samples S4,2 and S7,4).

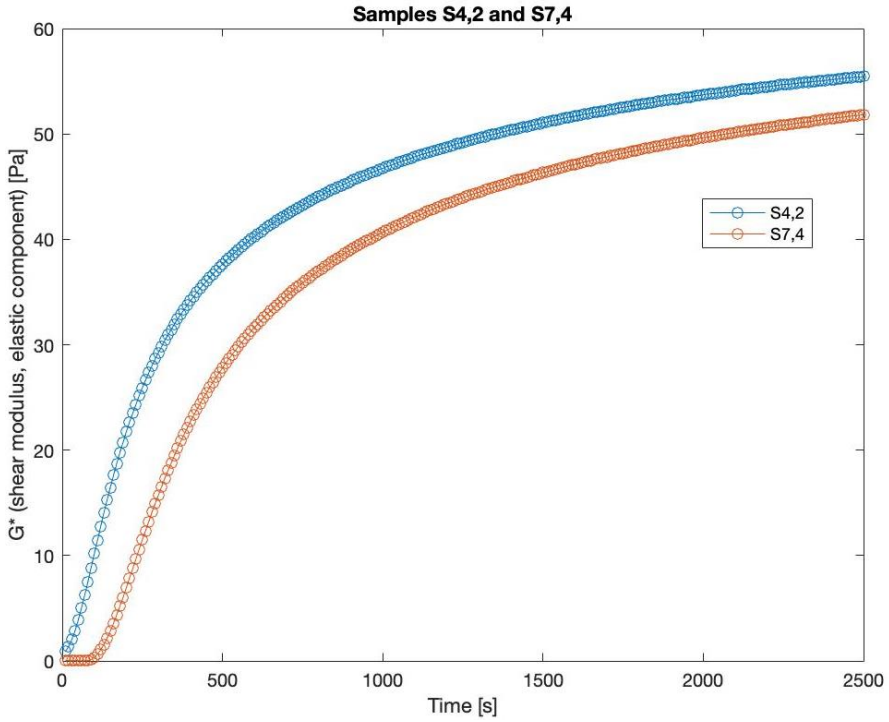

Figure B11 G' [Pa] plotted against time [s] for duplicate 11 (samples S4,2 and S7,4).

In Figure B12, the G’ [Pa] is plotted against Time [s] for duplicate 12 (samples S5,2 and S2,4).

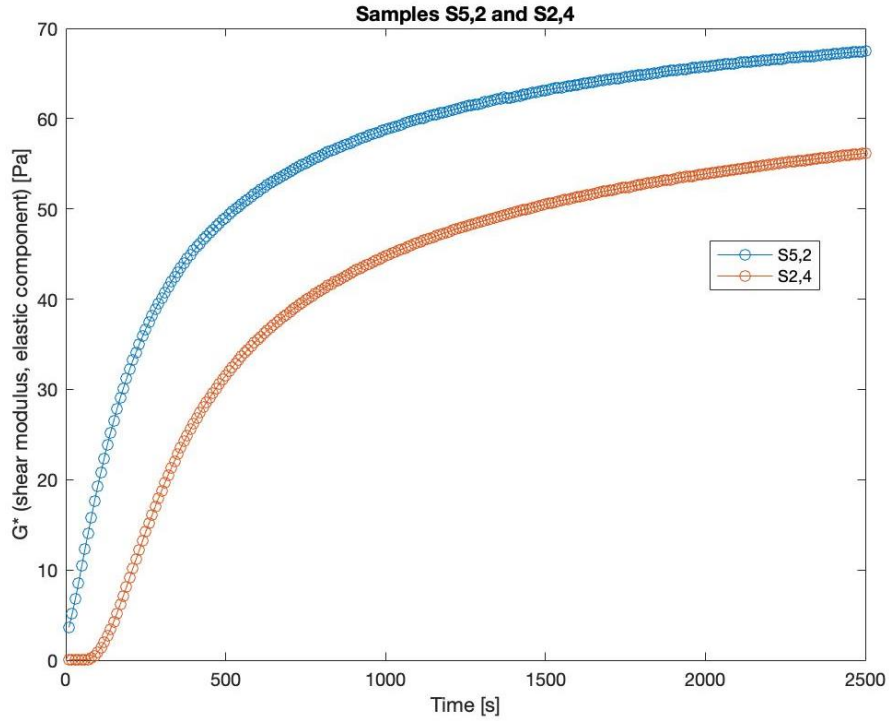

Figure B12 G' [Pa] plotted against time [s] for duplicate 12 (samples S5,2 and S2,4).

In Figure B13, the G’ [Pa] is plotted against Time [s] for duplicate 13 (samples S6,2 and S3,4).

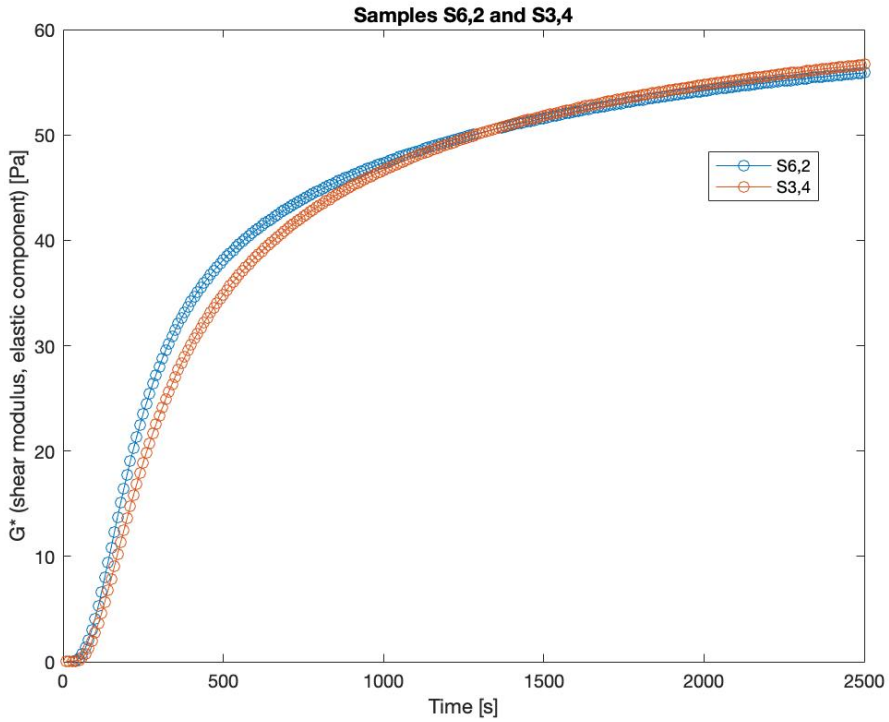

Figure B13 G' [Pa] plotted against time [s] for duplicate 13 (samples S6,2 and S3,4).

In Figure B14, the G’ [Pa] is plotted against Time [s] for duplicate 14 (samples S7,2 and S5,4).

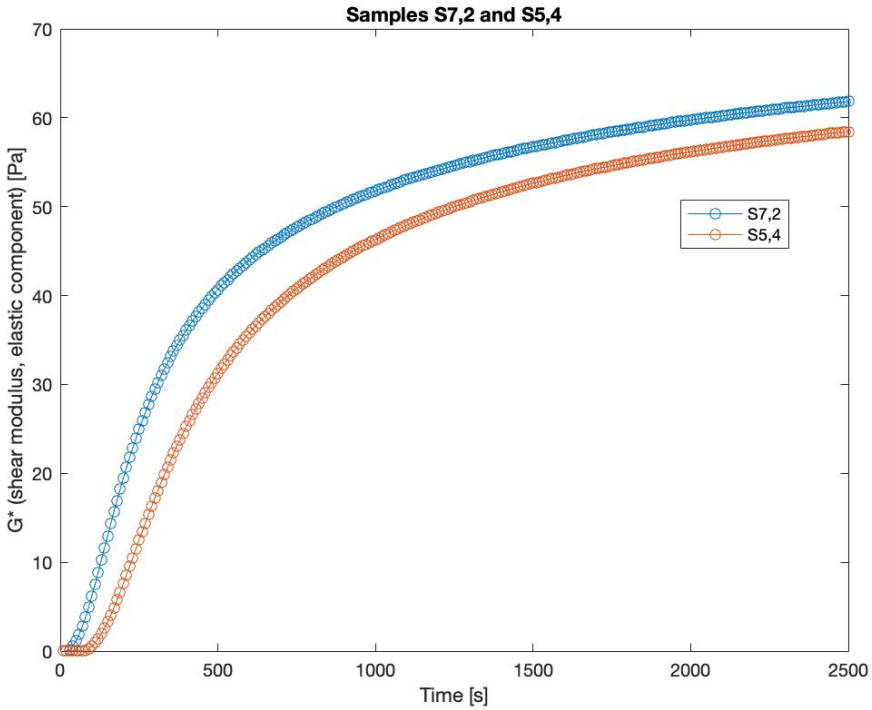

Figure B14 G’ [Pa] is plotted against Time [s] for duplicate 13 (samples S7,2 and S5,4).

Appendix C

In this appendix, the ΔBS [%] is plotted against Time [s] for the two samples of each duplicate in the Response Surface Method trial. This result was obtained using the Turbiscan.

In Figure C1, the ΔBS [%] is plotted against Time [s] for duplicate 1 (samples S1,1 and S3,3).

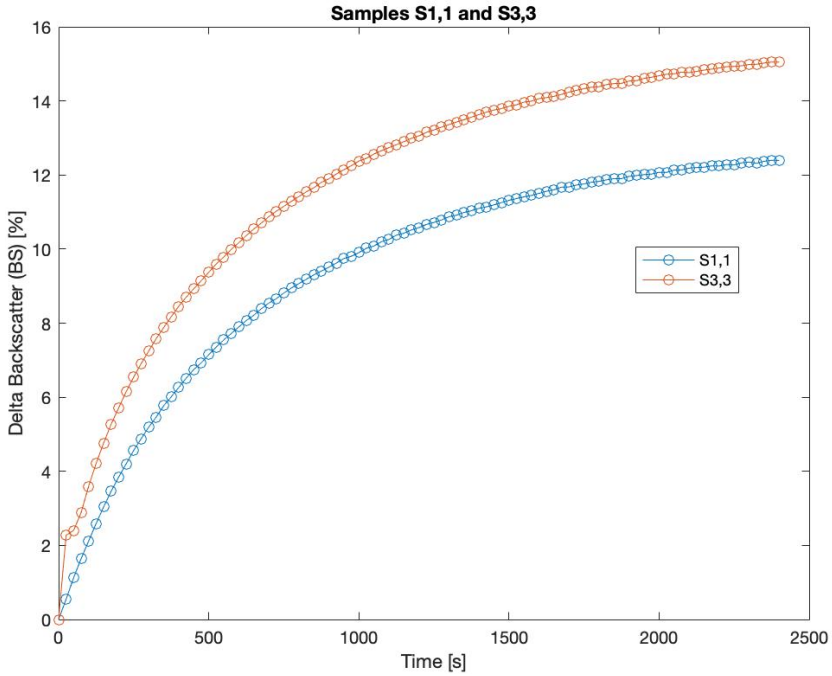

Figure C1 ΔBS [%] is plotted against time [s] for duplicate 1 (samples S1,1 and S3,3).

In Figure C2, the ΔBS [%] is plotted against Time [s] for duplicate 2 (samples S2,1 and S5,3).

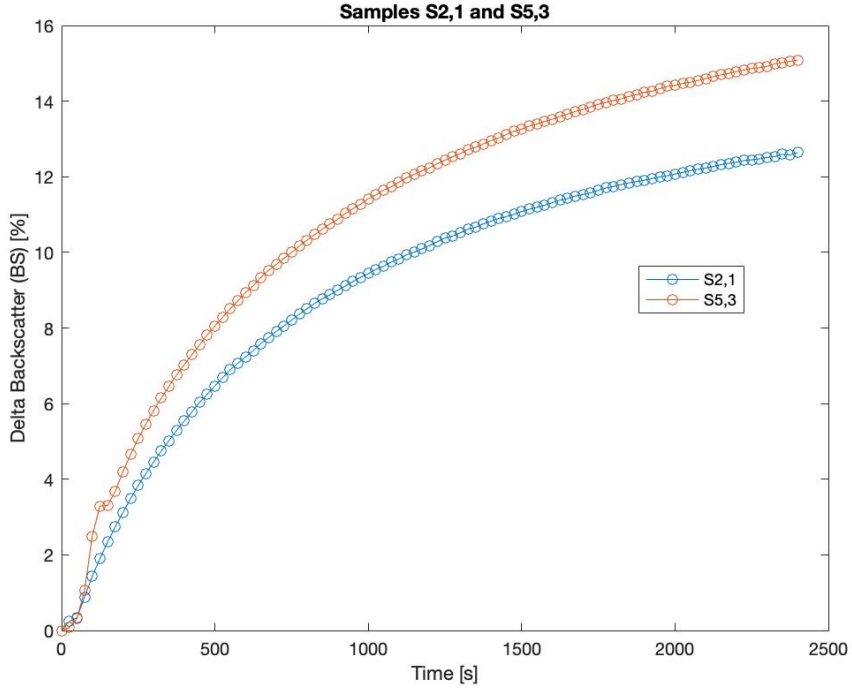

Figure C2 ΔBS [%] is plotted against time [s] for duplicate 2 (samples S2,1 and S5,3).

In Figure C3, the ΔBS [%] is plotted against Time [s] for duplicate 3 (samples S3,1 and S4,3).

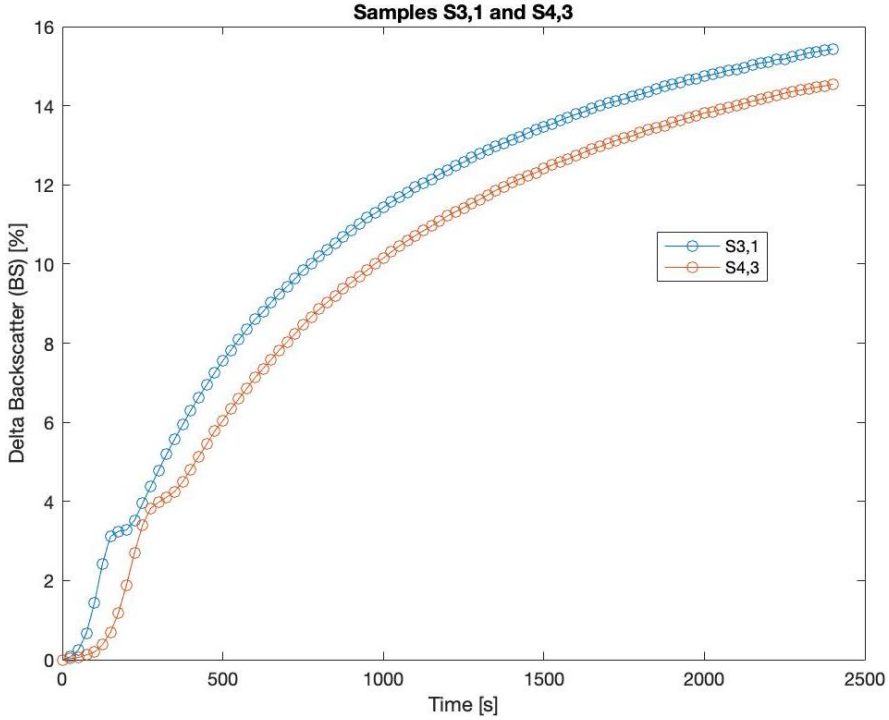

Figure C3 ΔBS [%] is plotted against time [s] for duplicate 3 (samples S3,1 and S4,3).

In Figure C4, the ΔBS [%] is plotted against Time [s] for duplicate 4 (samples S4,1 and S2,3).

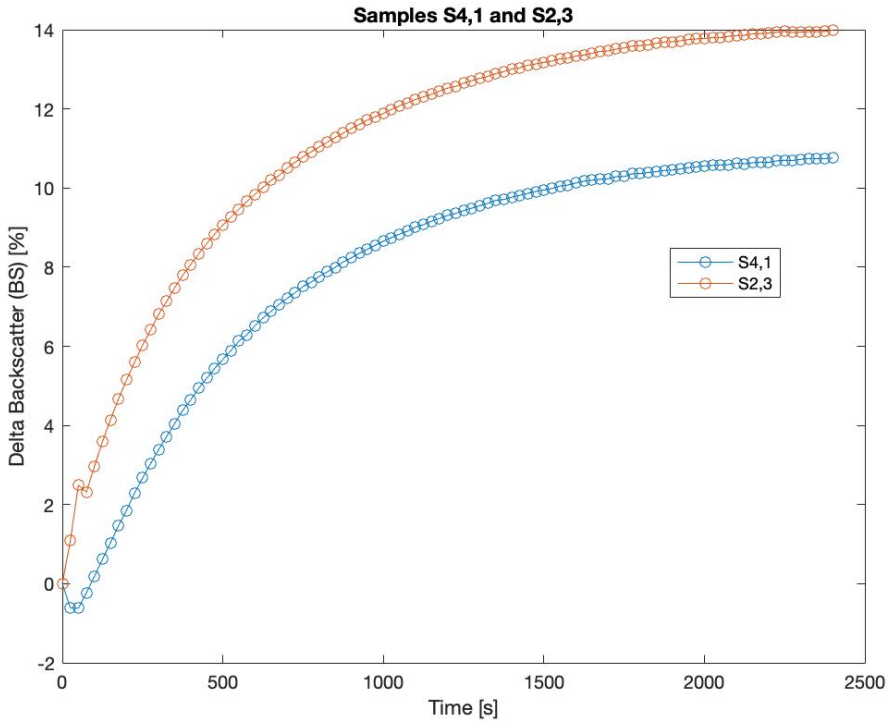

Figure C4 ΔBS [%] is plotted against time [s] for duplicate 4 (samples S4,1 and S2,3).

In Figure C5, the ΔBS [%] is plotted against Time [s] for duplicate 5 (samples S5,1 and S6,3).

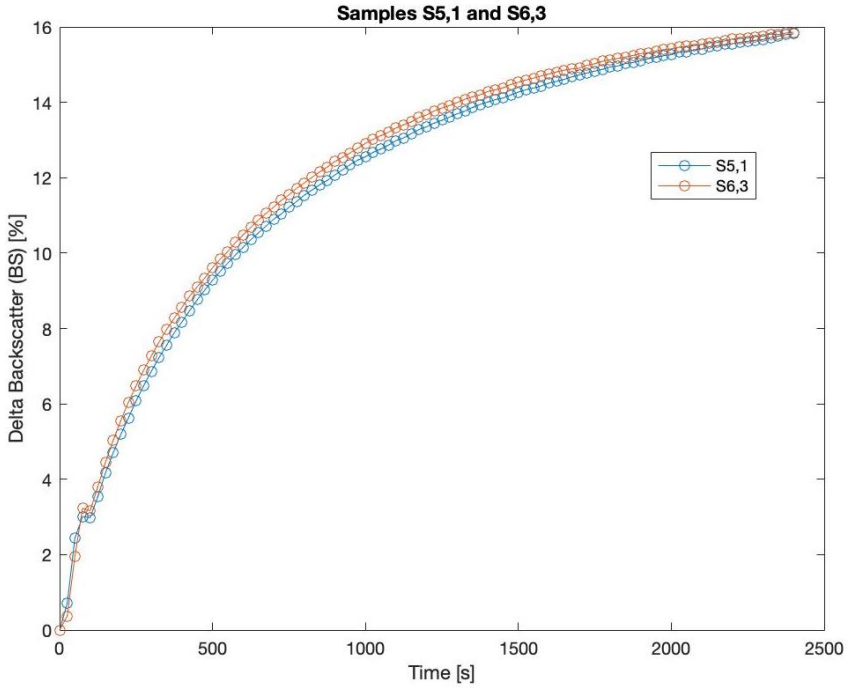

Figure C5 ΔBS [%] is plotted against Time [s] for duplicate 5 (samples S5,1 and S6,3).

In Figure C6, the ΔBS [%] is plotted against Time [s] for duplicate 6 (samples S6,1 and S1,3).

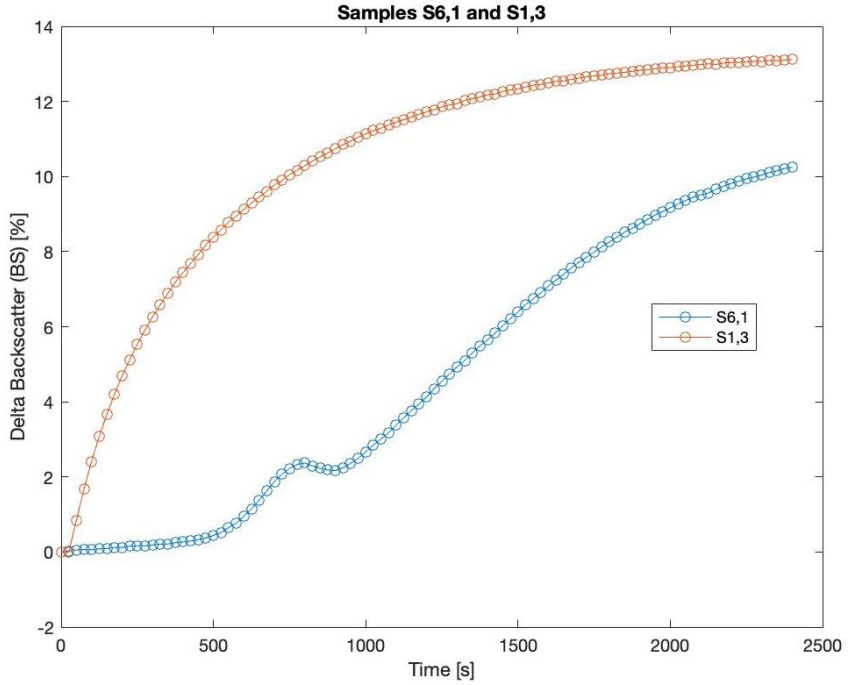

Figure C6 ΔBS [%] is plotted against Time [s] for duplicate 6 (samples S6,1 and S1,3).

In Figure C7, the ΔBS [%] is plotted against Time [s] for duplicate 7 (samples S7,1 and S7,3).

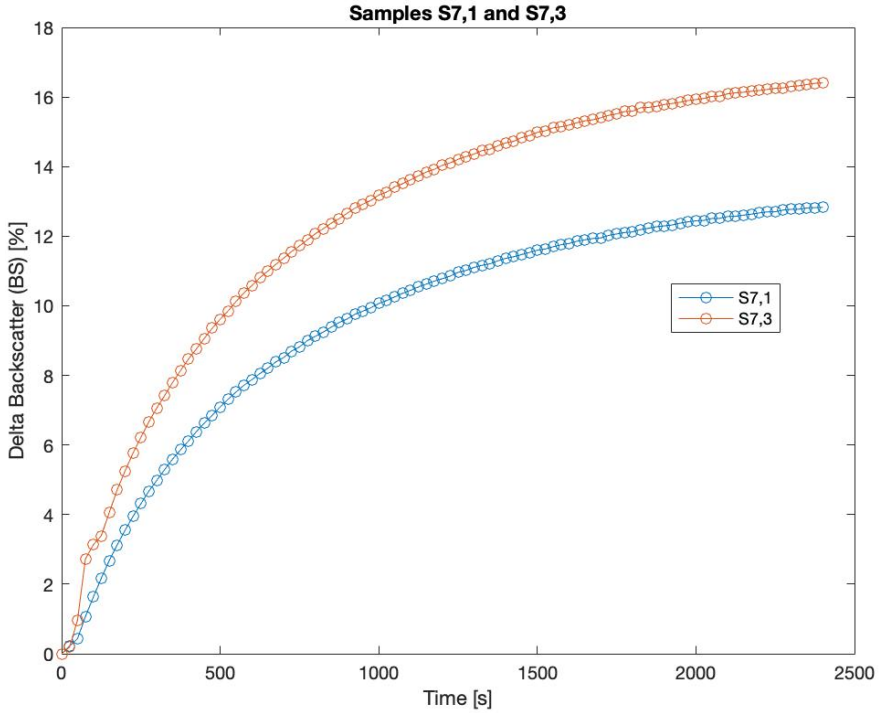

Figure C7 ΔBS [%] is plotted against time [s] for duplicate 7 (samples S7,1 and S7,3).

In Figure C8, the ΔBS [%] is plotted against Time [s] for duplicate 8 (samples S1,2 and S4,4).

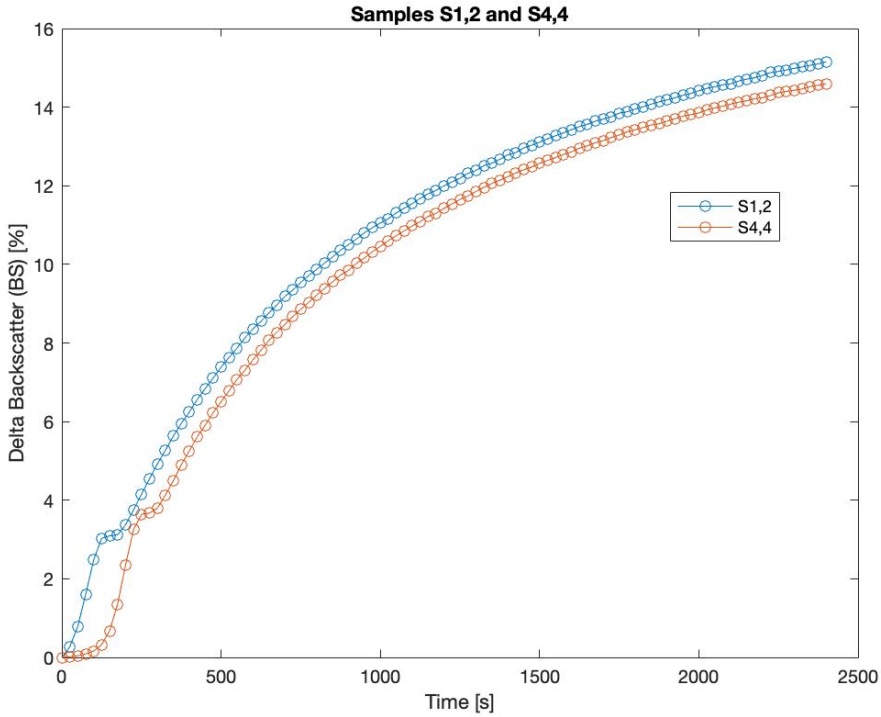

Figure C8 ΔBS [%] is plotted against Time [s] for duplicate 8 (samples S1,2 and S4,4).

In Figure C9, the ΔBS [%] is plotted against Time [s] for duplicate 9 (samples S2,2 and S1,4).

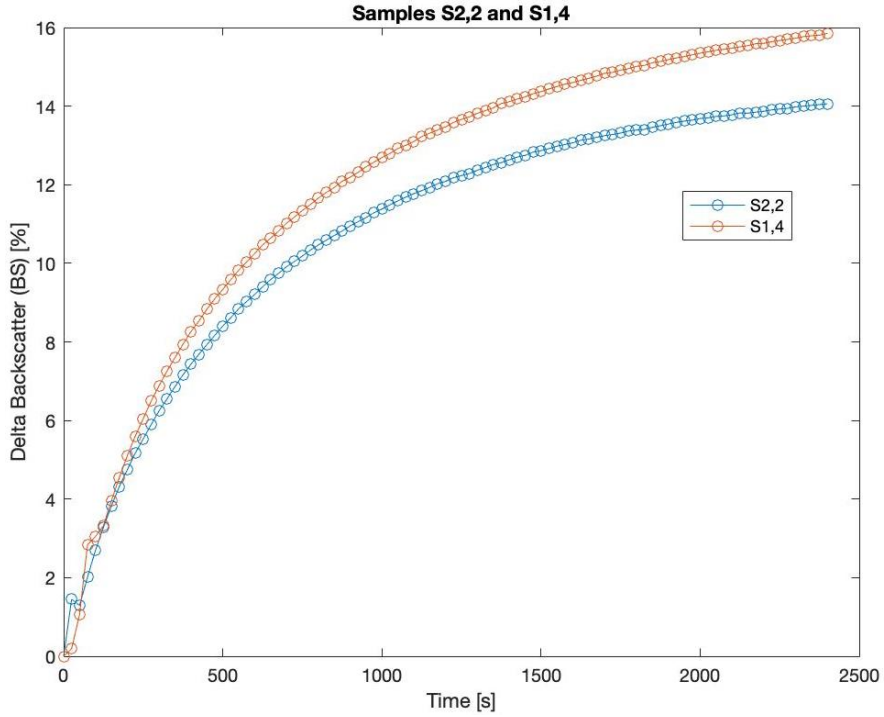

Figure C9 ΔBS [%] is plotted against time [s] for duplicate 9 (samples S2,2 and S1,4).

In Figure C10, the ΔBS [%] is plotted against Time [s] for duplicate 10 (samples S3,2 and S6,4).

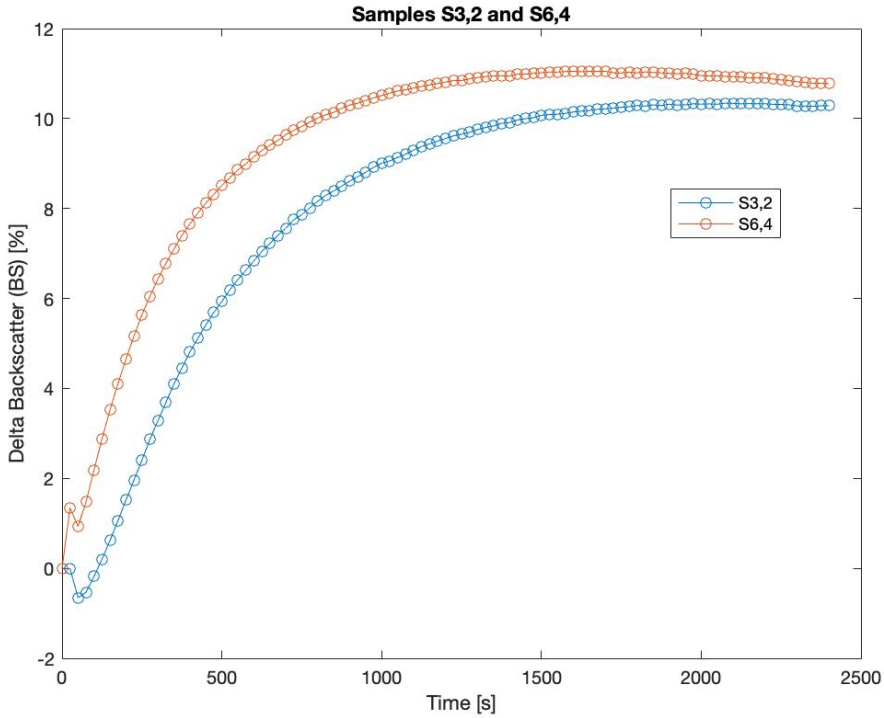

Figure C10 ΔBS [%] is plotted against Time [s] for duplicate 10 (samples S3,2 and S6,4).

In Figure C11, the ΔBS [%] is plotted against Time [s] for duplicate 11 (samples S4,2 and S7,4).

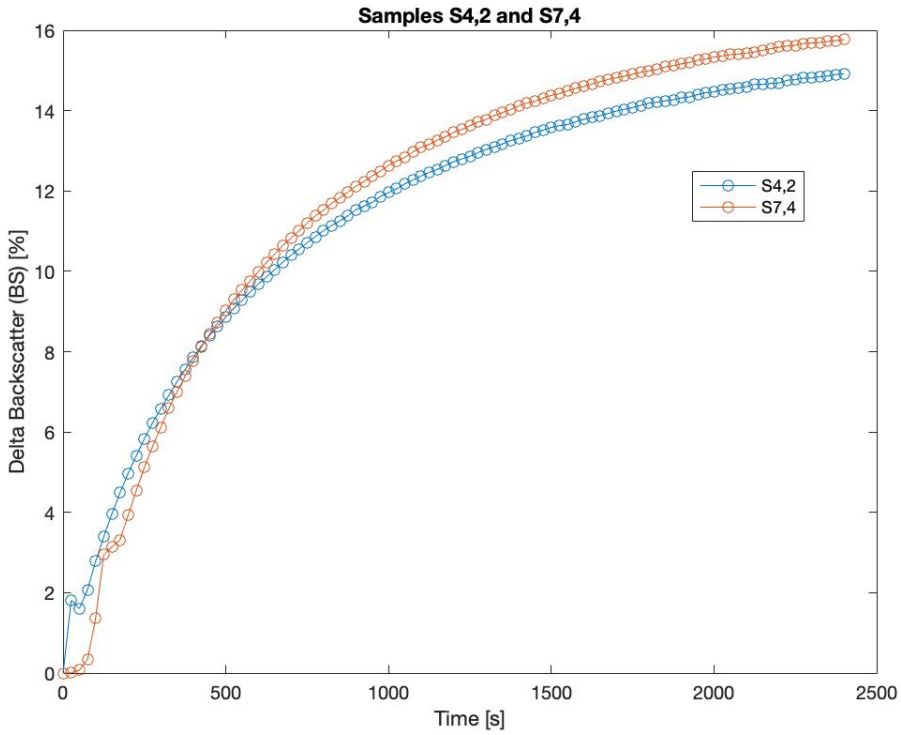

Figure C11 ΔBS [%] is plotted against time [s] for duplicate 11 (samples S4,2 and S7,4).

In Figure C12, the ΔBS [%] is plotted against Time [s] for duplicate 12 (samples S5,2 and S2,4).

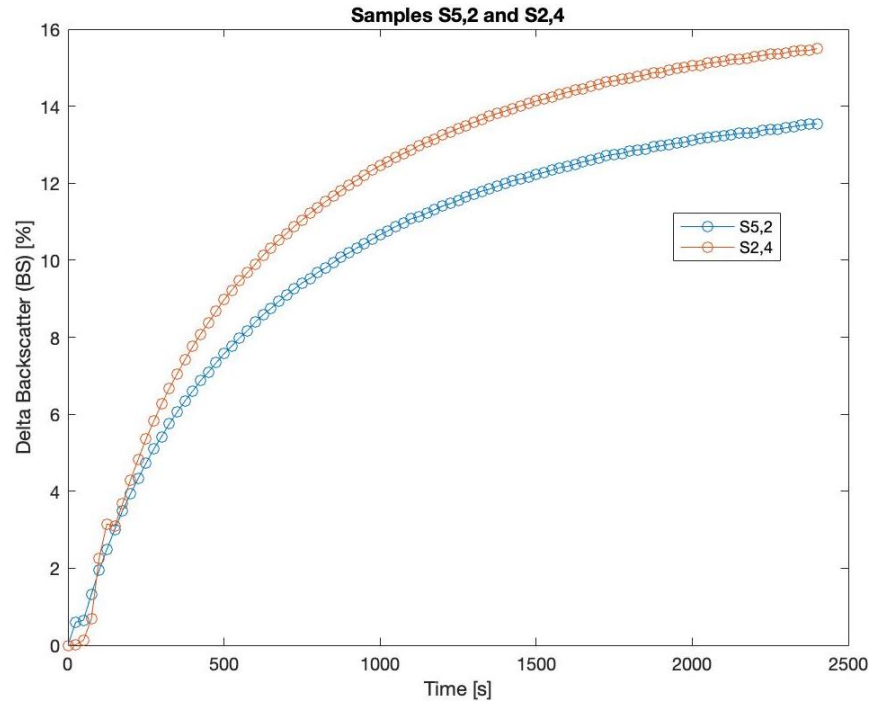

Figure C12 ΔBS [%] is plotted against time [s] for duplicate 12 (samples S5,2 and S2,4).

In Figure C13, the ΔBS [%] is plotted against Time [s] for duplicate 13 (samples S6,2 and S3,4).

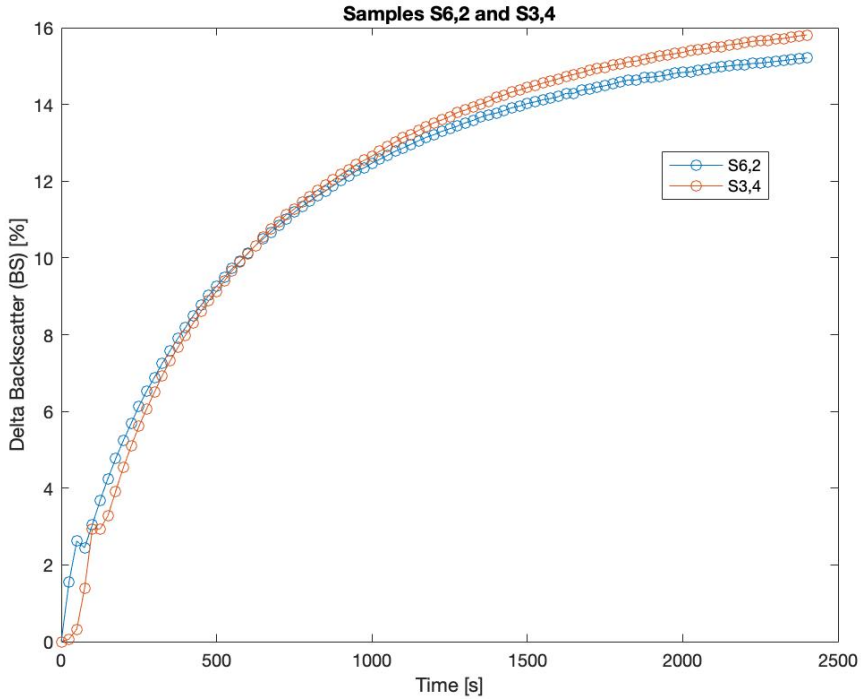

Figure C13 ΔBS [%] is plotted against time [s] for duplicate 13 (samples S6,2 and S3,4).

In Figure C14, the ΔBS [%] is plotted against Time [s] for duplicate 14 (samples S7,2 and S5,4).

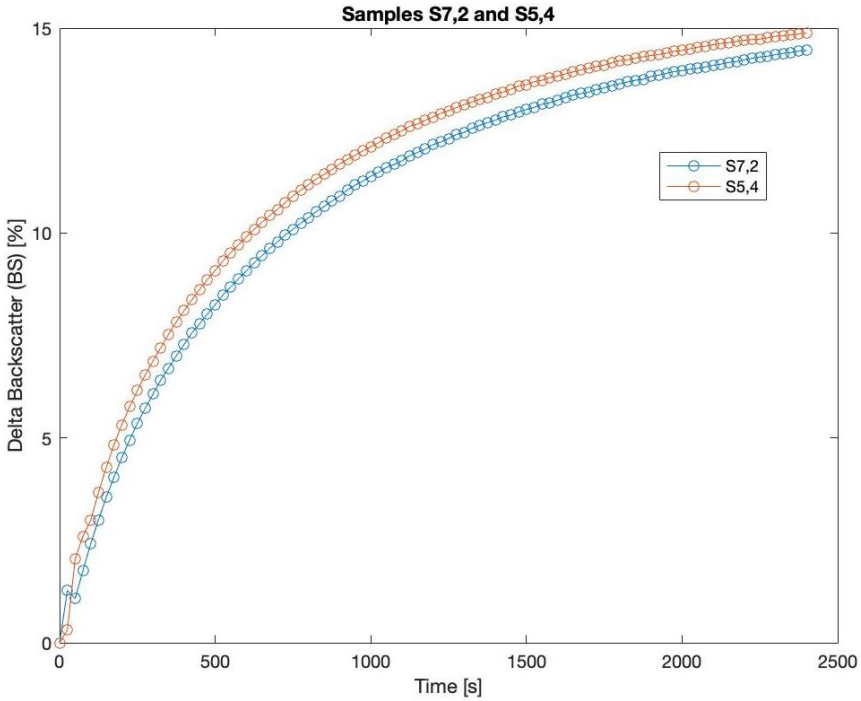

Figure C14 ΔBS [%] is plotted against time [s] for duplicate 14 (samples S7,2 and S5,4).

Appendix D

In this appendix, the G' [Pa] is plotted against Time [s] for the two samples of each duplicate in the Effect of fat on gelation-trial. This result was obtained using the Rheometer.

In Figure D1, the G' [Pa] is plotted against Time [s] for duplicate A (samples SSM3,1 and SSM3,2).

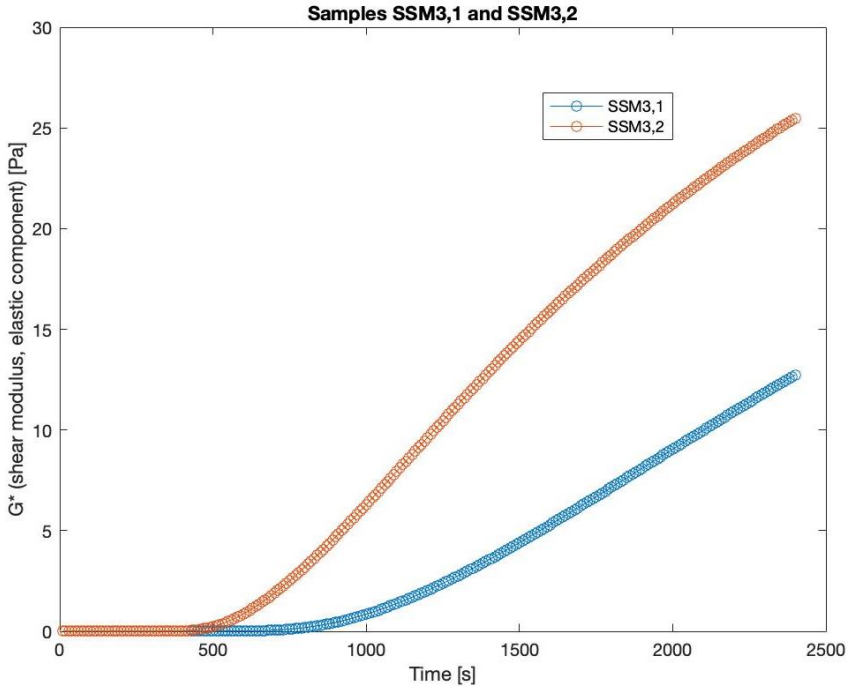

Figure D1 G' [Pa] is plotted against Time [s] for duplicate A (samples SSM3,1 and SSM3,2).

In Figure D2, the G' [Pa] is plotted against Time [s] for duplicate B (samples SM3,1 and SM3,2).

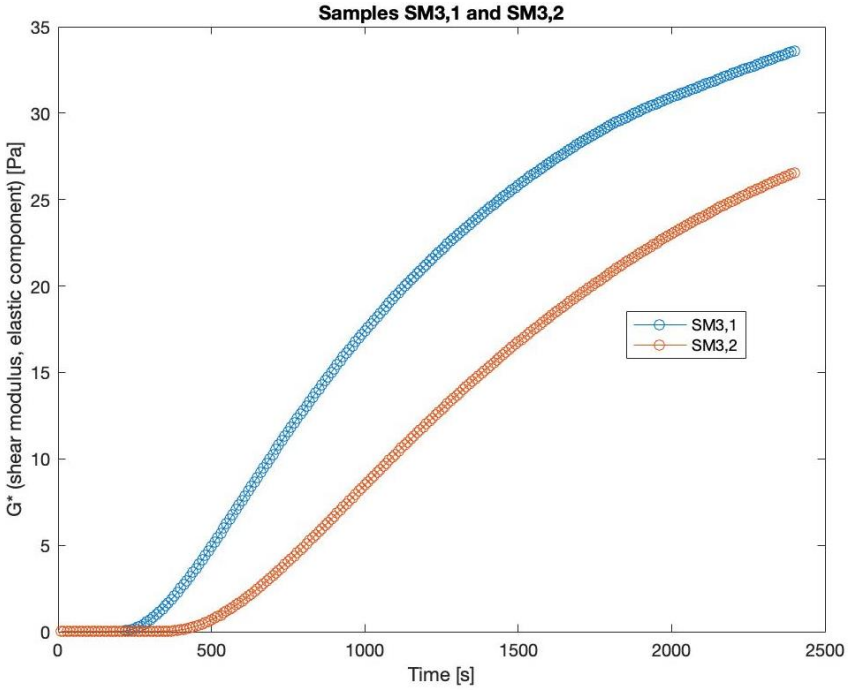

Figure D2 G' [Pa] is plotted against Time [s] for duplicate B (samples SM3,1 and SM3,2).

In Figure D3, the G' [Pa] is plotted against Time [s] for duplicate C (samples SSM2,1 and SSM2,2).

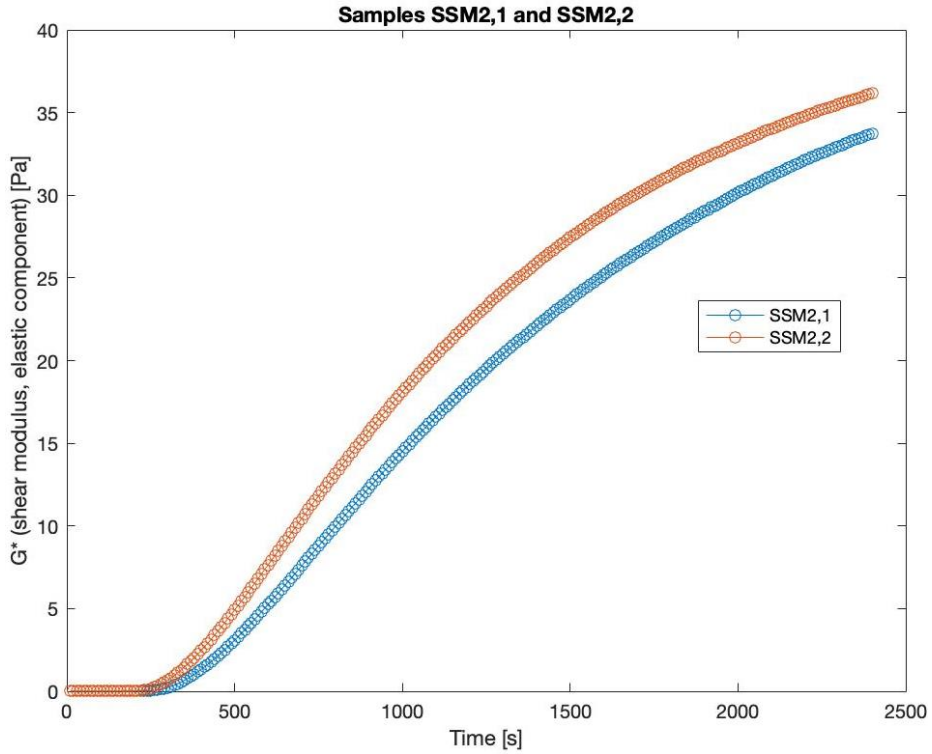

Figure D3 G' [Pa] is plotted against Time [s] for duplicate C (samples SM3,1 and SM3,2).

In Figure D4, the G' [Pa] is plotted against Time [s] for duplicate D (samples SM2,1 and SM2,2).

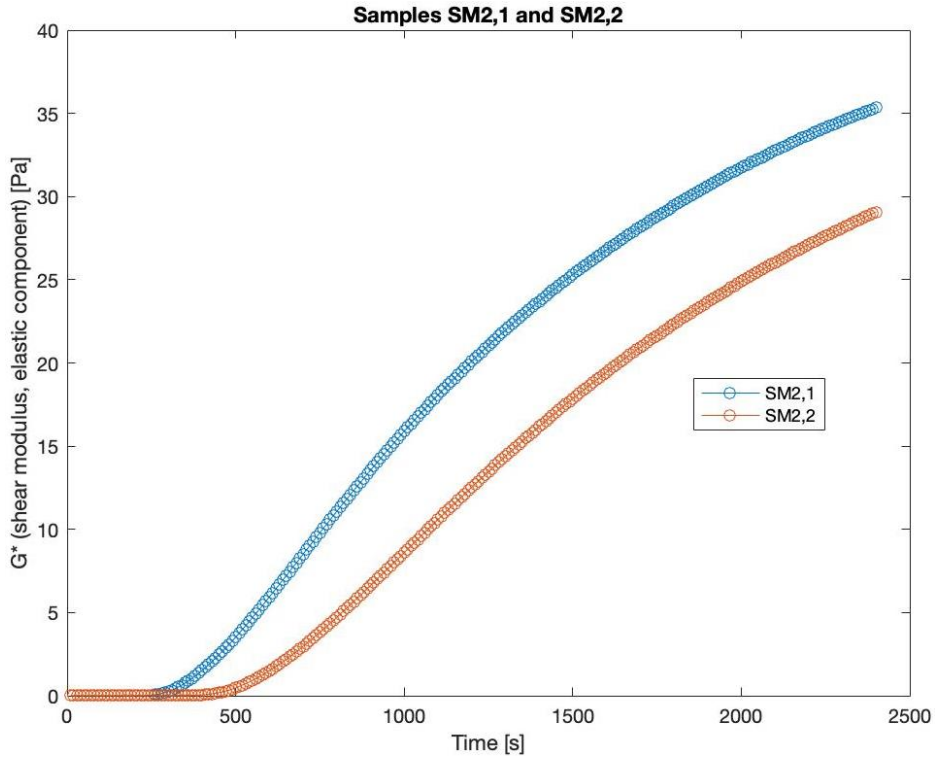

Figure D4 G' [Pa] is plotted against Time [s] for duplicate D (samples SM2,1 and SM2,2).

Appendix E

In this appendix, the ΔBS [%] is plotted against Time [s] for the two samples of each duplicate in the Effect of fat on gelation-trial. This result was obtained using the Turbiscan.

In Figure E1, the ΔBS [%] is plotted against Time [s] for duplicate A (samples SSM3,1 and SSM3,2).

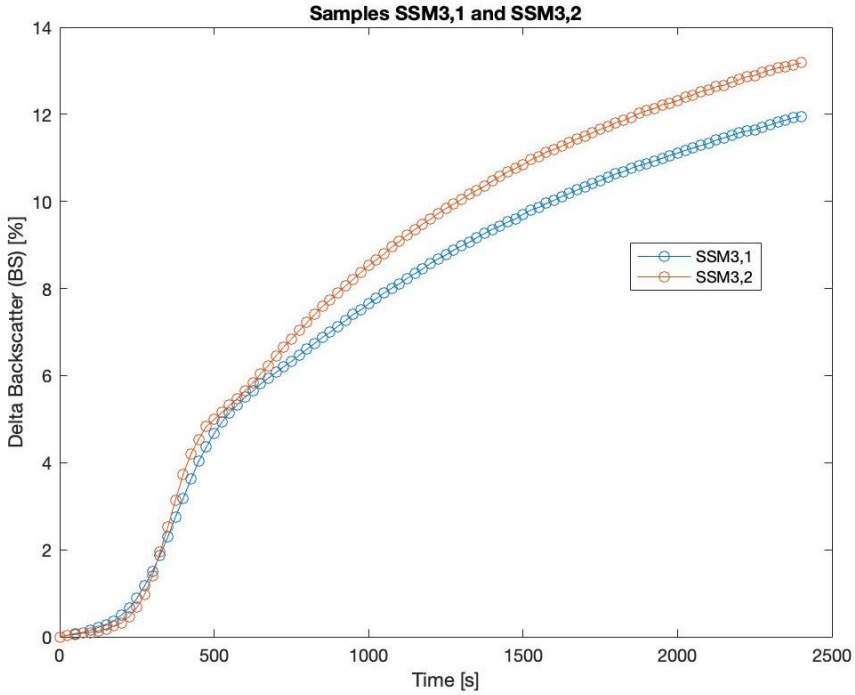

Figure E1 ΔBS [%] is plotted against Time [s] for duplicate A (samples SSM3,1 and SSM3,2).

In Figure E2, the ΔBS [%] is plotted against Time [s] for duplicate B (samples SM3,1 and SM3,2).

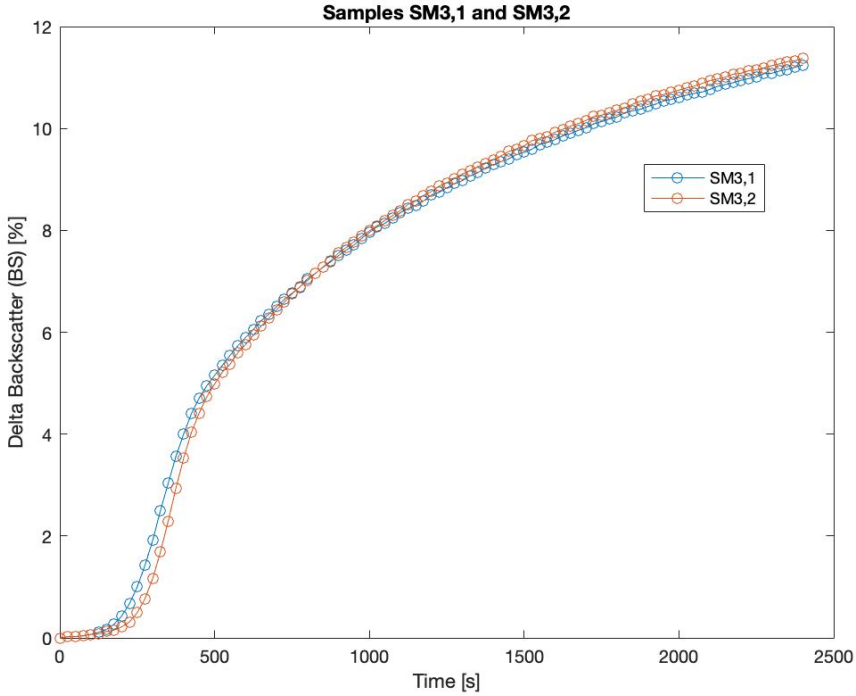

Figure E2 ΔBS [%] is plotted against Time [s] for duplicate B (samples SM3,1 and SM3,2).

In Figure E3, the ΔBS [%] is plotted against Time [s] for duplicate C (samples SSM2,1 and SSM2,2).

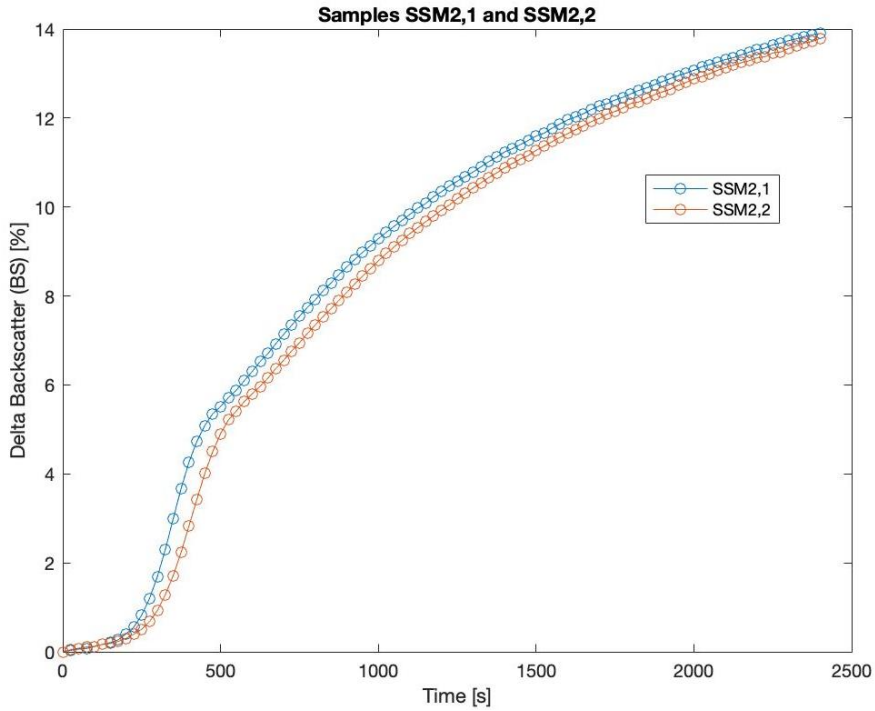

Figure E3 ΔBS [%] is plotted against Time [s] for duplicate C (samples SSM2,1 and SSM2,2).

In Figure E4, the ΔBS [%] is plotted against Time [s] for duplicate D (samples SM2,1 and SM2,2).

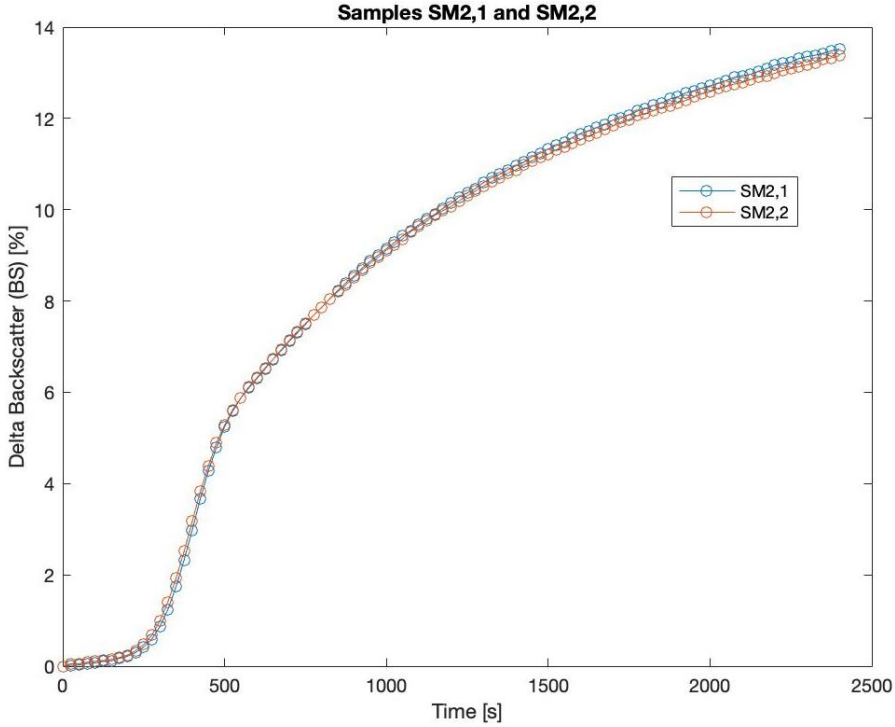

Figure E4 ΔBS [%] is plotted against Time [s] for duplicate D (samples SM2,1 and SM2,2).

Printed by Media-Tryck, Lund 2021 NORDIC SWAN ECOLABEL 3041 0903

LUND UNIVERSITY

LUND UNIVERSITY
Faculty of Engineering
Food Technology, Engineering, and Nutrition